LBL-30005
Preprint

Lawrence Berkeley Laboratory

UNIVERSITY OF CALIFORNIA

APPLIED SCIENCE DIVISION

To be submitted to Indoor Air

Modeling Radon Entry into Florida Houses with Concrete Slabs and Concrete-Block Stem Walls

K.L. Revzan, W.J. Fisk, and R.G. Sextro

October 1991

APPLIED SCIENCE DIVISION

LBL-30005
Copy 2
LOAN COPY
Circulates
for 4 weeks
Bldg. 50 Library.

Prepared for the U.S. Department of Energy under Contract Number DE-AC03-76SF00098

DISCLAIMER

This document was prepared as an account of work sponsored by the United States Government. While this document is believed to contain correct information, neither the United States Government nor any agency thereof, nor the Regents of the University of California, nor any of their employees, makes any warranty, express or implied, or assumes any legal responsibility for the accuracy, completeness, or usefulness of any information, apparatus, product, or process disclosed, or represents that its use would not infringe privately owned rights. Reference herein to any specific commercial product, process, or service by its trade name, trademark, manufacturer, or otherwise, does not necessarily constitute or imply its endorsement, recommendation, or favoring by the United States Government or any agency thereof, or the Regents of the University of California. The views and opinions of authors expressed herein do not necessarily state or reflect those of the United States Government or any agency thereof or the Regents of the University of California.

To be submitted to
Indoor Air

LBL-30005

MODELING RADON ENTRY INTO FLORIDA HOUSES WITH CONCRETE SLABS AND CONCRETE-BLOCK STEM WALLS

K.L. Revzan, W.J. Fisk, R.G. Sextro
Indoor Environment Program
Applied Science Division
Lawrence Berkeley Laboratory
1 Cyclotron Road
Berkeley, CA 94720

October, 1991

This work was supported by the U.S. Environmental Protection Agency (EPA) through Interagency Agreement DW89934620-0 with the U.S. Department of Energy (DOE). This work was also supported by the Assistant Secretary for Conservation and Renewable Energy, Office of Building Technologies, Building Systems and Materials Division and by the Director, Office of Energy Research, Office of Health and Environmental Research of DOE under contract DE-AC03-76SF00098.

Abstract

We model convective radon entry through soil into a typical Florida house. The part of the house included in the model comprises a concrete slab supported by a permeable concrete-block stem wall and a concrete footing. The slab rests on backfill material; the same material is used to fill the footing trench. A region of undisturbed soil extending 10 m beyond and below the footing is also included. The Laplace equation, resulting from Darcy's law and the continuity equation, and the mass-transport equation are solved using a steady-state finite-difference model to determine the pressure and radon concentration fields in the soil. The house and soil are represented as cylindrically-symmetric in order to increase resolution and computing efficiency without significant loss of generality. Isothermal conditions are assumed and spatial variations in soil moisture content are ignored. The soil is assumed homogeneous and isotropic except for certain simulations in which soil layers of high permeability or radium content are introduced. From the pressure and concentration fields, we calculate radon entry rates through openings in the slab, through gaps between the stem wall and slab and between the stem wall and footer, and through the permeable stem wall. These rates are determined for variable soil, backfill, and stem wall permeability, slab opening width and position, soil, slab, and stem wall radium content, slab and stem wall diffusivity, and water table depth. The variations in soil permeability and radium content include cases of horizontally stratified soil. We also consider the effect of a gap that restricts the passage of soil gas from the interior of the stem wall into the house. The model predicts that the total radon entry rate is relatively low unless the soil or backfill permeability or radium content is high. Apart from soil characteristics, the backfill permeability is the major factor determining radon entry rates. Stem wall permeability is a relatively unimportant factor in radon entry when small openings through the slab into the house are also present. Radon entry through the stem wall may be controlled by ensuring that the pressure in the interior is very nearly atmospheric, but entry through slab openings increases when this is done, so that the net reduction in radon may be only a factor of 2-3.

Nomenclature

Symbol	Name	Units
C	Radon concentration in soil	$Bq\ m^{-3}$
D	Bulk diffusivity of radon in soil	$m^2\ s^{-1}$
E_s	Entry rate of soil gas	$m^3\ s^{-1}$
E_r	Normalized entry rate of radon	$m^3\ s^{-1}$
g	Gravitational constant	$m\ s^{-2}$
k	Permeability of soil	m^2
P	Absolute pressure	Pa
P_A	Atmospheric pressure	Pa
p	Disturbance pressure	Pa
r	Radial coordinate	m
S	Radon production rate in soil	$Bq\ s^{-1}$
t	Thickness of gap or opening	m
w	Width of gap or opening	m
z	Vertical coordinate, positive downward	m
$\vec{v}$	Velocity of soil gas	$m\ s^{-1}$
ε	Porosity of soil	-
λ	Radon decay rate	s^{-1}
μ	Viscosity of air	$kg\ m^{-1}\ s^{-1}$
ρ	Density of air	$kg\ m^{-3}$
σ	Element of area of gap or opening	m^2

Introduction

Indoor radon (^{222}Rn) concentrations arise mainly from convective flow of radon-bearing gas from soil into the building interior and diffusion of radon from soil or from building materials (Nazaroff *et al.*, 1988; Nero and Nazaroff, 1984; DSMA 1983). In houses with elevated radon concentrations, convective flow of soil gas is the dominant source in almost all cases. In this situation, flow of gas, in response to a pressure difference between the soil and the building interior, will depend on both the type and location of openings or other flow pathways between the building and soil and on the characteristics of the surrounding soil. The building substructure -- usually either a basement, slab-on-grade, or crawlspace (or some combination of these) -- has a significant role in defining the nature of these pathways and openings.

As in other regions of the U.S., elevated indoor radon concentrations have been observed in a number of areas of Florida (Geomet, 1988). In response, the State of Florida, along with the U.S. Environmental Protection Agency, has established the Florida Radon Research Program with the broad objectives of conducting research on radon entry into Florida housing and of developing building codes and construction

standards designed to restrict radon entry into buildings (Sanchez *et al.*, 1990). Since a large fraction of houses built in the state utilize one of several variants of slab-on-grade construction (Scott and Findlay, 1983; Acres 1990), much of the research and code development has focused on these substructures. An important objective is to understand how details of the construction techniques used, both those in current practice and those that might be adopted in response to new building and construction codes, affect indoor radon concentrations.

We have developed a steady-state finite difference model of radon transport through soils and into buildings (Loureiro *et al.*, 1990; Revzan *et al.*, 1990) to investigate the dependence of radon and soil gas entry on a variety of parameters, including features of the soil and building system. For the present study, the steady-state finite difference model has been modified to account for the details of one form of the slab-on-grade substructure. We neglect the effect of variations in atmospheric pressure, which may increase radon entry rates when the soil permeability is relatively low (Narasimhan *et al.*, 1990). For this study, we also neglect the effect of inhomogeneity and anisotropy of soil permeability. Preliminary modeling indicates that anisotropy of soil due to layering produces significantly increased radon entry rates. Inhomogeneities such as fractures, which have not yet been studied, are also likely to increase entry rates. Validation of the model under controlled conditions is proceeding (Fisk, *et al.*, 1989).

We present here the predictions of the steady-state model, utilizing a set of soil and building substructure characteristics that are typical of Florida soils and houses. We then discuss the influence of variations in certain characteristics of the substructure and soil-fill system, taken as parameters of the model, on soil gas and radon entry. Because the model is not yet validated, the results should be viewed as providing a measure of the relative, rather than absolute, effect of varying these parameters.

Model Description

We model soil-gas and radon transport for a system comprising undisturbed soil, soil backfill, and building substructure as shown in Figures 1 and 2, The model incorporates an above-grade concrete slab floor, supported at the perimeter by a concrete-block stem wall that rests on a concrete footing. The slab and footing are considered to be impermeable to air, but the permeability of the stem wall may exceed that of the soil. The stem wall is represented by inner ("house-side") and outer ("soil-side") permeable layers separated by an open zone. The layers are assumed continuous, *i.e.*, the changes in permeability at the mortar joints between blocks are ignored. The slab rests on fill material elevated above the natural grade level. The footer trench is filled with the same material. The area modeled includes the slab, stem wall, and footer of the house, the fill, and a section of the undisturbed soil. Radon-bearing air ("soil gas") is assumed to enter the interior of the stem wall through gaps between the stem wall and footer, through gaps between the stem wall and slab, and through the permeable sides of the concrete blocks. All air entering the interior of the stem wall is assumed to pass into the house through

gaps between the stem wall and the slab. Air may also enter the house directly through an opening in the slab itself, *e.g.*, a crack or an opening for utilities. A vertical cross-section of the region, with the dimensions used in this paper, is shown in Figure 1. A detail of the neighborhood of the stem wall, with the width of the gaps greatly exaggerated, is shown in Figure 2. It may be seen that the walls of the footer trench have been modeled as vertical, rather than sloping, for simplicity. The part of the house above the slab is not modeled.

Assuming that the cross-section of the stem walls is uniform, and assuming that we are willing to limit the discussion of slab openings to those that are cylindrically-symmetrical, the slab, stem walls, and footers can be modeled as cylinders with only the loss of corner effects, which have been shown to be unimportant in the case of basements (Revzan, *et al.*, 1990). The region from which a house draws soil gas depends on the positions of adjacent houses, the extent of their depressurization, and the characteristics of the soil. The exact boundaries of this region are likely to be important in particular cases, but in the general case, the soil may be represented as well by a cylinder as by a box. The entire region may therefore be modeled in cylindrical coordinates, which permits greater resolution, shorter solution time (with lower cost), or a combination of the two.

We use a finite-difference steady-state model (Loureiro, 1987; Loureiro, *et al.*, 1990; Revzan, *et al.*, 1990) that, assuming isothermal soil conditions, comprises two difference equations, each of which is obtained from a differential equation. First, the pressure field is found from Darcy's law,

$$\vec{v}(r,z) = -\frac{k(r,z)}{\mu}\nabla p(r,z), \tag{1}$$

where $\vec{v}$ is the bulk velocity (flow rate divided by total cross-sectional area), k is the permeability of the soil, μ the viscosity of air (1.8×10^{-5} kg m^{-1} s^{-1}), and r and z are the radial and vertical coordinates, respectively. The disturbance pressure, p, *i.e.*, the pressure change in the soil that is produced by the difference between house and atmospheric pressures, is defined by

$$p(r,z) = P(r,z) - P_A - \rho g z, \tag{2}$$

where P is the absolute pressure, P_A the atmospheric pressure, assumed constant in a steady-state model, ρ the density of air, which is constant when conditions are isothermal, and g the gravitational acceleration. Under isothermal conditions, the equation of continuity may be written

$$\nabla\cdot\vec{v}(r,z) = 0. \tag{3}$$

Combining Equations 1 and 3, we have the first equation of the model:

$$\nabla \cdot \left\{ \frac{k(r,z)}{\mu} \nabla p(r,z) \right\} = 0. \tag{4}$$

The boundaries for the solution of Equation 4 are the outer limits of the soil block (chosen 10 m from the footer in both the r- and z-directions, far enough from the house that insignificant change in radon entry rate results from their extension), the soil surface, the bottom of the slab, the outer surfaces of the footer, the inner surfaces of the permeable concrete blocks of the stem wall, including the parts forming the sides of the gaps, the interfaces between gaps or openings and the backfill, and the outside of the part of the stem wall that is above the soil surface. Since the area modeled does not extend above the slab, the top of the soil-side stem wall layer is treated as a boundary. Transport within the slab and footer is excluded from the model, *i.e.*, the velocity is set to zero at all nodes in these regions. Special techniques, described below, are used to determine the velocities in the narrow gaps, since numerical modeling of such areas offers no advantages to offset the considerable decrease in computing speed.

At the outer soil boundaries and at all concrete surfaces, the normal derivative of the pressure must vanish, *i.e.*, there is no flow of air across these boundaries. At the soil surface, the disturbance pressure vanishes. At the backfill side of a gap, the pressure is determined by the difference between the house pressure and the pressure drop across the gap. Temperature differences between a house and the outside, the effect of wind, and the operation of heating, ventilation, and air-conditioning systems produce a pressure at the floor which is generally lower than P_A (Feustel and Sherman, 1989; Sherman, *et al.*, 1979; see also Revzan, *et al.*, 1988; 1989). The difference between the pressure at the house side of a gap and P_A is written as ΔP_b. This is assumed to be the pressure at the top of the slab. In the general case, it is also assumed to be the pressure inside the stem wall. Two special cases are also considered: 1) the stem wall is filled with an impermeable material, so that the normal derivative of the pressure vanishes inside the stem wall, *i.e.*, flow of air into the house occurs only through the wall-slab gap and the top of the house side of the stem wall (the part of the wall adjacent to the gap); 2) there is considered to be a restriction between the inside of the stem wall and the house (*i.e.*, the gap between the edge of the slab and the inside of the stem wall is small), so that the pressure inside the stem wall is the difference between ΔP_b and the pressure drop caused by flow through the restriction.

The pressure drop across a gap, ΔP_g, is determined from an algorithm due to Baker, *et al.* (1989):

$$|\Delta P_g| = \frac{12\mu t}{w^2} |v| + \frac{\rho(1.5+n)}{2} v^2. \tag{5}$$

Here, t is the length of the gap in the direction of flow, w is the width of the gap perpendicular to the flow, v is the average speed of air in the gap, *i.e.*, the flow rate through the gap divided by the area, and n is the number of bends in the gap which is always 1 for the

configuration discussed here. For a restriction between the house and the interior of the stem wall, treated as a gap, the flow into the gap is determined by summing all flows into the interior of the wall through the permeable inner and outer layers and the wall-footer and wall-slab gaps. This summed flow includes the flow of outside air, considered to be radon-free, through the above-grade part of the wall. Air flow through the permeable layers is not, in general, horizontal, *i.e.*, parallel to the soil surface, so that air can flow from a layer into a gap. Such a flow cannot be incorporated into Equation 5, so that we have excluded it from the model by requiring that the edges of gaps in the stem wall layers be no-flow boundaries. This choice of boundary condition is unlikely to affect total radon entry rates significantly, but it does slightly exaggerate the fraction of radon entering through the layers at the expense of the fraction entering through the gaps. The top of the soil-side stem wall layer is also treated as a no-flow boundary.

Once a solution to Equation 4 is obtained, the soil-gas velocity is found from Equation 1 and the soil-gas entry rate, E_s, from

$$E_s = \int_{\Sigma} \vec{v}(r_g, z) \cdot d\vec{\sigma}(r_g, z), \tag{6}$$

where $\vec{\sigma}$ is an element of area and Σ indicates an integral over the entire area of interest. In the case of the soil-side stem wall layer, the soil-gas entry rate is found by subtracting the air flow through the above-grade part of the outside surface of the layer from the total air and soil-gas flow through the inside surface. In practice, we calculate soil-gas entry rates through each of the gaps, through the house-side stem wall layer, and through the soil-side stem wall layer. In addition, we calculate the flow rate of air through the soil surface for comparison with the total soil-gas entry rate through all gaps and permeable walls.

After the pressure field in the soil, permeable stem wall layers, and gaps or openings is found from Equation 4, the radon concentration, C, may be obtained from the steady-state mass-transport equation (Nazaroff, *et al.*, 1988),

$$\vec{v}(r,z) \cdot \nabla C(r,z) = \nabla \cdot [D(r,z) \nabla C(r,z)] - \varepsilon(r,z) \lambda C(r,z) + \varepsilon(r,z) S(r,z), \tag{7}$$

where ε is the porosity, D the bulk radon diffusivity (the effective diffusivity is found by dividing D by ε), λ the radon decay constant, and S the rate of release of radon per unit pore space volume. For gaps and openings, we assume $\varepsilon = 1$ and $S = 0$. For any material, the theoretical maximum concentration at distances far from the influence of surface boundary conditions, C_∞, is given by

$$C_\infty = \frac{S}{\lambda}. \tag{8}$$

In general, the radon concentration in materials other than the undisturbed soil is less than C_∞ for that material.

In the general case, the boundaries for the solution of Equation 7 are the outer soil boundaries, the soil surface, the basement side of the slab, the interior of the stem wall, and the portion of the stem wall exterior that is above the soil surface. At the soil surface, we assume C = 0; because radon concentrations in soil gas are typically high compared to those in the atmosphere, the assumption of a non-zero soil-surface concentration has a negligible effect on the result. We also assume C = 0 inside the stem wall, since the flow of low-radon air through the soil-side layer is much greater than the flow of high-radon air through the house-side layer. At the outer and lower boundaries of the soil, we assume that the normal derivative of C vanishes, which is equivalent to the assumption that there is no passage of radon by diffusion across these boundaries. Since passage of radon by convection has been excluded by the boundary conditions used in solving Equation 4, these are no-flow boundaries for radon. When the stem wall is filled with an impermeable material, the boundary is the top of this material, which is considered to be at zero concentration.

From previously-determined velocities and a solution to Equation 7, we find the radon entry rate, E_r, and the average radon concentration, <C>, for any entry area of interest, from the equations

$$E_r = \int_{\Sigma} (\vec{v}(r,z)C(r,z) - D\nabla C)\cdot d\vec{\sigma}(r,z) \tag{9}$$

and

$$<C> = \frac{\int_{\Sigma} C(r,z)\,d\sigma(r,z)}{\int_{\Sigma} d\sigma(r,z)}, \tag{10}$$

where σ and Σ have the same meaning as for Equation 6.

Configurations and Procedures

Base Configuration

We define a "base configuration" for the substructure, soil, and fill. The characteristics of the base substructure were determined from a review of typical construction practices (Acres, 1900; Scott and Findlay, 1983) and in discussions with Florida researchers (Pugh, 1990; Dixon, 1990); the base-case soil and fill properties were determined from available studies of soil and fill properties (Nielson and Rogers, 1990; Roessler, *et al.*, 1990). In this configuration (Figures 1 and 2), the outer edge of the

concrete-block wall is 7 m from the center of the slab and the concrete blocks are 0.19 m wide in total, with a central air space of 0.134 m and two concrete layers 0.028 m thick. (The sections of concrete that connect the inner and outer concrete layers in actual blocks have been ignored, since they have little effect on the vertical flow of air.) The slab is 0.1 m thick. The footer is 0.45 m wide by 0.30 m high. There are gaps between the inside of the stem wall and the slab, between the inside of the stem wall and the footer, and between the outside of the stem wall and the footer; all of these gaps are 0.003 m wide. There is an opening in the slab 3 m from the center; this opening is also 0.003 m wide.

The distance between the bottom of the slab and the soil surface is 0.3 m and that between the soil surface and the top of the footer is 0.2 m, so that the distance between the bottom of the slab and the top of the footer is 0.5 m. The areas between the bottom of the slab and the soil surface and between the top of the footer and the soil surface (the footer trench) are assumed to be filled with a material ("fill") that may be different from the undisturbed soil. The outer edge of the soil is 10 m beyond the outer edge of the footer, i.e., 17.13 m from the center of the slab. The depth of the soil block is 10 m greater than the bottom of the footer, i.e., 10.5 m below the soil surface or 10.9 m below the top of the slab. These distances are great enough that no significant increase in the radon entry rate results from their extension.

The base-case permeabilities, diffusivities, pore-space radon concentrations, and porosities of the materials included in the model are shown in Table 1. The indicated radon concentrations are those that would be found sufficiently far from surfaces that the effect of boundary conditions is negligible, *i.e.*, C_∞ as defined by Equation 8. For the narrow slab and stem wall, concentrations are generally lower than the value shown in the table; for the the soil, the value is the concentration a few meters below the soil surface.

The pressure at the top of the slab and inside the concrete block wall is fixed at -2.4 Pa with respect to the atmosphere, which is a typical indoor-outdoor pressure difference.

Parametric Evaluations

We evaluate the effect on soil-gas and radon entry of varying the following parameters individually, the others retaining the values of the base configuration:

- permeability of the soil as a whole ($10^{-12} - 10^{-9}$ m^2);
- permeability of soil layer 0.0-1.0 m below surface ($10^{-12} - 10^{-9}$ m^2);
- permeability of soil layer 0.5-1.5 m below surface ($10^{-12} - 10^{-9}$ m^2);
- permeability of the fill - house and soil sides ($10^{-15} - 10^{-9}$ m^2);
- permeability of the fill - soil side only ($10^{-15} - 10^{-9}$ m^2);
- permeability of the stem wall - both sides ($10^{-15} - 10^{-9}$ m^2);
- permeability of the stem wall - house side ($10^{-15} - 10^{-9}$ m^2);
- permeability of the stem wall - soil side ($10^{-15} - 10^{-9}$ m^2);
- width of the opening in the slab (0.001-0.1 m);
- distance of the opening in the slab from the center (0-7 m);

- depth of the water table (0.5-10 m);
- relative (to base case) radium content of the fill (0.1 – 10);
- relative radium content of the soil below 1 m depth (0.1 – 10);
- relative radium content of the soil below 5 m depth (0.1 – 10);
- relative radium content of the concrete slab (0.1 – 10);
- relative radium content of the stem wall blocks (0.1 – 10);
- effective diffusivity of the concrete slab ($10^{-9} - 10^{-6}$ m^2 s^{-1});
- effective diffusivity of the stem wall blocks ($10^{-9} - 10^{-6}$ m^2 s^{-1});

We also evaluate the following situations: 1) varying the soil permeability for high (10^{-9} m^2) and low (10^{-15} m^2) fill permeabilities; 2) varying the soil and fill permeabilities (independently) when the slab opening is the only entry point; 3) varying the soil, fill, and stem wall permeabilities (independently) when the stem wall is filled with impermeable concrete; 4) varying the stem wall permeability when the two wall-footer gaps are completely closed; 5) varying the width of a restriction between the interior of the stem wall and the house, *e.g.*, a gap between the side of the slab and the concrete block of the stem wall.

Results and Discussion

For the base configuration, the predicted air and soil-gas entry rate into the house through the substructure is 6.9×10^{-3} m^3 s^{-1}, of which 93% is outside air that enters the soil-side of the stem wall. The soil-gas entry rate is 4.5×10^{-4} m^3 s^{-1}. As a check on the mass-balance, the flow of air across the soil surface is calculated. This differs from the total soil-gas entry rate by less than 0.005%, which indicates that the mass-balance is within acceptable limits. The fraction of the soil gas that enters through each of the areas of interest is shown in Table 2. 92% of the total entry is through the soil side of the stem wall, including the gap, 6% through the house side of the stem wall, including the gaps, and 2% through the slab opening. The flow of outside air through the above-surface part of the stem wall is a factor of 14 greater than the total flow of soil gas through the remainder of the entry areas.

The predicted radon entry rate into the house is 2.3 Bq s^{-1}. If there is no pressure difference between the inside and outside of the house, the predicted entry rate is 1.2 Bq s^{-1}, so that 1.1 Bq s^{-1} may be attributed to convection. This "convective" entry rate may not be due to convection in the strict sense, but may combine convection and an increase in diffusion due to an increased radon concentration at the point of entry. The fraction of the diffusive, convective (in the sense of the previous sentence), and total radon entry rates through each of the areas of interest are shown in Table 2. The average radon concentration for the each of the areas as a fraction of C_∞ is also shown; this is to be understood as the concentration at the soil side of each of the areas, since the concentrations at the basement side of the slab and the interior of the stem wall are zero. Of the diffusive entry, 43% is through the house side of the stem wall, including the two gaps,

4% is through the soil side of the stem wall, including the gap, 10% is through the slab opening, and 43% is through the slab. Of the non-diffusive entry, 56% is through the house side of the stem wall, including the two gaps, 24% is through the soil side of the stem wall, including the gap, 17% is through the slab opening, and 2% is through the slab. The "convective" entry through the slab is not truly convective, since that is excluded by our choice of boundary conditions, but is rather an increase in diffusive entry. Of the total radon entry, 50% is through the house side of the stem wall, including the two gaps, 14% is through the soil side of the stem wall, including the gap, 13% is through the slab opening, and 23% is through the slab. The differences between the fractional soil-gas and radon entry rates at the several entry points are due to the differing radon concentrations in the soil gas at the several points of entry; these differences are due, in turn, primarily to the differing flow-path lengths from soil surface to opening. The radon concentration at the soil side of the stem wall is 0.02 C_∞ or less, depending on proximity to the surface. At the inner wall, the concentration is 0.64 C_∞, while at the slab the concentration rises to 0.77 C_∞. The predicted pressure and radon concentration fields for the base configuration are shown in Figures 3 and 4, respectively. (The pressure field near the outside block wall appears blank on Figure 3 because the gradient is too steep to be shown.)

Elimination of the slab opening from the base configuration has little effect: the total soil-gas entry rate is unchanged, while the total radon entry rate diminishes from 2.3 to 2.2 Bq s^{-1} because of the difference between the radon concentration at the center of the slab and at the stem wall. In contrast, removal of all of the entry points in the stem wall has a major influence on both soil-gas and radon entry. The soil-gas entry rate becomes 1.5×10^{-5} m^3 s^{-1}, the 97% reduction being due primarily to the closure of the soil side of the stem wall. The radon entry rate is then 1.3 Bq s^{-1}, a reduction of 43% due to sealing the stem wall. If, the stem wall remaining sealed, the width of the slab opening is increased to 0.1 m, so that the entry area increases from 0.019 to 1.9 m^2, the radon entry rate rises to 1.7 Bq s^{-1}, which is 74% of the base rate. The radon entry rate is reduced from that of the base configuration even if the slab opening is moved to the vicinity of the stem wall: for an opening 6.5 m from the center of the slab with a width of 0.003 m (area 0.12 m^2), the radon entry rate is 1.6 Bq s^{-1}, 70% of the base rate. Since the diffusive entry rate through the slab (23% of the total base entry rate) is essentially unchanged by the sealing of the stem wall and moving of the slab opening, the reduction in the convective entry rate is greater than would be indicated by the numbers given above. Thus, the model indicates that elimination of all openings at the stem wall, as might be accomplished by employing a one-piece concrete footer, stem wall, and slab, would be effective in reducing convective radon entry.

We now examine in detail the effect of variations in the parameters on radon entry. In each case, all parameters other than the one under consideration, have their base configuration values, except where noted. A summary of the results, showing the parameter, the range considered, and the ranges of soil-gas and radon entry rates is given in Table 3. In each case, the discrepancy between the total soil-gas entry rate and the entry rate of air at the soil surface is less than 0.01%. Certain of the results, as noted below,

are shown in Figures 5 and 6. Figures showing variations in the soil-gas and radon entry rates through each of the entry points for each of the parameters are provided in an appendix; a key to the appendix figures is given in Table 3. Figures showing soil-gas radon concentration variations at each of the entry points are also provided in the appendix for cases where the variations are significant.

Soil Permeability:

Soil permeability is permitted to vary from 10^{-12} m^2, below which convective entry becomes relatively insignificant, to 10^{-9} m^2. As the soil permeability increases, the soil-gas entry rates through all entry points also increase, those on the soil side of the block wall more dramatically. Although there is a significant diminution in radon concentration at all entry points on the house side, the increase in soil-gas entry rates is sufficient to produce a considerable increase in the radon entry rates (1.48 to 13.4 Bq s^{-1}, see Figure 5). The fraction of the total radon entry due to passage of soil gas through the house side of the block wall increases from 0.38 to 0.85 as the soil permeability increases.

If the stem wall is filled with an impermeable material (such as concrete), so that there is no entry except through the upper house side gap, radon entry rates increase from 0.70 to 1.70 Bq s^{-1} as the soil permeability increases (see Figure 5). These relatively low values are somewhat misleading, since the reduction due to the presence of the concrete is greatest at very high soil permeabilities, whose occurrence is unusual. At the base permeability of 10^{-11} m^2, the reduction is 59%, but the reduction in the entry rate through all entry points except the slab is 69%, which is high enough to indicate that filling the stem wall with impermeable material is an effective remedial measure. If the stem wall is made impermeable and all stem-wall gaps closed, so that radon entry occurs only through the slab, the range of radon entry rates is 0.97 to 1.90 Bq s^{-1}. These values are slightly higher than in the case of the filled stem wall because diffusion through the stem wall is permitted to occur.

When the permeabilities of the backfill and the undisturbed soil differ from one another, soil-gas entry is limited by the smaller of the two values. For that reason, the radon entry rate increases very little as the soil permeability increases beyond the base fill permeability. If the fill permeability is increased to 10^{-9} m^2, the upper limit of the radon entry rate, at a soil permeability of 10^{-9} m^2, becomes 44.4 Bq s^{-1}. For this fill permeability and a high, but more reasonable, soil permeability of 5×10^{-11} m^2, the entry rate is 7.85 Bq s^{-1}, which produces an indoor radon concentration of 113 Bq m^{-3} (3.1 pCi L^{-1}) in a house of air exchange rate 0.5 h^{-1} and volume 500 m^3. This concentration is 3.4 times the base concentration but still below the EPA guideline of 150 Bq m^{-3} or 4 pCi L^{-1}. Hence, the model indicates that, even with highly permeable soil and fill, above-average soil radium concentrations are necessary to produce indoor radon concentrations that exceed the EPA guideline.

Since the backfill can be the limiting factor in soil-gas entry, it is of interest to find the variation in radon entry rates with soil permeability when the backfill permeability is very small. Taking the latter to be 10^{-15} m^2, the lower limit of permeabilities of naturally-occurring soil, the model predicts that neither the soil-gas nor the radon entry

rate varies with soil permeability. The latter rate is 1.00 Bq s^{-1}, a 57% reduction from the base rate. However, gaps or cracks in the fill might compromise its effectiveness in limiting soil-gas and radon entry.

To determine the effect of soil stratification on radon entry, we independently consider two horizontal layers, each 1 m thick, the first beginning at the soil surface and the second 0.5 m below the surface. The permeability of each layer is allowed to vary between 10^{-12} and 10^{-9} m^2. The first layer is in contact with the backfill, whose permeability is $4x10^{-11}$ m^2, while the second is separated from the backfill by a 0.5 m layer of the base soil, whose permeability is 10^{-11} m^2. For layer permeabilities of 10^{-10} m^2, the radon entry rates for the two configurations are 204% and 137%, respectively, of the base rate, which is indicative of the importance of the placement of the layer with respect to the backfill. If the backfill is of low permeability, however, the placement of the high-permeability layer is unimportant. For a backfill permeability of 10^{-12} m^2, all other parameters remaining the same, the radon entry rates for the two configurations are 64% and 62% of the base rate.

Backfill Permeability:

As the backfill permeability is reduced from 10^{-9} to 10^{-15} m^2, the soil-gas entry rate decreases by nearly five orders of magnitude. Since most of this decrease occurs on the soil side of the stem wall, where the radon concentration is low, the radon entry rate decreases by only a factor of 2.2 (2.66 to 1.2 Bq s^{-1}, see Figure 5). However, this relatively small reduction is misleading, since the reduction in the convective entry rate (as we have defined it above) is much greater. At the base fill permeability, an entry rate of 1.14 Bq s^{-1} is attributable to the presence of the pressure field. For fill permeabilities of 10^{-15} and 10^{-12} m^2, this convective entry rate becomes 0.01 (>99% reduction) and 0.22 Bq s^{-1} (81% reduction), respectively. Reducing the backfill permeability is a highly effective method of reducing convective radon entry.

It has been suggested that radon entry be reduced by using a low-permeability material to fill in just the soil-side part of the footer trench. The soil-gas entry rate can, in fact, be reduced by a factor of 12 by reducing the fill permeability in this region from the base value of $4x10^{-11}$ m^2 to 10^{-15} m^2. Unfortunately, the radon entry rate is reduced only slightly, from 2.33 to 2.11 Bq s^{-1}. The reductions in the entry rates through the soil-side block wall and wall-footer gap are indeed dramatic, but the radon concentration on the soil side is so low that the effect on the total radon entry rate is almost negligible. Changing the permeability of the soil-side fill has essentially no effect on the radon concentrations at the several entry points.

Filling the stem walls with concrete reduces the radon entry rate by roughly a factor of 2 over the range of fill permeabilities considered (see Figure 5). The effect of elimination of all entry at the stem wall, so that the only entry point is the slab opening, depends strongly on the fill permeability. Between the lowest and highest permeabilities considered, the reduction from the base rate diminishes from a factor of 2.6 to a factor of 1.02. The influence of the fill permeability increases as the opening is moved toward the center of the house.

Stem-wall Permeability:

It would seem that decreasing the permeability of the concrete-block walls, through which 41% of the radon enters in the base case, would significantly reduce the radon entry rate. Decreasing the wall permeability to 10^{-12} m^2 does reduce soil-gas entry by 76%, but radon entry is reduced by only 13%. A further decrease to 10^{-15} m^2 gives only another 6% reduction in soil-gas entry and another 4% reduction in radon entry, since the entry rates through the slab opening and the three gaps are now dominant and essentially constant. Because the largest part of the reduction in soil-gas entry rate occurs at the soil side of the stem wall, where the radon concentration is low, there is only a small diminution in the radon entry rate (see Figure 5). It does not appear that reducing the permeability of the stem wall concrete blocks is an effective remedial measure.

We also considered the effect of varying the permeability of the soil and house sides of the concrete blocks independently and of varying the permeability of both sides of the blocks while: 1) eliminating the gaps between the lowest block and the footer and 2) filling the concrete blocks with concrete. As indicated in Table 3, none of these measures has a significant effect on radon entry.

We have indicated that a reduction in the soil-gas entry rate through the block walls, caused by decreasing their permeability, is offset by an increase in the entry rate through the wall-slab and wall-footer gaps. In the latter case, the pressure gradient near the gaps is much greater than in the former: at roughly corresponding points on the house side of the wall, the pressures are -2.3 and -1.8 Pa, respectively, compared to the house pressure of -2.4 Pa. The larger the interface (permeable material, gap, or opening) between house and soil or fill, the lower the pressure gradient; increased entry area (due to the block walls becoming permeable) is offset by diminished soil-gas velocity.

Slab Opening:

So long as the stem wall remains relatively permeable, the width of the opening in the slab has little effect on either the total soil-gas or total radon entry rate. The total radon entry rate changes by only 17% for widths ranging from 0.001 to 0.1 m. As the width increases, the slight increase in the entry rate through the slab opening is nearly offset by a slight diminution in the entry rate through the stem wall on the house side; the other entry rates are all but unaffected. The effect on soil-gas entry rates is similar. The radon concentrations at the entry points remain essentially unchanged.

The distance of the slab opening from the center also has little effect on the entry rates. The radon entry rate reaches a maximum when the opening is approximately 5 m from the center and diminishes as it approaches either the center or the stem wall. The radon entry rate through the opening itself changes more dramatically, but the change is somewhat offset by compensating changes in the entry rates at the house side of the stem wall. The entry rates through the soil side gap and block wall are essentially unaffected. The pattern of changes in soil-gas entry rates is similar. The radon concentration at the mouth of the slab opening diminishes from nearly 0.78 C_∞ when the opening is near the center to 0.47 C_∞ when it is near the block wall; the radon concentrations at the other entry points are unaffected.

Water Table Depth:

The effect of a reduction in the water table depth is modeled by changing the lower boundary of the soil, i.e., we assume that no air flows through water-saturated soil. The depth of the water table has little effect on the radon entry rate until it is reduced to ~2 m, at which point the rate is 2.1 Bq s^{-1}. The rate diminishes to 1.6 Bq s^{-1} at a water table depth of 0.5 m. The diminution is a consequence of lower soil-gas entry rates through the entry areas on the house side of the wall.

Radium Content:

If the radium content of all soil beneath the house, including the backfill material, is changed uniformly, the radon entry rate changes proportionally (soil-gas entry is not affected). If the radium content of just a part of the soil is changed, however, the situation must be modeled to determine the effect of the change on radon entry. We examine three configurations: in the first, the radium content of the fill material varies; in the second and third, the radium content of all soil 1 and 5 m below the surface, respectively, varies over the same range, with the remaining soil and the fill retaining the base value. We also consider the effect of varying the radium content of the slab and the stem wall independently. In all cases, the radium is allowed to vary between 0.1 and 10.0 times the base value.

Since radium content has no effect on soil-gas entry rates, radon entry rates reflect the concentrations at the entry points. When the radium content of the fill is changed, the radon concentrations at the entry points and the radon entry rates also change. However, the undisturbed soil contributes radon to the soil gas in the fill and, hence, to the soil gas entering the house, so that the radon entry rates do not necessarily vary in proportion to the radium content of the fill. When the radium content of the fill is an order of magnitude greater than that of the soil, the total radon entry rate increases by a factor of 2.9 over the base value, with diffusive and convective entry increasing by approximately the same factor; the average sub-slab radon concentration is a factor of 3.2 greater than in the base case. If the radium content of the fill is a factor of 10 less than that of the soil, radon entry is reduced by 19%; the sub-slab concentration is 78% of the base value. The radon entry rate as a function of the relative radium content of the fill is shown in Figure 6.

While the radon entry rates increase with the radium content of the deep soil in both the second and third configurations, the magnitude of the increase is profoundly affected by the depth of the boundary between the low- and high-radium regions. When the boundary is 1 m below the surface, an increase in the relative deep soil radium by a factor of 10 ($C_\infty = 3.7 \times 10^5$ Bq m^{-3}) leads to an increase in radon concentration at the house side of the block wall from 2.4×10^4 to 8.9×10^4 Bq m^{-3} and an increase in the total radon entry rate by a factor of 3.6 over the base rate. When the boundary is 5 m below the surface, the concentration at the block wall is 2.5×10^4 Bq m^{-3} and the total radon entry rate is essentially unchanged. A similar effect is seen when the radium content of the deep soil is a factor of 10 lower than the base value. When the boundary is 1 m deep, the radon entry rate is reduced by a factor of 1.3; when it is 5 m, there is essentially no reduction. Radon entry rates as functions of the relative radium content of the deep soil

for the two cases are shown in Figure 6.

Stratification of the radium content of the soil affects entry rates on both the house and soil sides of the stem wall. If the influence of the high-radium deep soil were limited to the introduction of radon into the air flowing through the high-radium region itself, it would be expected that radon entry rates on the soil side would be unaffected, since air entering the entry points on the soil side does not pass through soil below the level of the stem wall. However, radon produced in the high-radium region diffuses into the low-radium region, increasing concentrations in that region and, hence, entry rates in general. This may be confirmed by examing the consequences of changing the diffusivity. If the radon diffusivity is increased by a factor of 5 throughout the soil and fill, and if the soil below 5 m depth has a radium content a factor of 10 greater than that of the soil above 5 m depth, the predicted radon entry rate is a factor of 1.80 greater than the base rate at the same diffusivity. At the base diffusivity, the factor is 1.05. At very low diffusivity, the factor is 1.00. The effect of the region below 5 m depth on radon entry is due entirely to diffusion. For the high-radium region beginning at 1 m depth, the equivalent factors are 5.8, 3.6, and 1.2, so that both diffusion and the flow of air through the region have an influence on radon entry rates, with diffusion being the more important in this case. In general, the relative importance of diffusion and convection is dependent on the soil permeability.

If the radium content of the concrete slab is reduced to 0.1 of the base value, the total radon entry rate is reduced by just 6%, all of the reduction being in entry through the slab itself. If the radium is increased to 10 times the base value, the total radon entry rate increases by 67%; 75% of the increase is due to increased entry through the slab, with the remainder due to an increase in radon concentration at all entry points. The radium content of the stem wall blocks has a much smaller effect: for radium content ranging from 0.1 to 10 times the base value, the total radon entry rate ranges from 99.6% to 107% of the base rate. The relative unimportance of the stem wall radium is a consequence of the low mass of the concrete block layers.

Diffusivity

Radon entry through the slab is highly dependent on the effective diffusivity of radon in concrete: an increase in the diffusivity from 10^{-9} to 10^{-6} m^2 s^{-1} increases radon entry through the slab from 0.04 to 3.77 Bq s^{-1} (7-700% of the base value). Because entry through the slab is a small fraction of the total entry when the diffusivity is small, the range of the total radon entry rate is 1.89 to 5.15 Bq s^{-1} (81-221% of the base value) for the same range of diffusivities. For the reasons given in the previous section, the radon diffusivity in the stem wall blocks has a much smaller influence on radon entry rates than does that of the slab. For the range of values considered, the total radon entry rate ranges from 99-114% of the base rate.

Increased Pressure in the Stem Wall Interior

When the interior of the stem wall is at less than atmospheric pressure, there is a considerable flow of outside air through the part of the wall that is above the soil surface, in addition to the flow through the below-grade part (Figure 2). For the base

configuration, this flow is 6.2×10^{-3} m^3 s^{-1}, which is a factor of 14 greater than the total flow of soil gas into the house. If there is a small gap between the edge of the slab and the outer (soil side) layer of the stem wall, *i.e.*, a flow restriction between the stem wall interior and the house, the pressure drop will cause the pressure in the stem wall interior to be greater (*i.e.*, less negative) than that in the house, so that the driving force of soil gas and radon entry through the stem wall, wall-footer gaps, and wall-slab gap will be diminished. (If air is permitted to flow vertically through the soil side of the stem wall, the flow restriction may be bypassed. In the model, we have used a no-flow boundary condition at the top of the soil side of the stem wall; in practice, sealing of this area may be necessary to prevent vertical flow.) For gap widths less than 0.008 m, the pressure on the house side of the stem wall is less than that in the interior, so that soil gas may flow through the concrete blocks without entering the house and radon entry rates through the stem wall are uncertain. At a gap width of 0.005 m, the total radon entry rate is 50% of the base rate or less, and the entry rate through the stem wall is 5% of the base rate or less, so that almost all of the radon entry is through the slab or the slab opening. The pressure drop across the gap is 2.2 Pa or 92% of the house depressurization. At a (perhaps more realistic) gap width of 0.001 m, the pressure drop is 58% of the house pressure, the radon entry rate through the stem wall is 54% of the base value, and the total radon entry rate is 79% of the base value.

It is possible to bring the interior stem wall pressure even closer to atmospheric by increasing the permeability of the above-surface part of the soil side of the stem wall. If the remaining parts of the wall are maintained at low permeability, the radon entry rate through the wall may be greatly diminished. For the base configuration, with a house-stem wall gap of 0.001 m, an above-surface wall permeability of 10^{-9} m^2, and the remainder of the wall of permeability 10^{-12} m^2, the pressure drop is 2.2 Pa (92% of base), the total radon entry rate is 1.14 Bq s^{-1} (49% of base), and the entry rate through the stem wall is just 0.07 Bq s^{-1} (4% of base). These values are similar to those obtained for the 0.0005 m gap with the stem wall retaining its base permeability.

Summary and Discussion

The model predicts that the radon entry rate into a house of the type considered here will be low or moderate unless the slab, soil, or backfill radium content is high or there is a high permeability path within the soil between the soil surface and the backfill.

We used the model to assess the dependence of radon entry on a variety of changes to the design or construction of the house's substructure, for example sealing various cracks, filling the stem wall with concrete, or decreasing the permeability of the stem wall. Most design or construction changes had little effect on the radon entry rate because reductions in radon entry through one pathway were offset by increased radon entry elsewhere. However, two types of structural changes each reduced the radon entry rate by at least two thirds and, therefore, are worthy of further consideration. In the first case, all openings in the vicinity of the stem wall, including the permeable blocks, are

eliminated. This might be accomplished by constructing a one-piece concrete footer, stem wall, and slab assuming that cracks do not develop near the stem wall. This type of substructure is sometimes used in Florida. In the second case, the stem wall of permeable concrete blocks is retained but the pressure within the stem wall is increased (thus decreasing radon entry) by: (1) decreasing the permeability of all sections of stem wall that contact soil or fill, possibly by application of a coating; (2) maintaining a high permeability in the remaining above- grade section of stem wall; (3) sealing the top of the soil side of the stem wall at the level of the soil surface; and (4) virtually eliminating the normally-large gap between the edge of the slab and the outer layer of the stem wall. We are unsure of the practicality of this second option.

We also examined the dependence of radon entry rate on soil and backfill permeability. The permeability of both materials has a large impact on the radon entry rate. The permeability of the soil cannot be changed, but low-permeability backfill could be emplaced beneath the slab. The predicted radon entry rate decreases by 81% when the permeability of the fill is decreased from 4×10^{-11} m^2 to 10^{-12} m^2 and convective radon entry is essentially eliminated by a backfill permeability of 10^{-15} m^2. This option should be considered further; however, we suspect that cracks in the backfill or gaps at the junction of the backfill and either the stem wall or substructural plumbing could develop and seriously compromise the effectiveness of the low permeability layer in inhibiting radon entry.

The dependence of radon entry on the radium content of the backfill and soil is the final important relationship examined. If the soil and fill are identical and homogeneous, the convective radon entry rate scales linearly with the radium content. However, increasing or decreasing the radium content of the fill has little impact on radon entry unless the fill's radium content is increased to more than three times the base case value. Consequently, efforts to obtain fill material with an unusually low radium content are probably not warranted unless the thickness of the fill is considerably greater than in our model. An increase in the radium content of the soil with depth is important if the high-radium soil is not too far below the slab. For example, a factor of ten increase in the radium content of all soil located one meter or more below the slab results in an increase in radon entry by a factor of 3.6. When the high radium soil starts at a depth of five meters below the slab, the radon entry rate increases insignificantly. The increases are due partly to radon diffusion from deeper layers into shallower ones, including the backfill, followed by convective flow of this radon into the house. The practical implication is that one need not be overly concerned about the effects of deep soil on radon entry into this type of house.

All results presented in this paper are predictions of a numerical model that does not include the superstructure of the house and has not yet been validated. We expect that the model appropriately indicates the relative magnitude of the dependence of radon entry rate on the different factors. However, the determination of the fraction of the radon entering the interior of the stem wall that actually enters the living space of the house and the validation of the model using well-characterized experimental structures remain to be done. Model validation is now being carried out by the Florida Radon

Research Program.

Acknowledgments

This work was supported by the U.S. Environmental Protection Agency (EPA) through Interagency Agreement DW89934620-0 with the U.S. Department of Energy (DOE). This work was also supported by the Assistant Secretary for Conservation and Renewable Energy, Office of Building Technologies, Building Systems and Materials Division and by the Director, Office of Energy Research, Office of Health and Environmental Research of DOE under contract DE-AC03-76SF00098. Although the research described here is partially supported by the EPA, it has not been subjected to EPA review and therefore does not necessarily reflect the views of EPA, and no official endorsement by EPA should be inferred.

References

Acres International Corporation (1990). Radon Entry Through Cracks in Slabs-on-Grade, Vol. 2, Sealants for Cracks and Openings in Concrete Slabs-On-Grade. Acres Report P09314. Amherst, NY.

Baker, P.H., Sharples, S., Ward, I.C. (1989). Air Flow Through Cracks. *Building and Environment*, **22(4)**, 293-304.

Dixon, R.W. (1990), State of Florida, Dept. of Community Affairs, Tallahassee, FL., personal communication.

DSMA Atcon Ltd. (1983). Review of Existing Instrumentation and Evaluation of Possibilities for Research and Development of Instrumentation to Determine Future Levels of Radon at a Proposed Building Site. Report INFO-0096. Atomic Energy Control Board, Ottawa, Canada.

Feustel, H.E. and Sherman, M.H. (1989). A Simplified Model for Predicting Air Flow in Multizone Structures. *Energy and Buildings*, **13**, 217-230.

Fisk, W.J., Flexser, S., Gadgil, A.J., Holman, H.-Y., Modera, M.P., Narasimhan, T.N., Nuzum, T., Revzan, K.L., Sextro, R.G., Smith, A.R., Tsang, Y.W., and Wollenberg, H.A. (1989). Monitoring and Modeling for Radon Entry into Basements: A Status Report for the Small Structures Project. Lawrence Berkeley Laboratory Report LBL-27962.

Garbesi, K., Sextro, R.G. (1990). Modeling and Field Evidence of Pressure-Driven Entry of Soil Gas into a House through Permeable Below-Grade Walls. *Environ. Sci. Technol.*, **23**, 1481-1487.

Geomet Technologies Inc. (1988). Florida Statewide Radiation Survey. Geomet Report IE-1808. Germantown, MD.

Loureiro, C. d'O. (1987). Simulation of the Steady-State Transport of Radon from Soil into Houses with Basements under Constant Negative Pressure. Lawrence Berkeley Laboratory Report LBL-24378. Berkeley, CA.

Loureiro, C.O., Abriola, L.M., Martin, J.E., and Sextro, R.G. (1990). Three Dimensional Simulation of Radon Transport into Houses Under Constant Negative Pressure. *Environ. Sci. Technol.* **24**, 1338-1348.

Narasimhan, T.N., Tsang, Y.W. and Holman, H.Y. (1990). On the Potential Importance of Transient Air Flow in Advective Radon Entry Into Buildings. *Geophysical Research Letters* **17**, 821-824.

Nazaroff, W.W., Moed, B.A. and Sextro, R.G. (1988). Soil as a Source of Indoor Radon: Generation, Migration, and Entry. In *Radon and Its Decay Products Indoors*, Nazaroff, W.W. and Nero, A.V., eds., pp 57-112. Wiley, New York.

Nero, A.V. and Nazaroff, W.W. (1984). Characterizing the Source of Radon Indoors. *Radiation Protection Dosimetry* **7**, 23-29.

Nielson, K.K. and Rogers, V.C. (1990). Correlation of Florida Soil-Gas Permeabilities with Grain Size, Moisture, and Porosity. Rogers and Associates Report RAE-8945-1. Salt Lake City, UT.

Pugh, T.D. (1990), Florida A & M University, Tallahassee, FL., personal communication.

Revzan, K.L., Turk, B.H., Harrison, J., Nero, A.V., and Sextro, R.G. (1988). Parametric Modelling of Temporal Variations in Radon Concentrations in Homes. *IEEE Trans Nucl Sci* **35(1)**, 550-555.

Revzan, K.L. (1989). Radon Entry, Distribution, and Removal in Two New Jersey Houses with Basements. Lawrence Berkeley Laboratory Report LBL-26830. Berkeley, CA.

Revzan, K.L., Fisk, W.J., and Gadgil, A.J. (1990). Modeling Radon Entry into Houses with Basements: Model Description and Validation. *Indoor Air,* **2**, 173-189.

Roessler, C.E., Smith, D.L., Bolch, W.E., Hintenlang, D.E., and Furman, R.A. (1990). Gas Permeabilities and Radon Content of Florida Fill Materials and Soils. University of Florida Report, Gainesville, FL.

Sanchez, D.C., Dixon, R., and Williamson, A.D. (1990). The Florida Radon Research Program: Systematic Development of a Basis for Statewide Standards. Presented at the 1990 International Symposium on Radon and Radon Reduction Technology, Atlanta, GA., Paper A-I-3, and to be published in the proceedings. U.S. EPA.

Scott, A.G. and Findlay, W.O. (1983). Demonstration of Remedial Techniques Against Radon in Houses on Florida Phosphate Lands. Report EPA 520/5-83-009, U.S. EPA, Montgomery, AL.

Sherman, M.H., Grimsrud, D.T., and Diamond, R.C. (1979). Infiltration-Pressurization Correlation: Surface Pressures and Terrain Effects. Lawrence Berkeley Laboratory Report LBL-8785.

Zapalac, G.H. (1983). A Time-Dependent Method for Characterizing the Diffusion of Radon-222 in Concrete. *Health Phys.*, **45(2)**, 377-283.

Table 1. Values of certain parameters in the base configuration.

Material	Permeability (m^2)	Bulk Diffusivity ($m^2\ s^{-1}$)	Pore Space Radon Concentration* ($Bq\ m^{-3}$)	Porosity
Gaps and openings		1.2×10^{-5}		
Concrete slab and footer		10^{-8}	3.7×10^{4}	0.2
Concrete blocks of stem wall	10^{-10}	10^{-8}	3.7×10^{4}	0.2
Backfill	4×10^{-11}	10^{-6}	3.7×10^{4}	0.5
Undisturbed soil	10^{-11}	10^{-6}	3.7×10^{4}	0.5

* Far from surfaces

Table 2. For the base configuration, as described in the text, the fractions of the air and diffusive, convective, and total radon entry rates for each of the areas described in the text. The convective entry rate is defined to be the difference between the total entry rates with and without a pressure field. The radon concentration given is the average at the soil side of the entry area, as a fraction of C_∞; the concentrations at the interior of the stem wall and the basement side of the slab are zero.

Entry Point	Fraction of soil gas Entry	Radon concen-tration	Fraction of radon entry (diffusive)	Fraction of radon entry (convective)	Fraction of radon entry (total)
House side of stem wall, top gap	9.6×10^{-4}	0.11	1.5×10^{-1}	5.1×10^{-2}	1.0×10^{-1}
House side of stem wall, side of block	6.2×10^{-2}	0.64	1.2×10^{-1}	4.6×10^{-1}	2.9×10^{-1}
House side of stem wall, bottom gap	9.9×10^{-4}	0.12	1.6×10^{-1}	4.9×10^{-2}	1.1×10^{-1}
Soil side of stem wall, side of block	9.0×10^{-1}	0.01	7.9×10^{-3}	2.3×10^{-1}	1.2×10^{-1}
Soil side of stem wall, bottom gap	1.6×10^{-2}	0.02	2.7×10^{-2}	9.6×10^{-3}	1.8×10^{-2}
Footer			1.3×10^{-2}	4.0×10^{-4}	6.6×10^{-3}
Slab opening	1.8×10^{-2}	0.70	9.0×10^{-2}	1.7×10^{-1}	1.3×10^{-1}
Slab		0.77	4.3×10^{-1}	2.3×10^{-2}	2.3×10^{-1}

Table 3. The parameters, the range of values of each parameter, and the ranges of total soil-gas and radon entry rates that result from variation of each parameter. The values of parameters other than the one varied are those of the base configuration, as described in the text. A key to the appendix figures is given in the last column.

Parameter	Range of Parameter	Soil-Gas Entry Rates ($m^3\ s^{-1}$)	Radon Entry Rates ($Bq\ s^{-1}$)	Appendix Figures
(Base)	-	4.5×10^{-4}	2.33	
Soil permeability	$10^{-12} - 10^{-9}\ m^2$	$4.0 \times 10^{-4} - 1.0 \times 10^{-3}$	1.48 – 13.4	A1S, A1C, A1R
Soil permeability (fill permeability $10^{-9}\ m^2$)	$10^{-12} - 10^{-9}\ m^2$	$3.3 \times 10^{-3} - 6.1 \times 10^{-3}$	1.59 – 44.4	A2S, A2C, A2R
Soil permeability (fill permeability $10^{-12}\ m^2$)	$10^{-12} - 10^{-9}\ m^2$	$5.0 \times 10^{-8} - 5.0 \times 10^{-8}$	1.20 – 1.20	
Soil permeability (slab opening only)	$10^{-12} - 10^{-9}\ m^2$	$3.9 \times 10^{-6} - 3.3 \times 10^{-5}$	0.97 – 1.90	A3S, A3C. A3R
Soil permeability (concrete-filled stem wall)	$10^{-12} - 10^{-9}\ m^2$	$4.6 \times 10^{-6} - 9.1 \times 10^{-5}$	0.70 – 1.70	A4S, A4C. A4R
Soil permeability of 0.4-1.4 m layer	$10^{-12} - 10^{-9}\ m^2$	$4.0 \times 10^{-4} - 9.5 \times 10^{-4}$	1.61 – 7.59	A5S, A5C, A5R
Soil permeability of 0.9-1.9 m layer	$10^{-12} - 10^{-9}\ m^2$	$4.3 \times 10^{-4} - 5.1 \times 10^{-4}$	1.72 – 3.90	A6S, A6C, A6R
Fill permeability	$10^{-15} - 10^{-9}\ m^2$	$5.0 \times 10^{-8} - 3.3 \times 10^{-3}$	1.20 – 2.66	A7S, A7C, A7R
Fill permeability (concrete-filled stem wall)	$10^{-15} - 10^{-9}\ m^2$	$3.3 \times 10^{-9} - 4.9 \times 10^{-5}$	0.66 – 1.20	A8S, A8C, A8R
Fill permeability (slab opening only)	$10^{-15} - 10^{-9}\ m^2$	$8.3 \times 10^{-10} - 4.5 \times 10^{-5}$	0.89 – 2.28	A9S, A9C, A9R
Soil side fill permeability	$10^{-15} - 10^{-9}\ m^2$	$3.9 \times 10^{-5} - 3.3 \times 10^{-3}$	2.11 – 2.33	A10S, A10R
Stem wall permeability	$10^{-15} - 10^{-9}\ m^2$	$8.3 \times 10^{-5} - 5.2 \times 10^{-4}$	1.93 – 2.35	A11S, A11R
House-side stem wall permeability	$10^{-15} - 10^{-9}\ m^2$	$4.5 \times 10^{-4} - 4.5 \times 10^{-4}$	2.11 – 2.34	A12S, A12R
Soil-side stem wall permeability	$10^{-15} - 10^{-9}\ m^2$	$8.9 \times 10^{-5} - 5.2 \times 10^{-4}$	2.17 – 2.34	A13S, A13R
Stem wall (concrete-filled) permeability	$10^{-15} - 10^{-9}\ m^2$	$2.9 \times 10^{-5} - 3.1 \times 10^{-5}$	0.97 – 0.95	A14S, A14R
Stem wall permeability (no wall-footer gaps)	$10^{-15} - 10^{-9}\ m^2$	$2.9 \times 10^{-5} - 5.2 \times 10^{-4}$	1.65 – 2.25	A15S, A15R
Slab opening width	$10^{-3} - 10^{-1}$ m	$4.5 \times 10^{-4} - 4.5 \times 10^{-4}$	2.28 – 2.67	A16S, A16R
Slab opening distance from center	0 – 7 m	$4.5 \times 10^{-4} - 4.5 \times 10^{-4}$	2.21 – 2.27	A17S, A17R
Water table depth	0.5 – 10 m	$4.3 \times 10^{-4} - 4.5 \times 10^{-4}$	1.63 – 2.33	A18S, A18C, A18R
Radium concentration of fill*	0.1 – 10	4.5×10^{-4}	1.89 – 6.70	A19C, A19R
Radium concentration of soil below 1 m*	0.1 – 10	4.5×10^{-4}	1.73 – 8.36	A20C, A20R
Radium content of soil below 5 m*	0.1 – 10	4.5×10^{-4}	2.30 – 2.45	A21C, A21R
House to stem wall interior gap width	0.0005 – 0.004 m	$4.6 \times 10^{-5} - 4.4 \times 10^{-4}$	1.17 – 2.31	A22S, A22C, A22R
Effective radon diffusivity (slab)	$10^{-9} - 10^{-6}\ m^2\ s^{-1}$	4.5×10^{-4}	1.89 – 5.15	A23C, A23R
Radium concentration of slab*	0.1 – 10	4.5×10^{-4}	2.18 – 3.89	A24C, A24R
Effective radon diffusivity (stem wall)	$10^{-9} - 10^{-6}\ m^2\ s^{-1}$	4.5×10^{-4}	2.31 – 2.66	A25C, A25R
Radium concentration of stem wall*	0.1 – 10	4.5×10^{-4}	2.32 – 2.49	A26R

*Relative to the remainder of the soil and/or fill

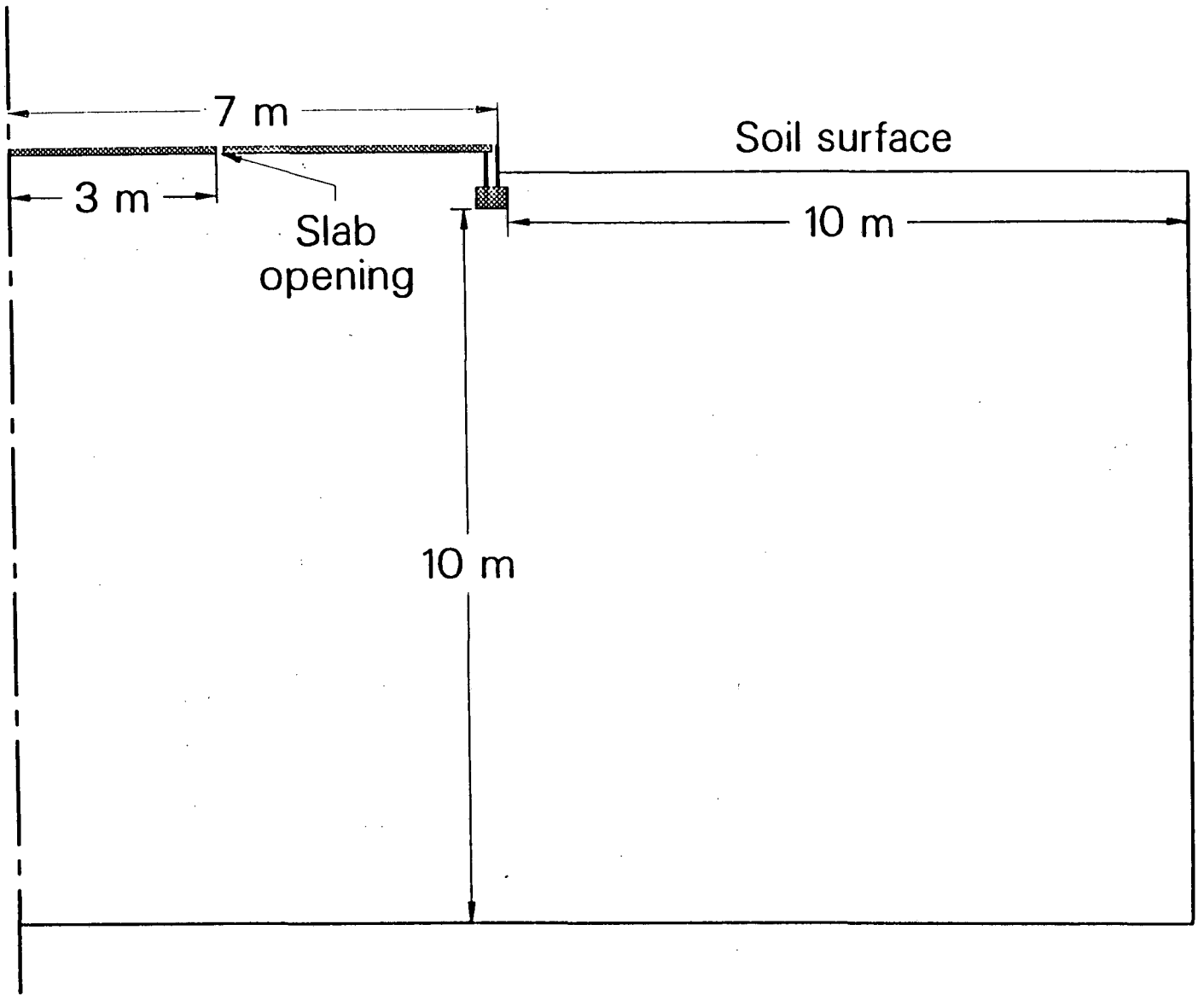

Figure 1.
Vertical cross-section of the region modeled; the shaded areas are the stem wall concrete blocks, the slab, and the footer. The dimensions are those of the base configuration, as described in the text. The slab opening is shown exaggerated; its width, in the base configuration, is 0.003 m.

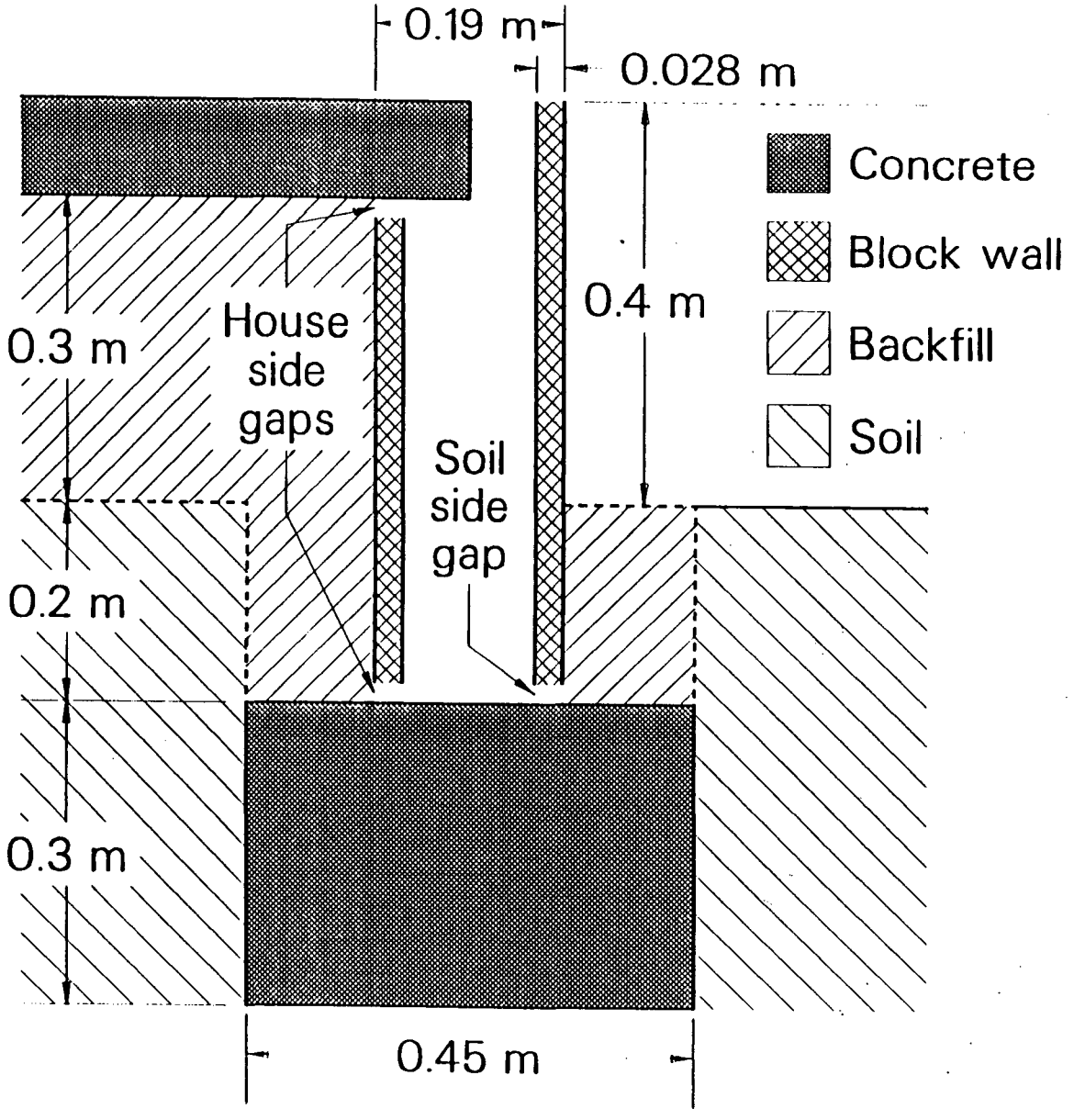

Figure 2.
Detail of the vertical cross-section of the region modeled, showing the footer, stem wall, and part of the slab. The dimensions are those of the base configuration, as described in the text. The three gaps are shown exaggerated; their widths, in the base configuration, are each 0.003 m.

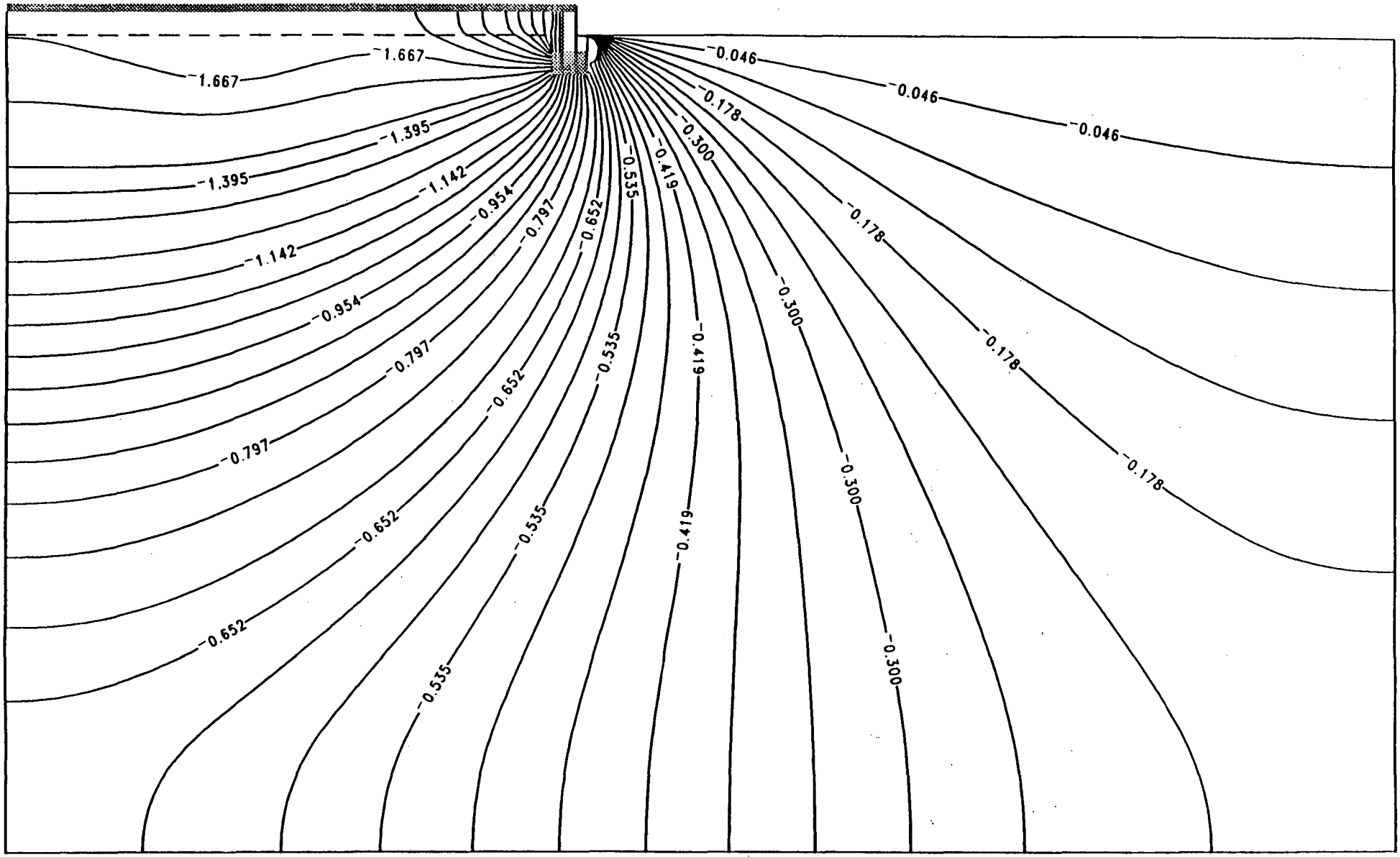

Figure 3.
Isobars for the base configuration, as described in the text. The regions above the slab and inside the hollow stem wall are 2.4 Pa below atmospheric pressure. The limits of the backfill are shown dashed. The pressure gradient very near the right (soil side) of the stem wall is too steep to be shown.

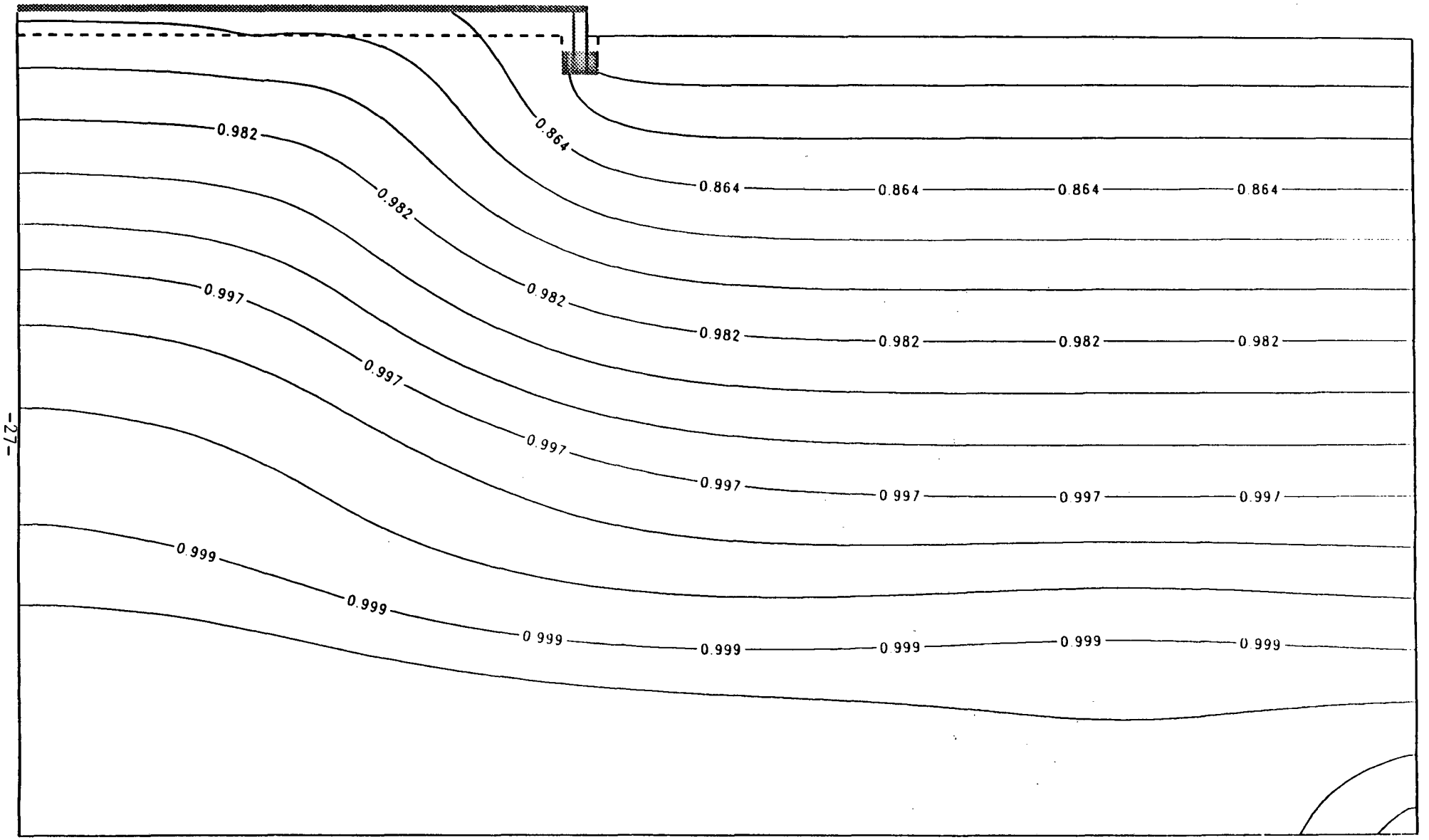

Figure 4.
Isopleths for the base configuration, as described in the text.
The field is shown normalized by C_∞.

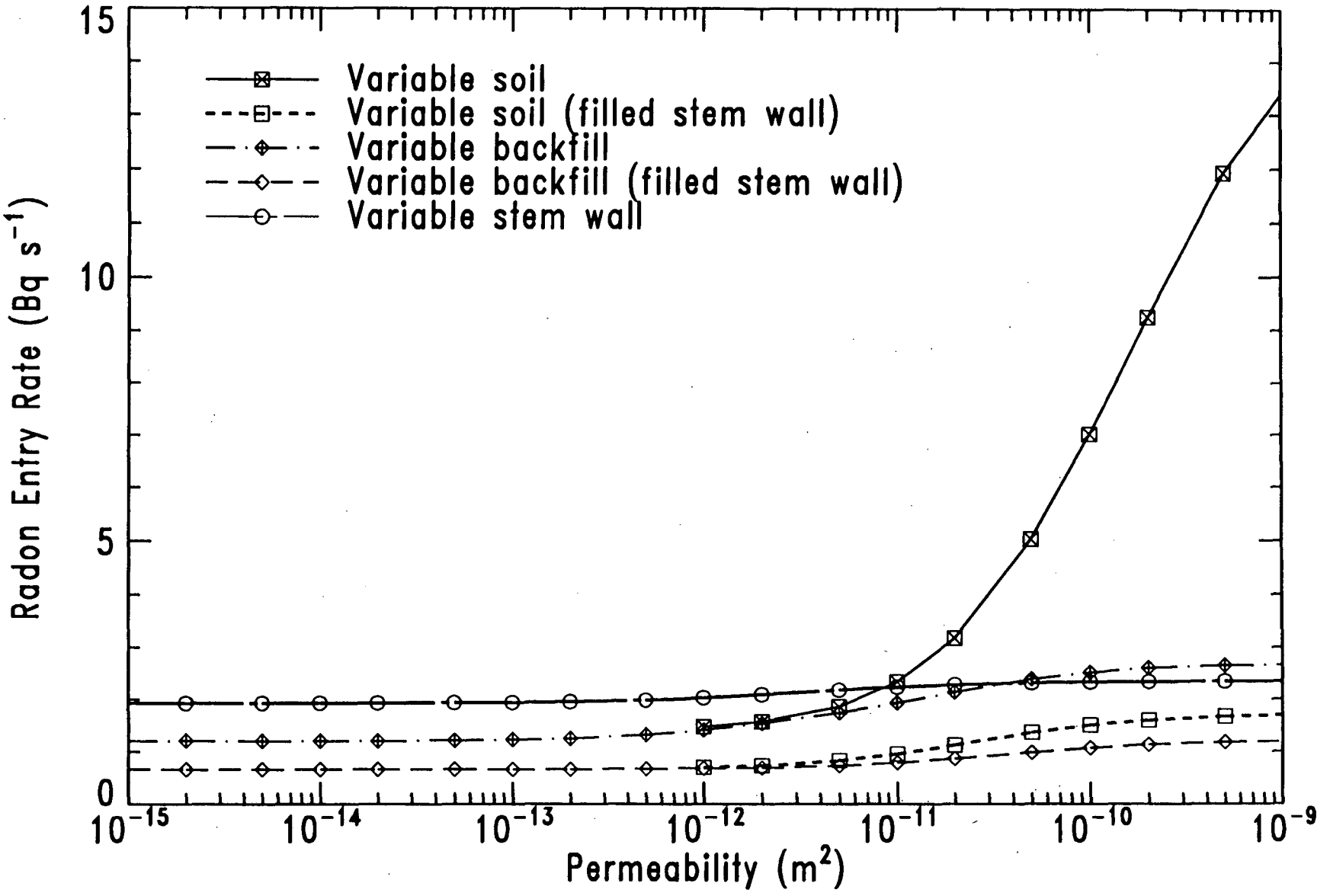

Figure 5.
Convective radon entry rates resulting from variations in the soil and backfill permeabilities for unfilled and concrete-filled stem walls, and by variations in the stem wall permeability for an unfilled stem wall.

09/30/91 14:24:46

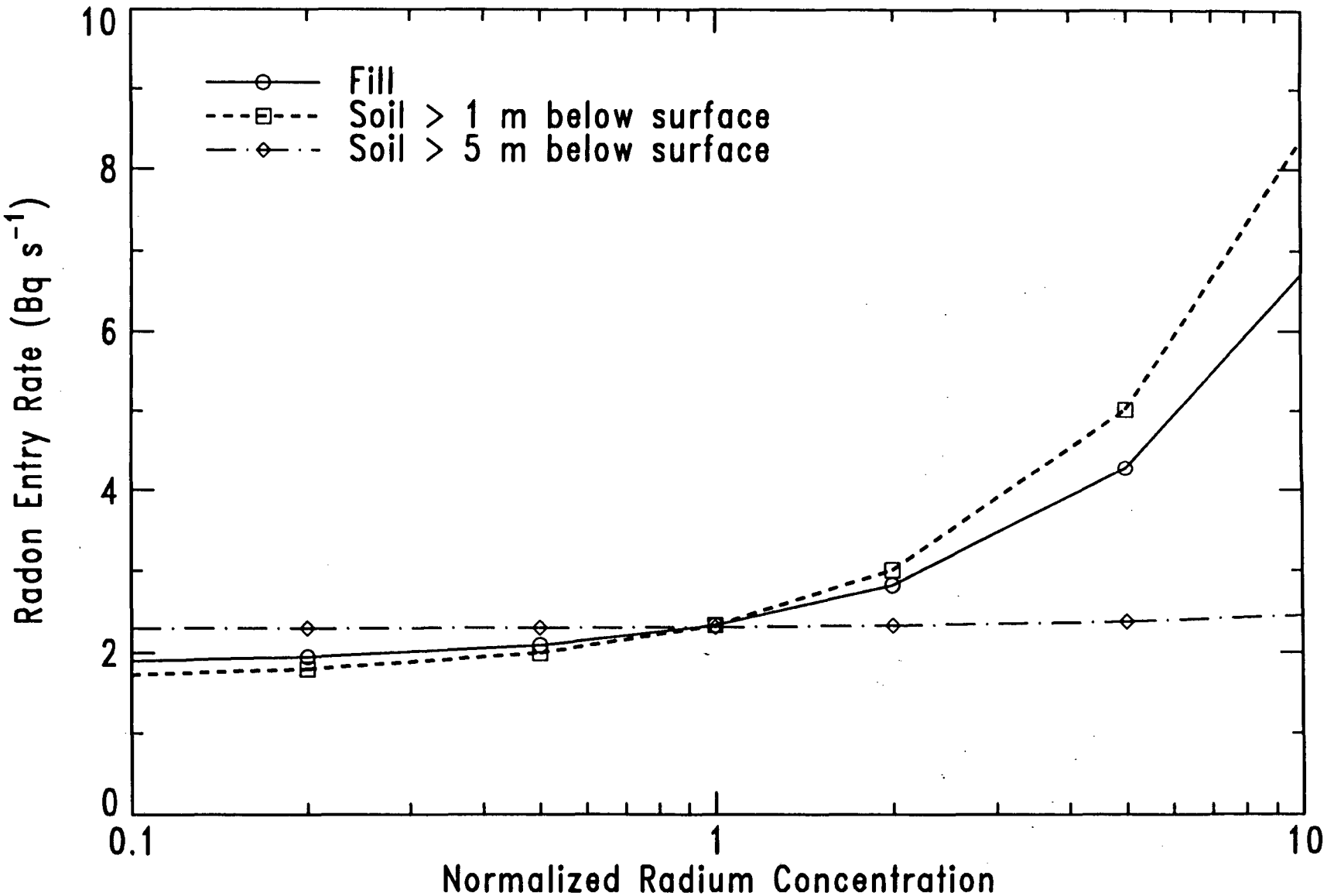

Figure 6.
Convective radon entry rates resulting from variations in the radium content of the fill, the soil at depth greater than 1 m below the surface, and the soil at depth greater than 5 m.

Appendix

This appendix consists of a number of figures in which the soil-gas entry rate, the radon concentration, or the radon entry rate is plotted against one of the parameters listed in the first column of Table 2 of the text. Soil-gas entry rate plots are provided for each of the cases listed in Table 2, except for the case of variable soil permeability with low-permeability fill, for which the entry rates are essentially constant, and the seven cases of variable radium or diffusivity, for which the soil-gas entry rates are unaffected. In most cases, seven curves are provided for each figure: these represent the total entry rate and the entry rates through the permeable house- and soil-side stem wall layers, the upper and lower gaps on the house side of the stem wall, the lower gap on the soil side of the stem wall, and the opening in the slab. In the cases where all entry except through the slab opening has been excluded, there is just a single curve. In the cases where a concrete-filled stem wall has been modeled, there are just three curves, since there is no entry through the wall-footer gaps or the stem wall layers. In the single case where it has been assumed that the wall-footer gaps are completely closed, there are five curves. The entry of outside air through the above-grade part of the soil-side stem wall is not represented.

Radon concentration plots show the average concentration over the soil side of each of the entry areas. The plots have not been provided only for those cases where there is significant variation in the concentration at one or more entry points. In addition to the curves shown on the soil-gas figures, there is one for the concrete slab, for which there is no soil gas entry; there is no curve corresponding to the total entry rate. The concentration is shown normalized by C_∞ (= 3.7×10^4 Bq m^{-3}); in the cases of variable radium, the normalized concentration can be greater than unity.

Radon entry rate plots are provided for all cases except that of variable soil permeability with low-permeability fill. In addition to the curves shown on the soil-gas figures, there is one showing entry through concrete slab. The entry rates given are based on a C_∞ of 3.7×10^4 Bq m^{-3}.

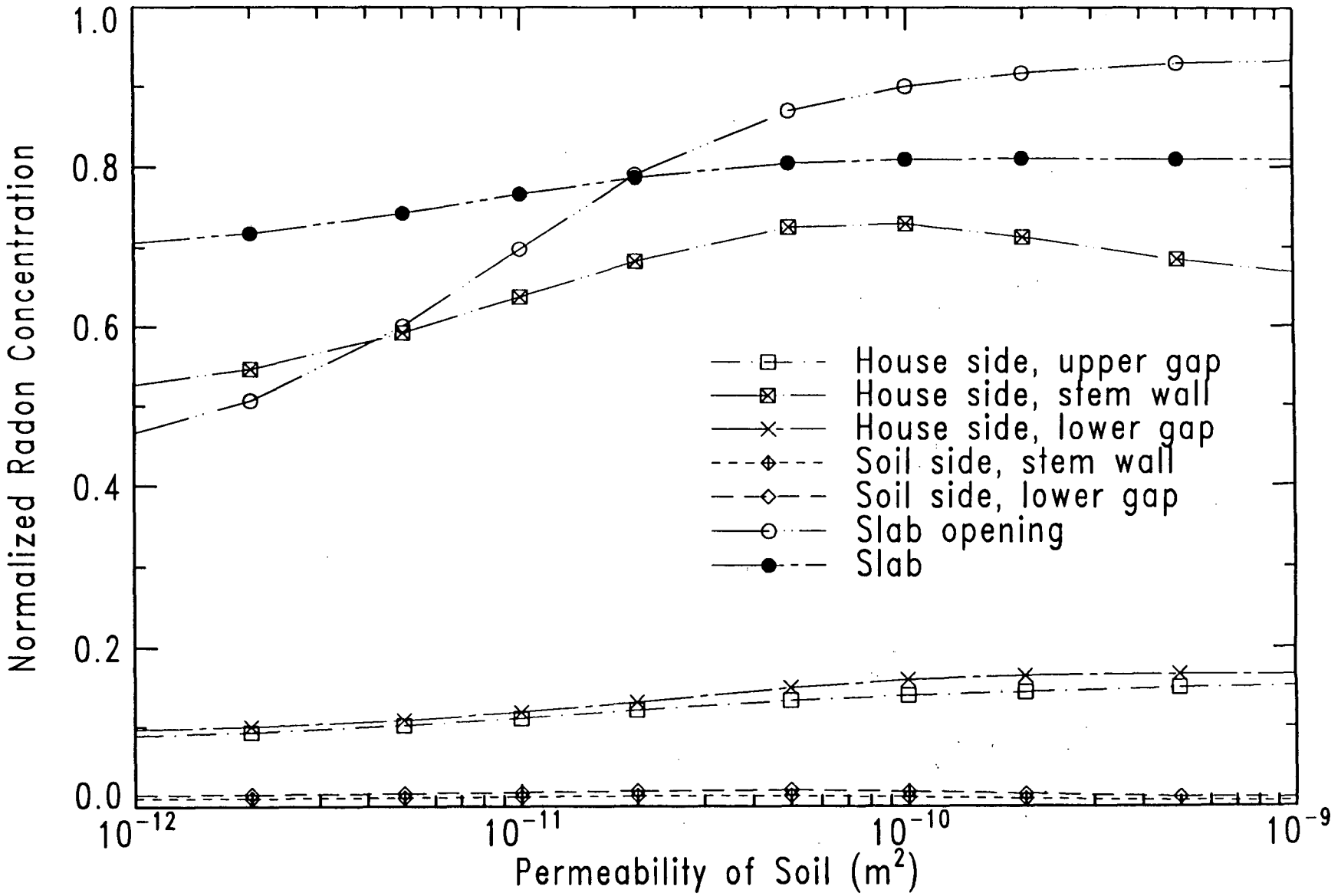

Figure A1C.
Normalized radon concentrations at the several entry points, with the soil permeability as parameter.

10/03/91 10:46:42

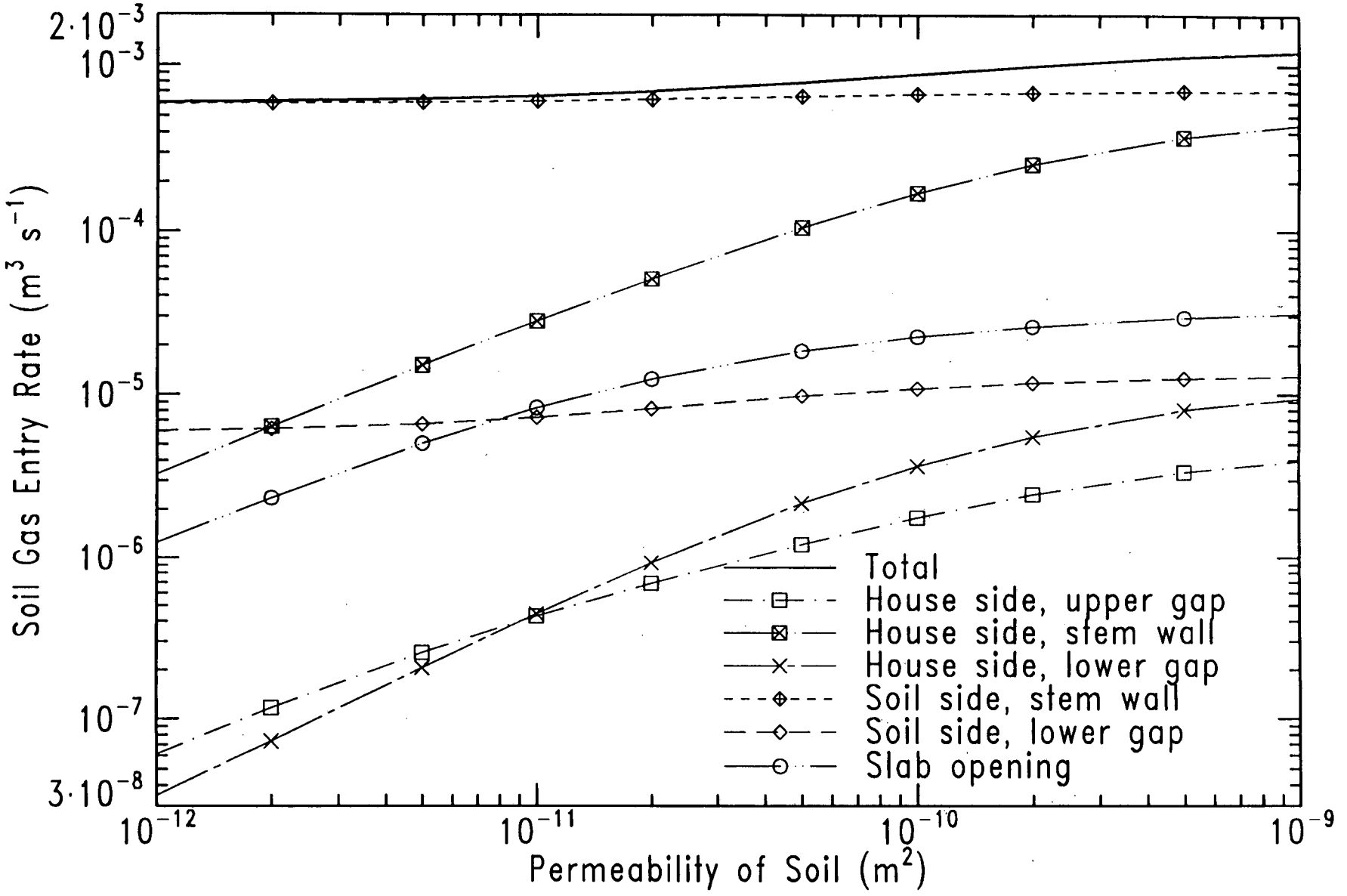

Figure A1S.
Soil-gas entry rates at the several entry points,
with the soil permeability as parameter.

10/03/91 10:38:07

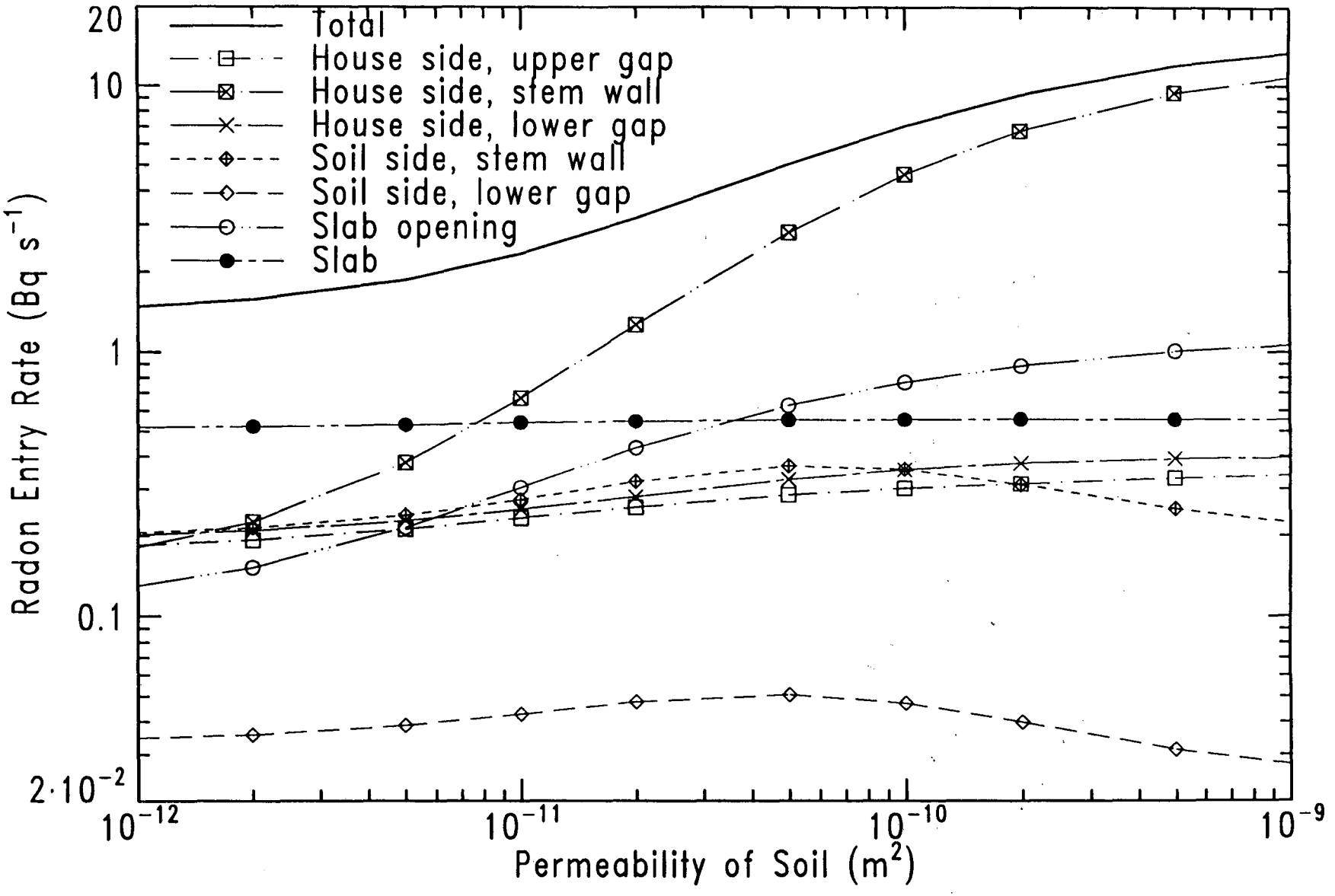

Figure A1R.
Radon entry rates at the several entry points,
with the soil permeability as parameter.

10/03/91 11:13:39

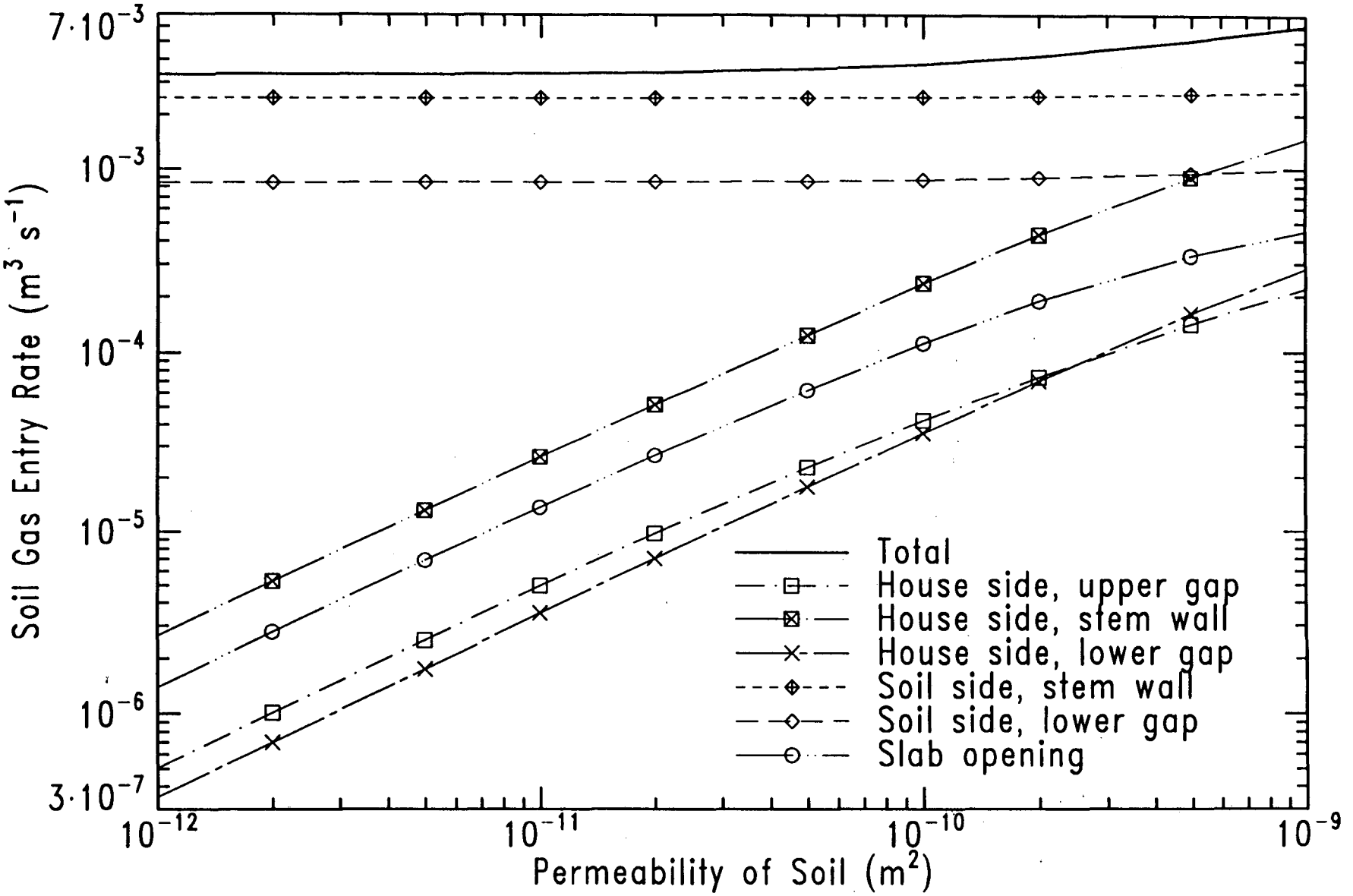

Figure A2S.
Soil-gas entry rates at the several entry points,
with the soil permeability as parameter
(backfill permeability 10^{-9} m^2).

10/03/91 11:09:38

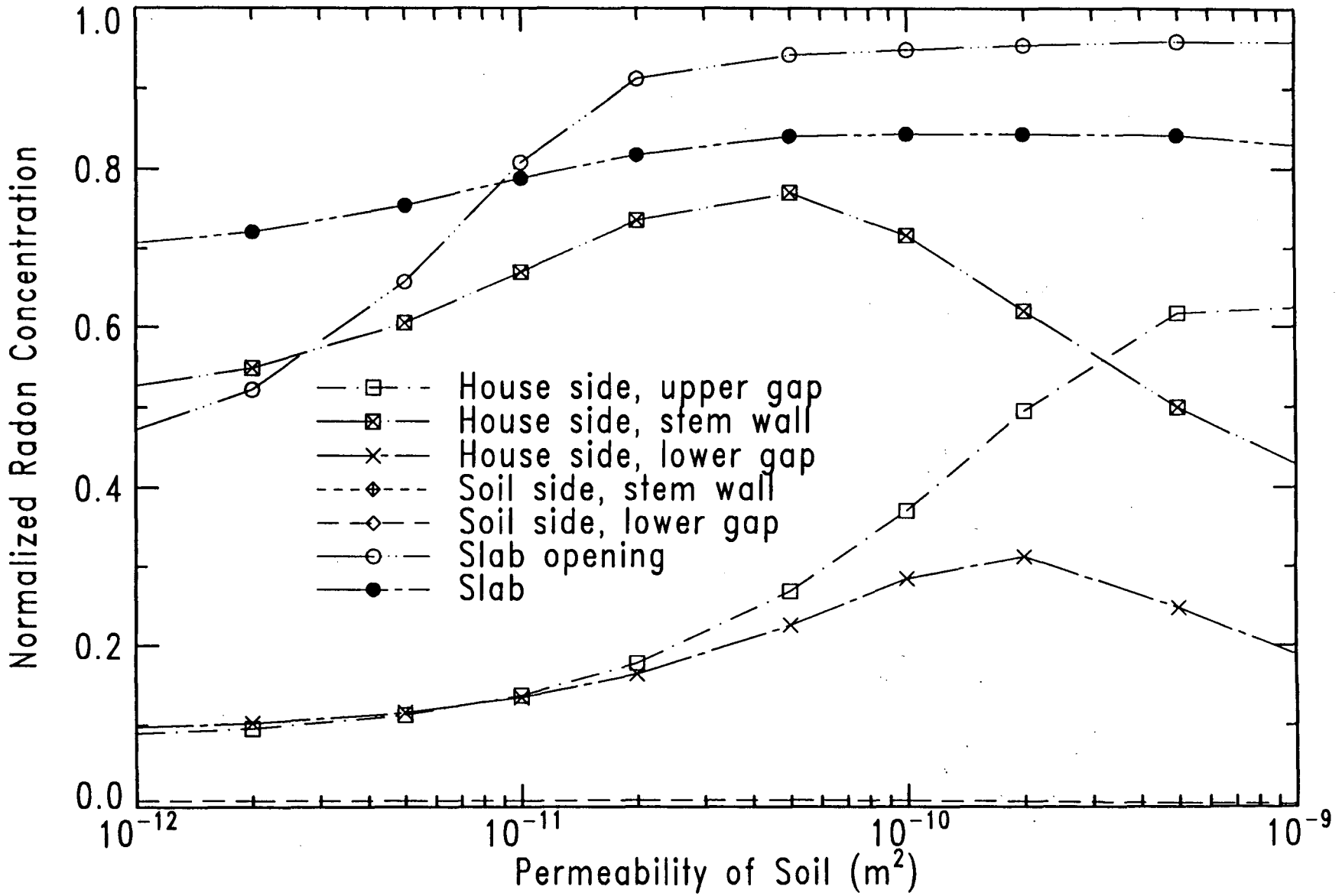

Figure A2C.
Normalized radon concentrations at the several entry points, with the soil permeability as parameter (backfill permeability 10^{-9} m^2).

10/03/91 11:19:09

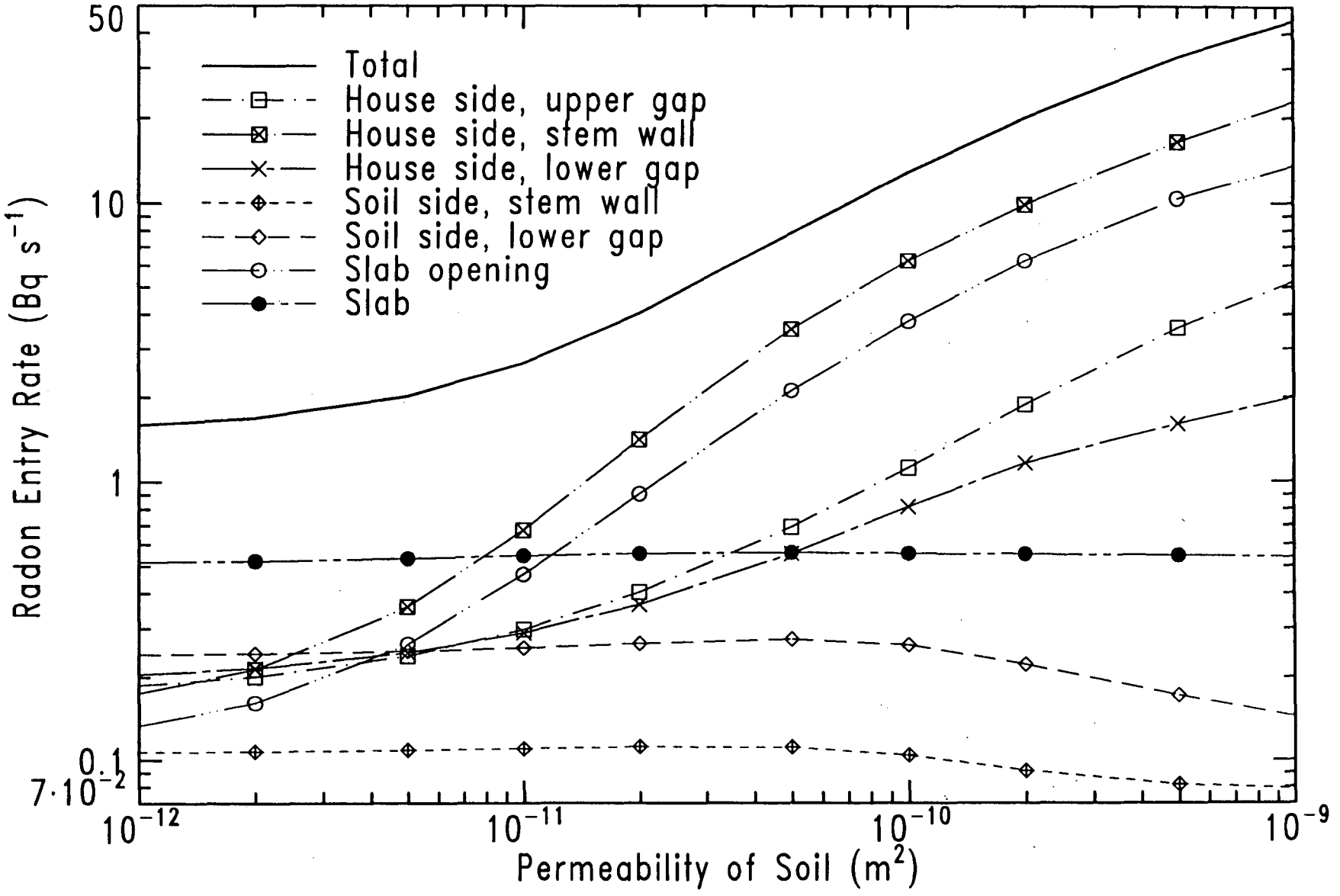

Figure A2R.
Radon entry rates at the several entry points,
with the soil permeability as parameter
(backfill permeability 10^{-9} m^2).

10/03/91 11:20:53

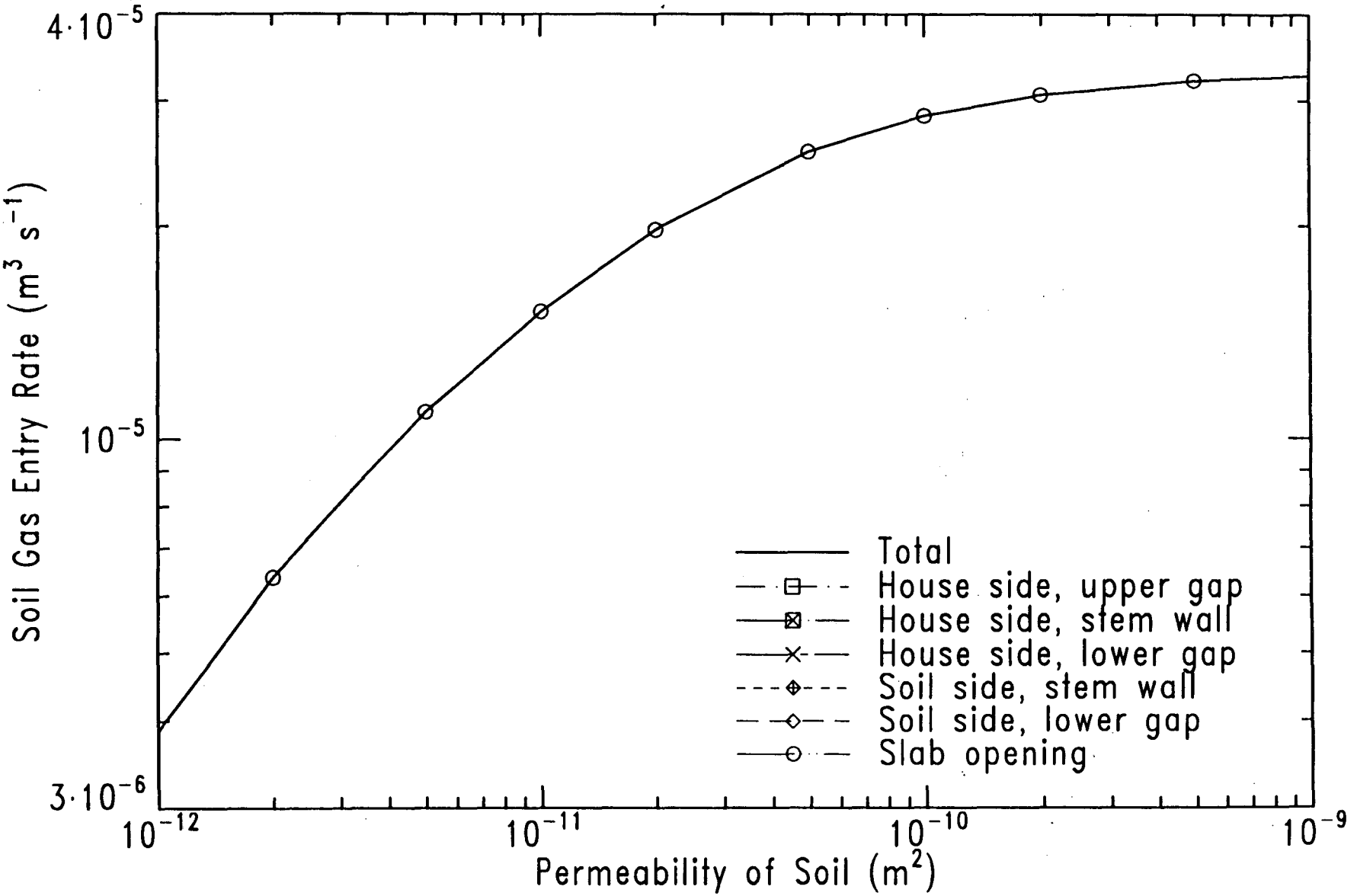

Figure A3S.
Soil-gas entry rates at the several entry points,
with the soil permeability as parameter
(no entry except at the opening in the slab).

10/03/91 10:38:18

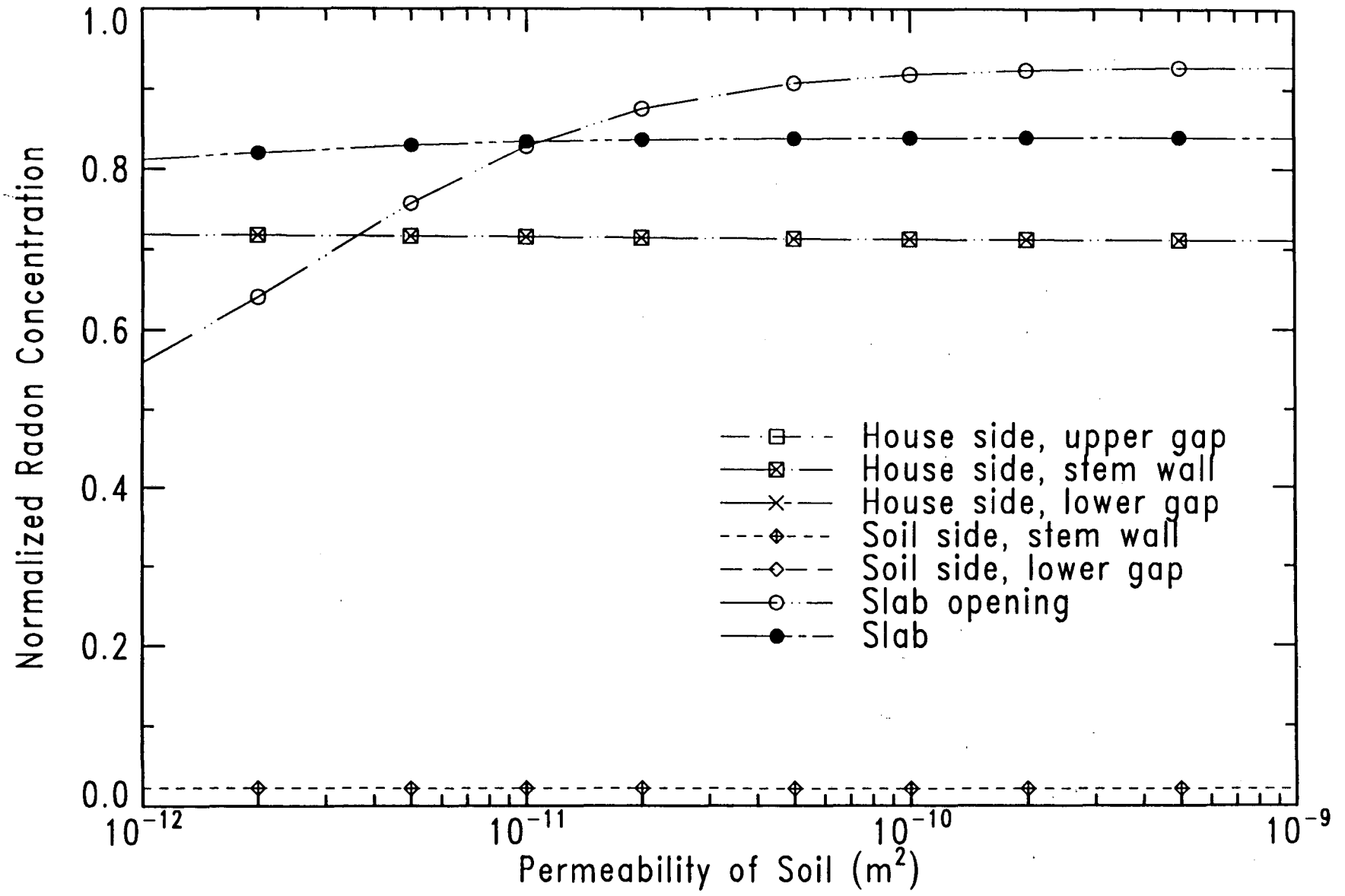

Figure A3C.
Normalized radon concentrations at the several entry points,
with the soil permeability as parameter
(no soil-gas entry except at the opening in the slab).

10/03/91 10:46:53

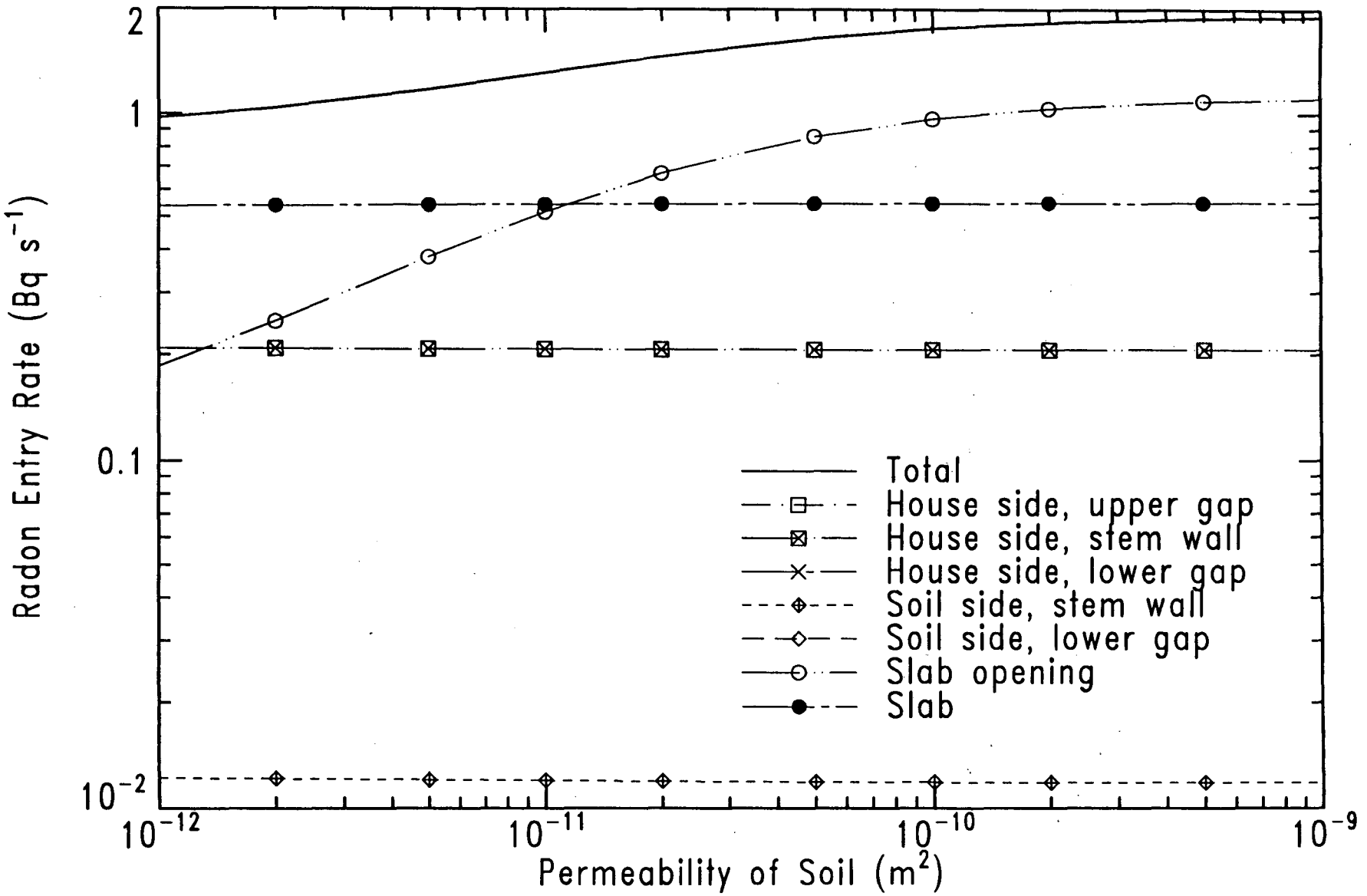

Figure A3R.
Radon entry rates at the several entry points,
with the soil permeability as parameter
(no soil-gas entry except at the opening in the slab).

10/03/91 11:13:53

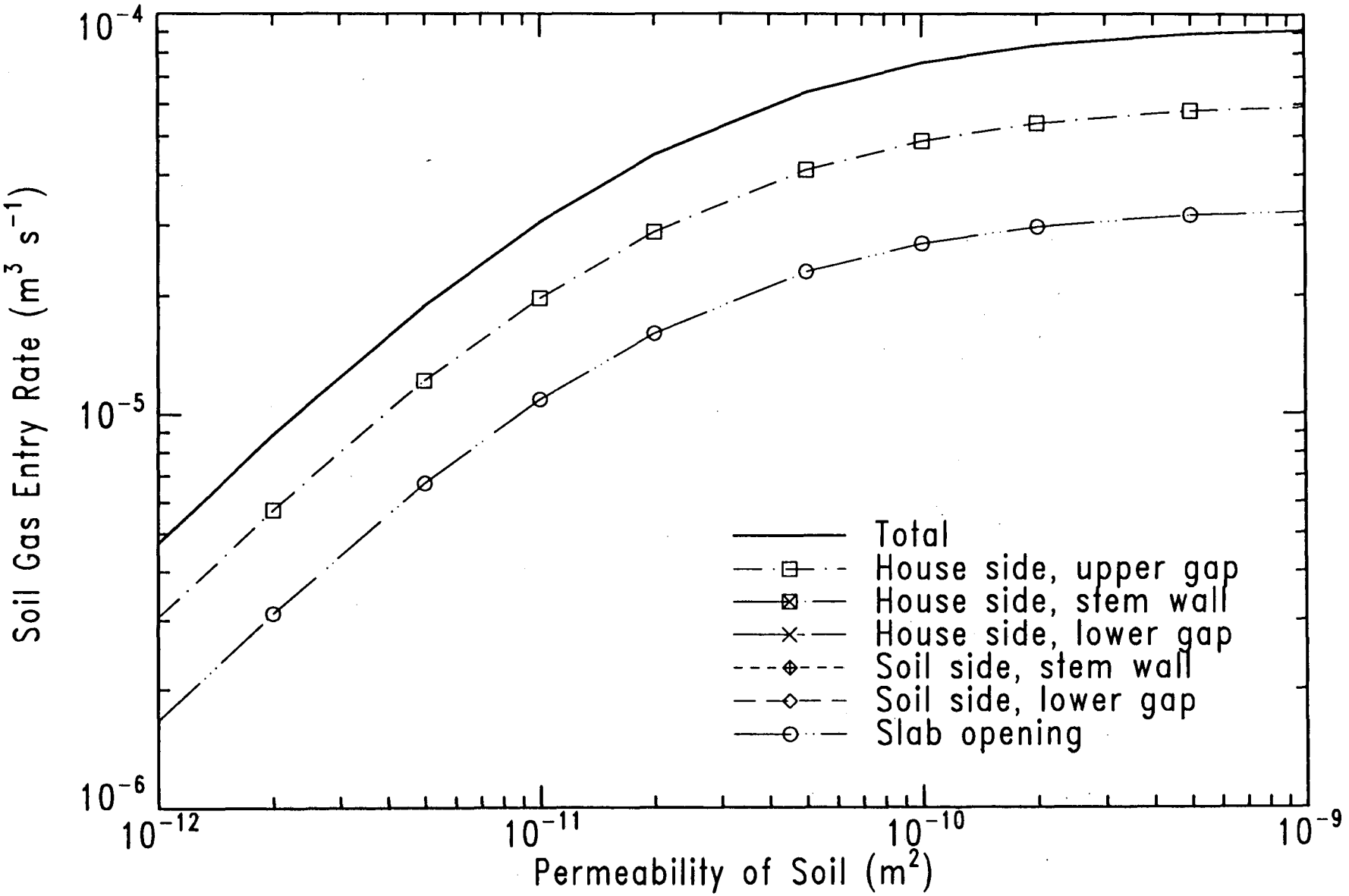

Figure A4S.
Soil-gas entry rates at the several entry points, with the soil permeability as parameter (concrete-filled stem wall simulated).

10/03/91 10:38:24

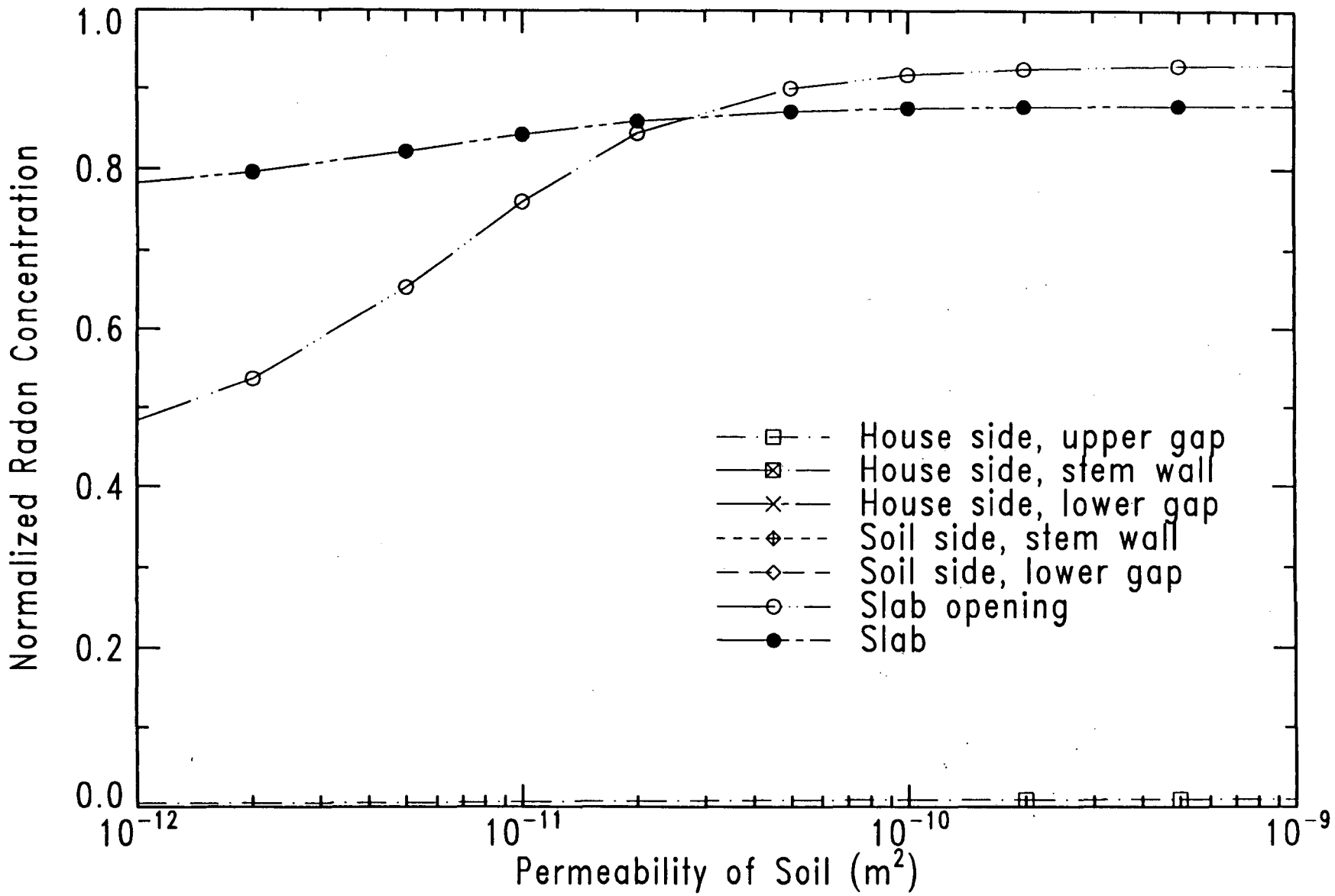

Figure A4C.
Normalized radon concentrations at the several entry points, with the soil permeability as parameter (concrete-filled stem wall simulated).

10/03/91 10:46:59

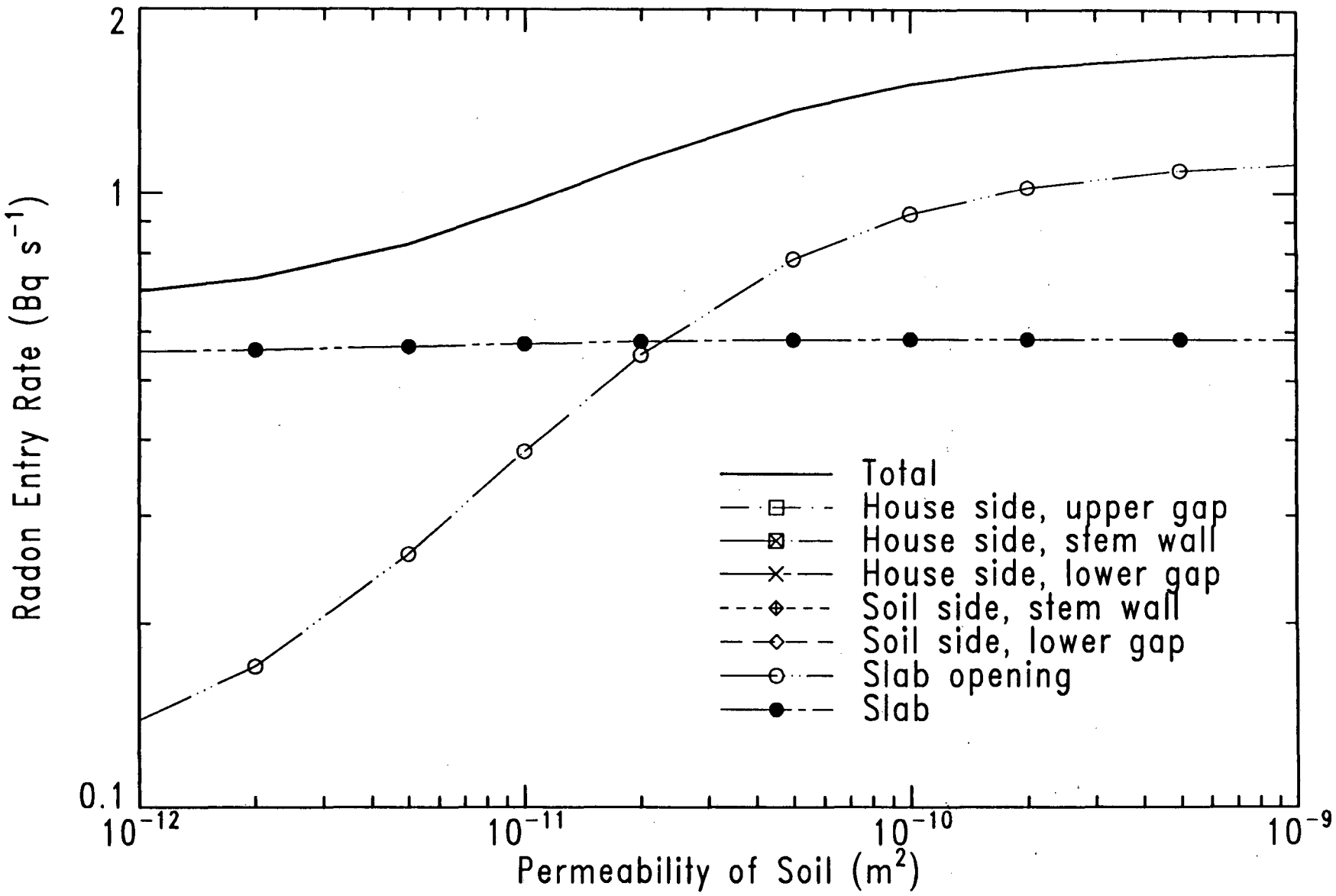

Figure A4R.
Radon entry rates at the several entry points,
with the soil permeability as parameter
(concrete-filled stem wall simulated).

10/03/91 11:13:59

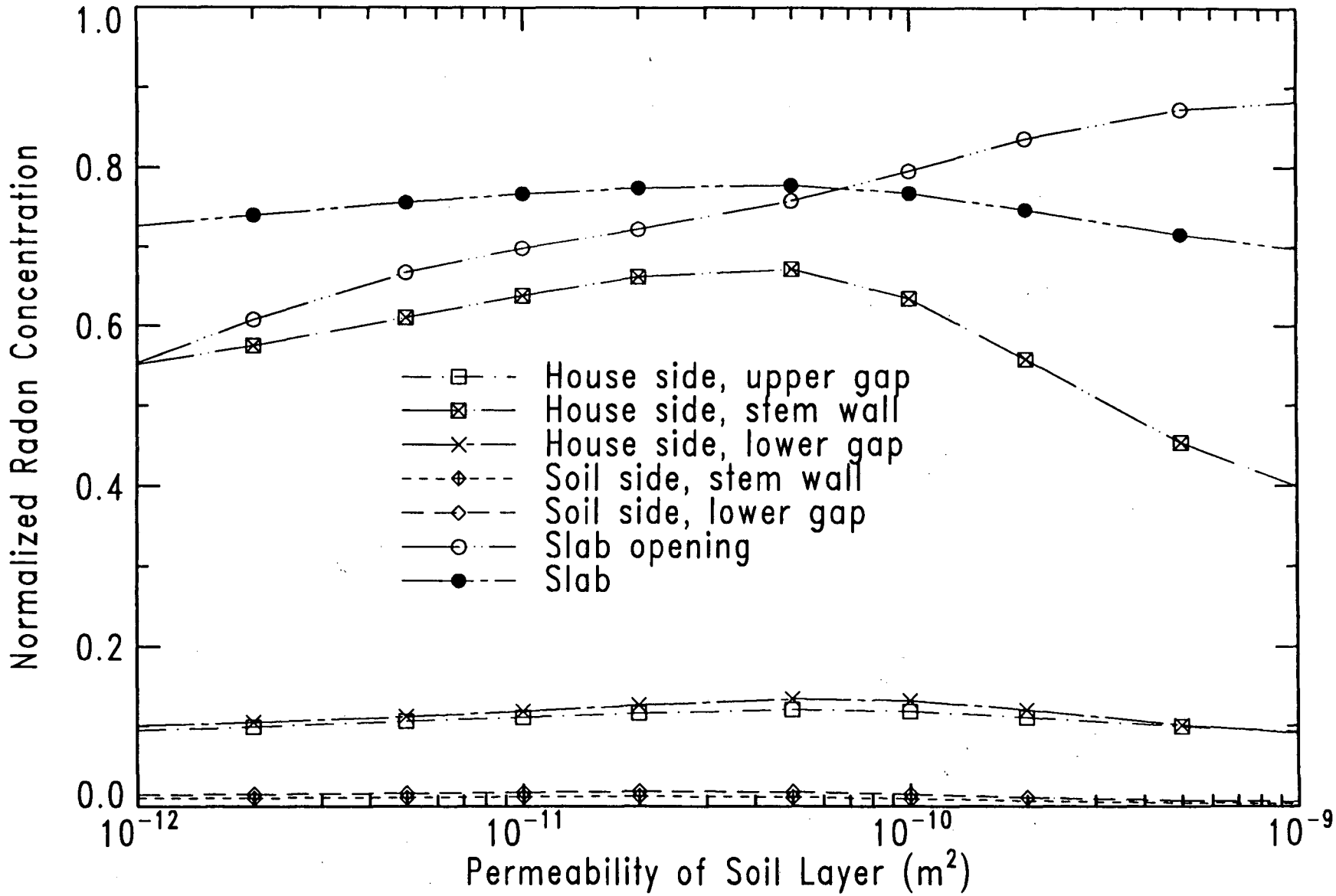

Figure A5C.
Normalized radon concentrations at the several entry points, with the permeability of a soil layer between 0 and 1 m as parameter.

10/03/91 10:47:05

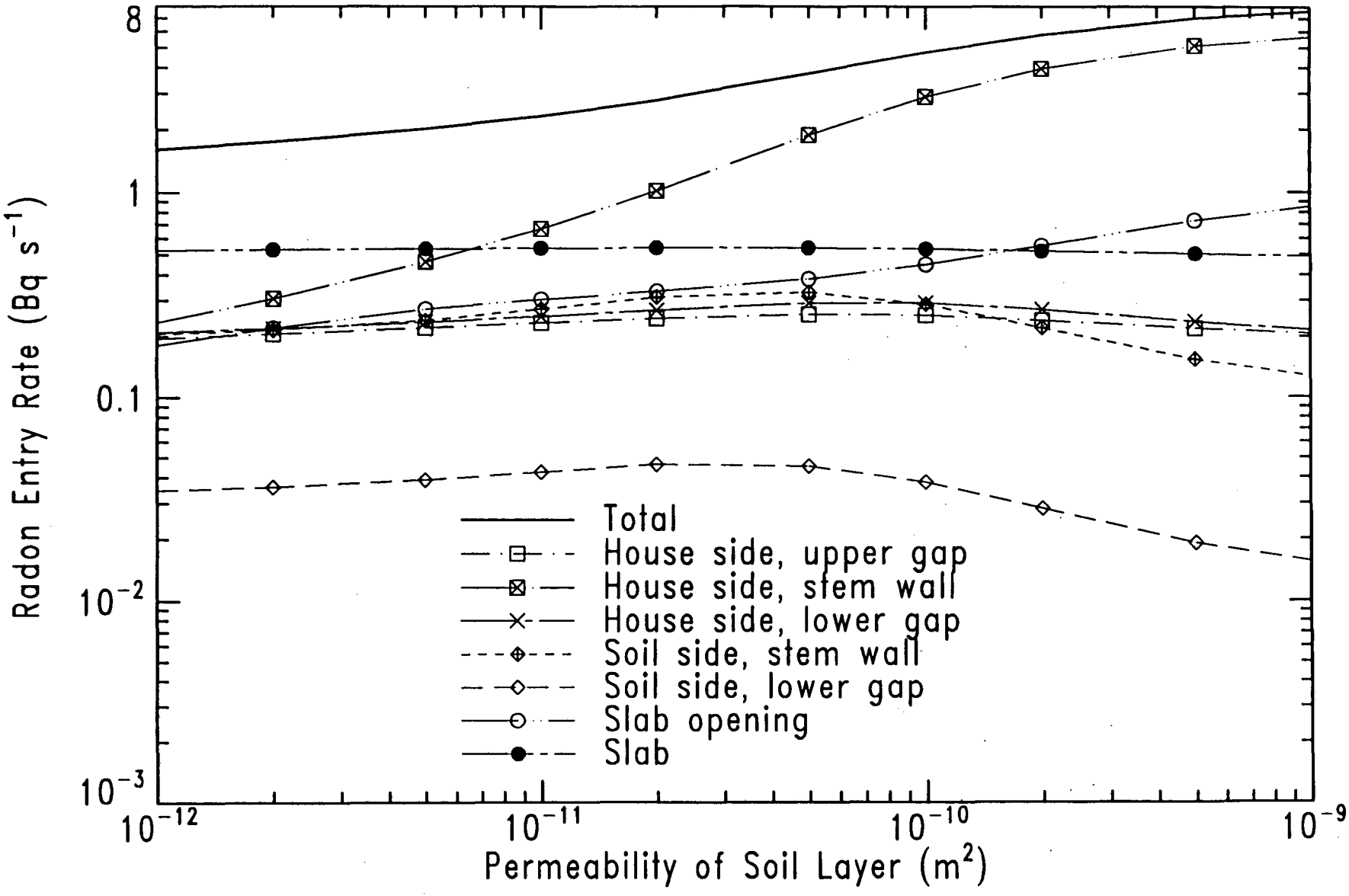

Figure A5R.
Radon entry rates at the several entry points, with the permeability of a soil layer between 0 and 1 m as parameter.

10/03/91 11:22:51

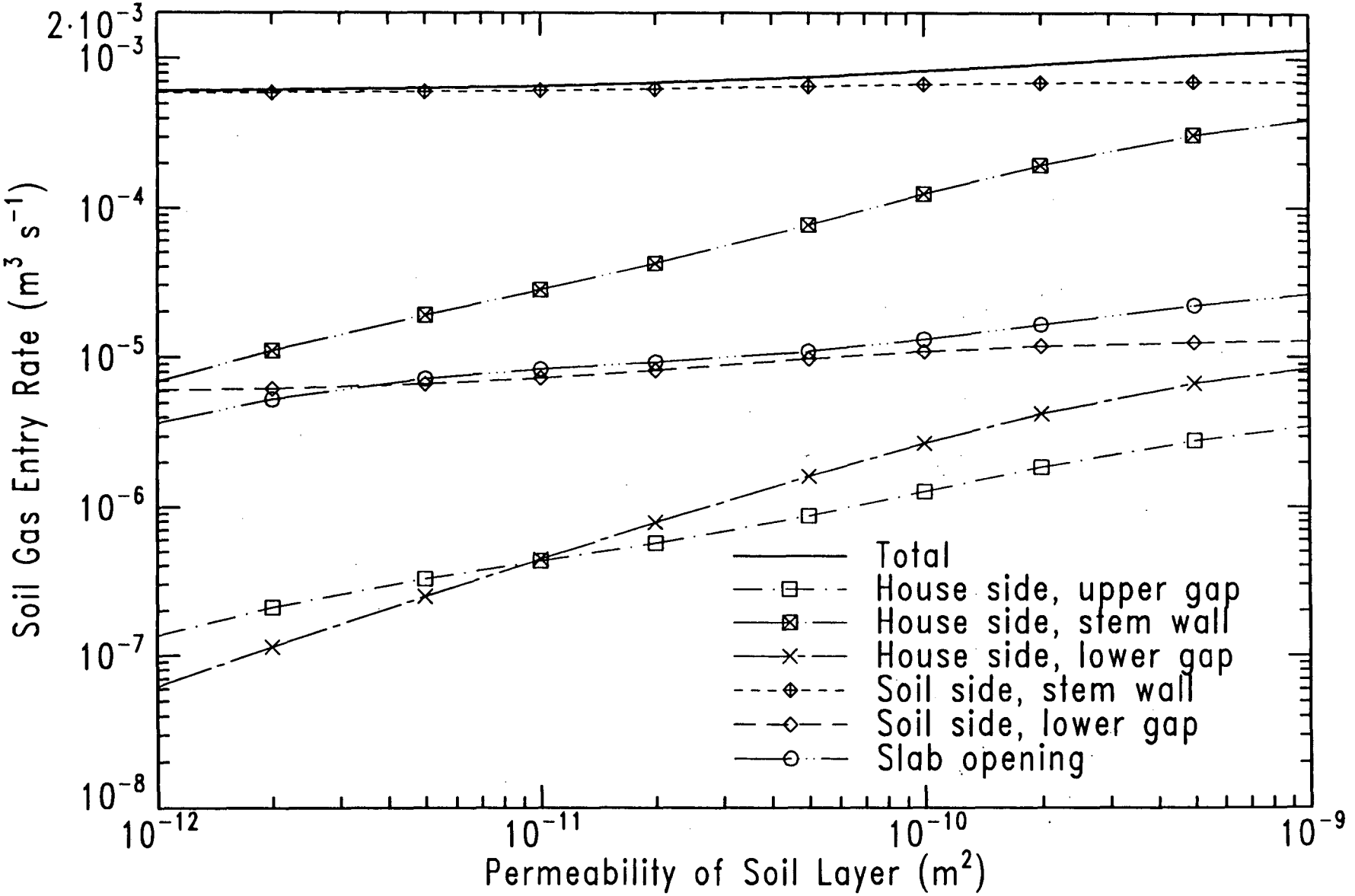

Figure A5S.
Soil-gas entry rates at the several entry points, with the permeability of a soil layer between 0 and 1 m as parameter.

10/03/91 11:05:54

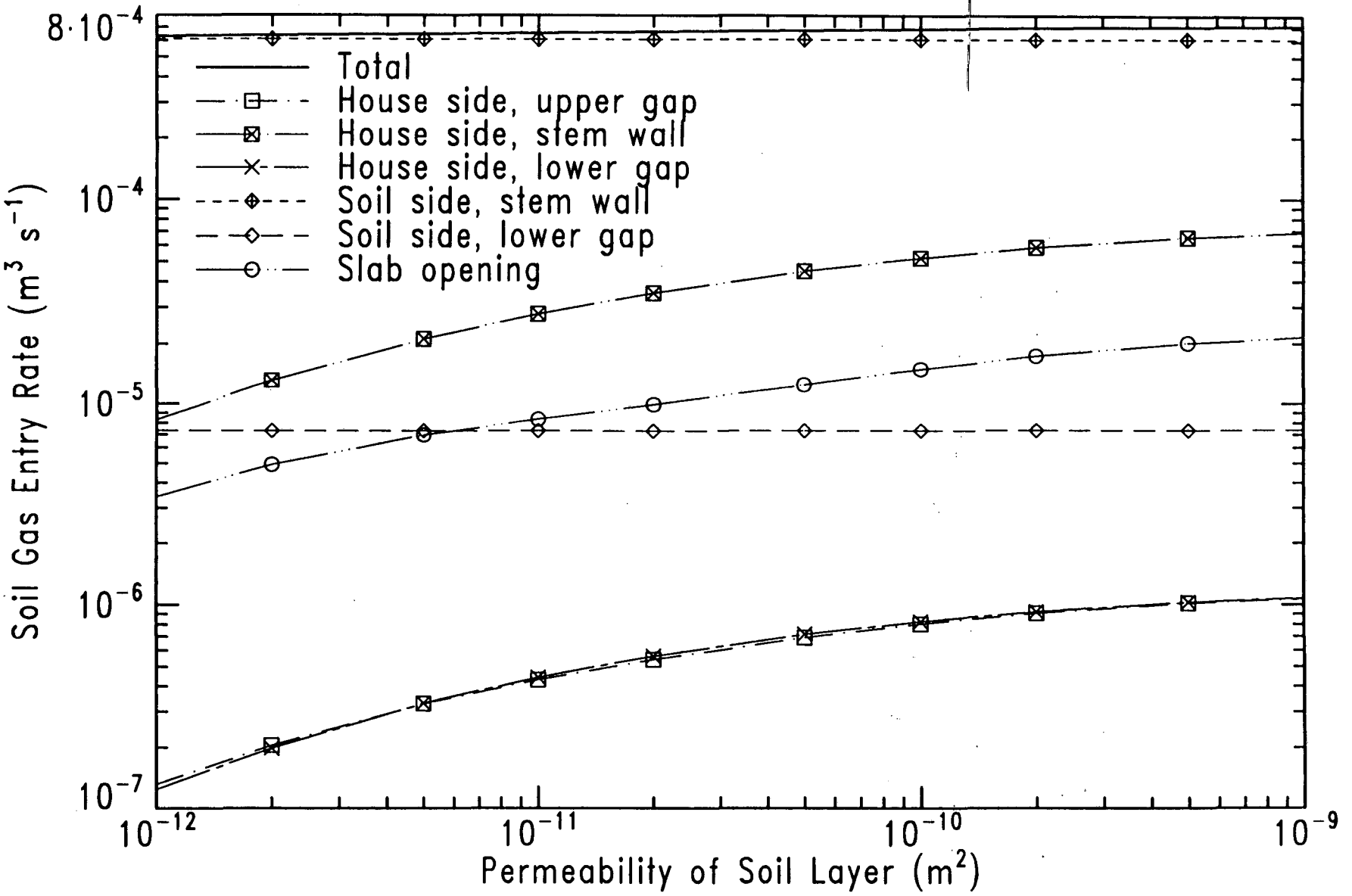

Figure A6S.
Soil-gas entry rates at the several entry points, with the permeability of a soil layer between 0.5 and 1.5 m as parameter.

10/03/91 10:38:35

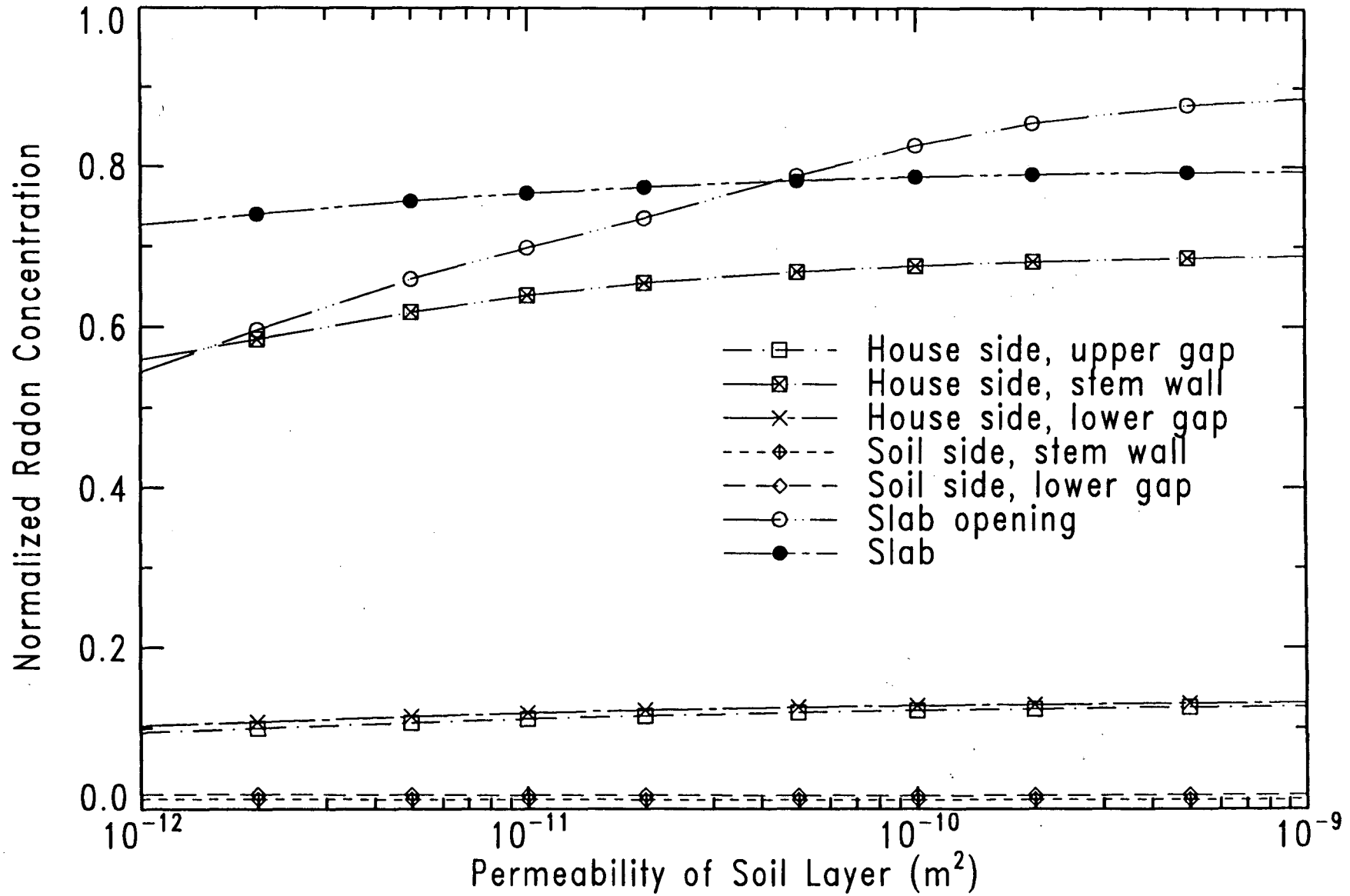

Figure A6C.
Normalized radon concentrations at the several entry points, with the permeability of a soil layer between 0.5 and 1.5 m as parameter.

10/03/91 10:47:10

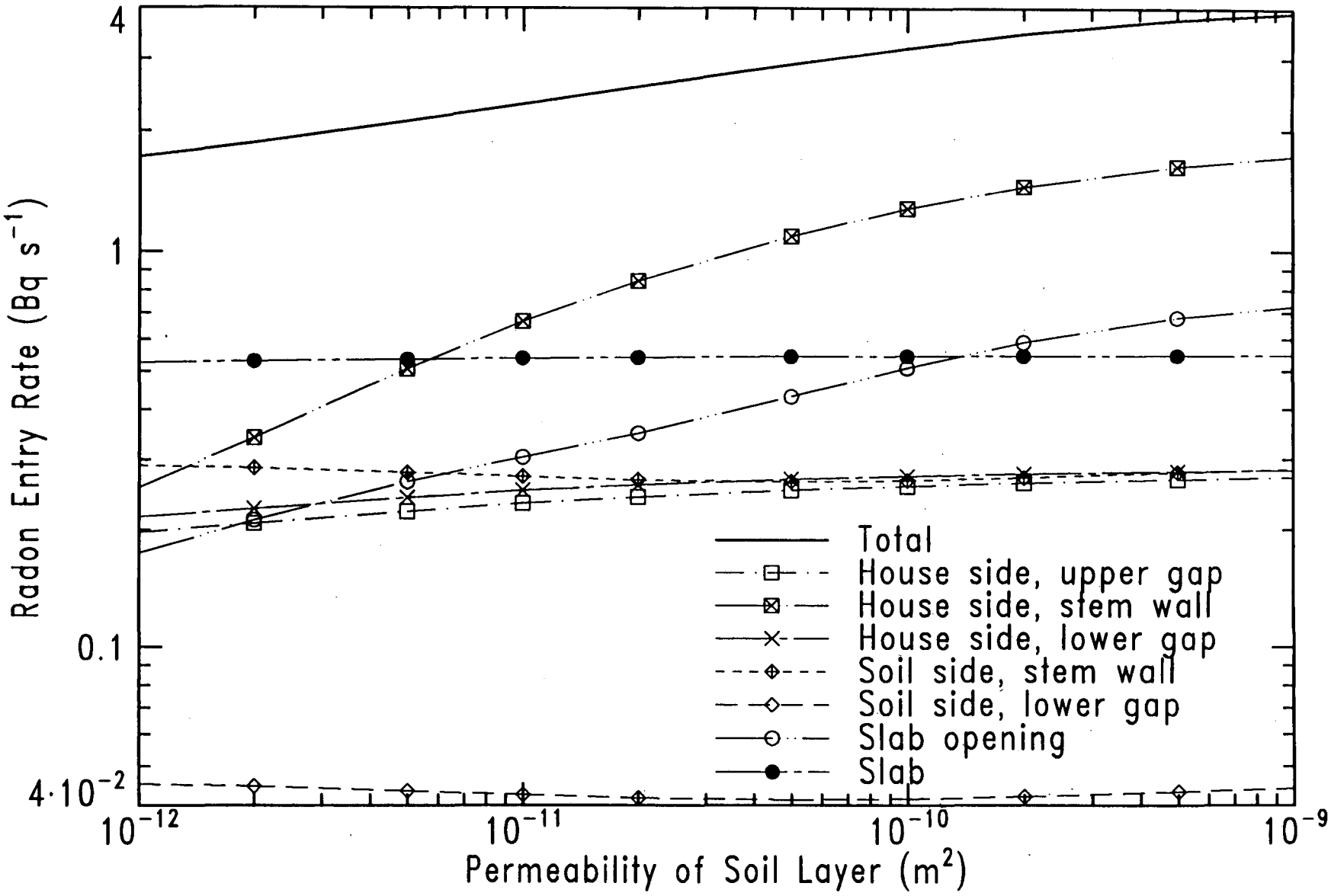

Figure A6R.
Radon entry rates at the several entry points, with the permeability of a soil layer between 0.5 and 1.5 m as parameter.

10/03/91 11:14:09

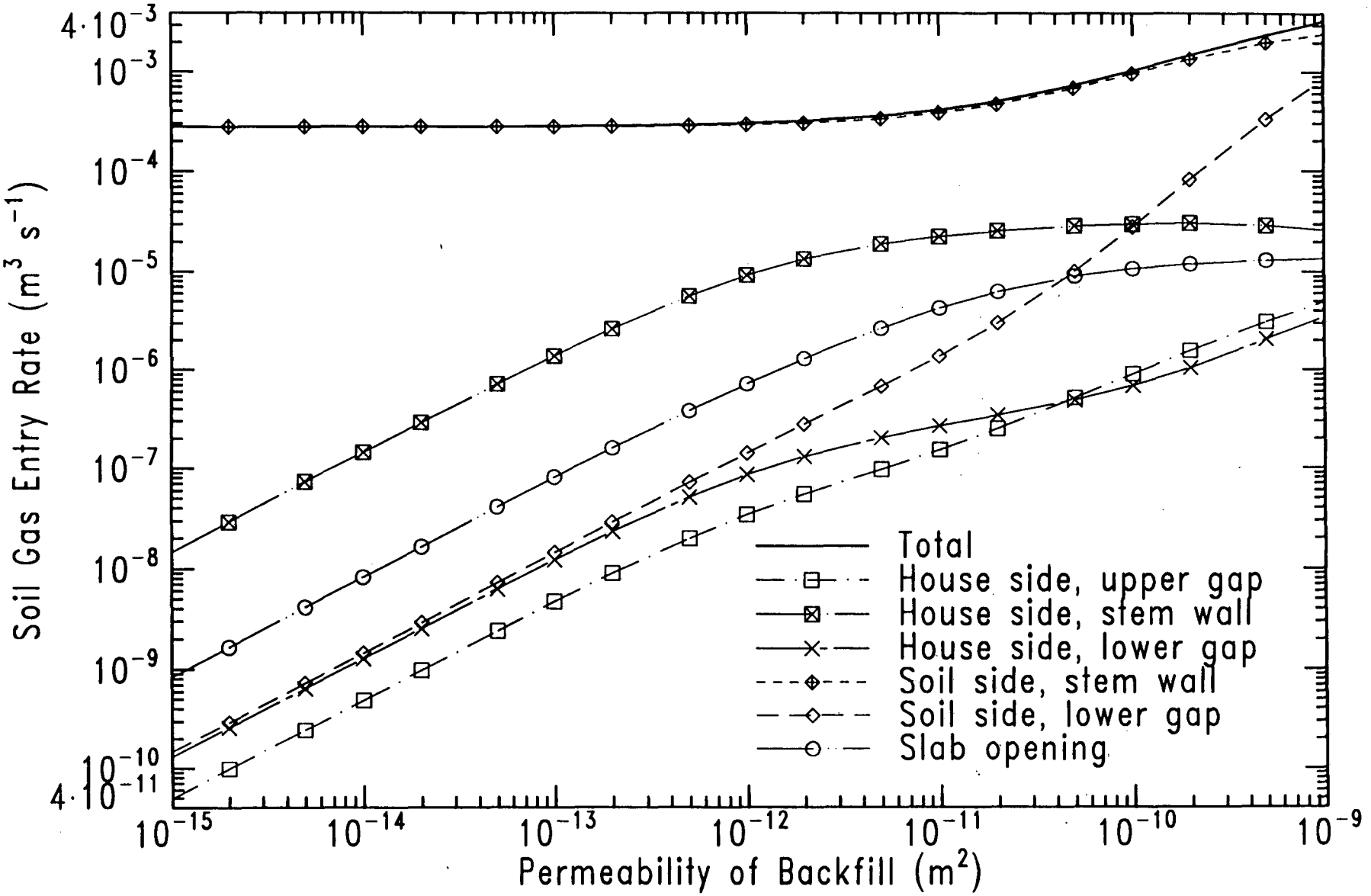

Figure A7S.
Soil-gas entry rates at the several entry points, with the backfill permeability as parameter.

10/03/91 10:38:42

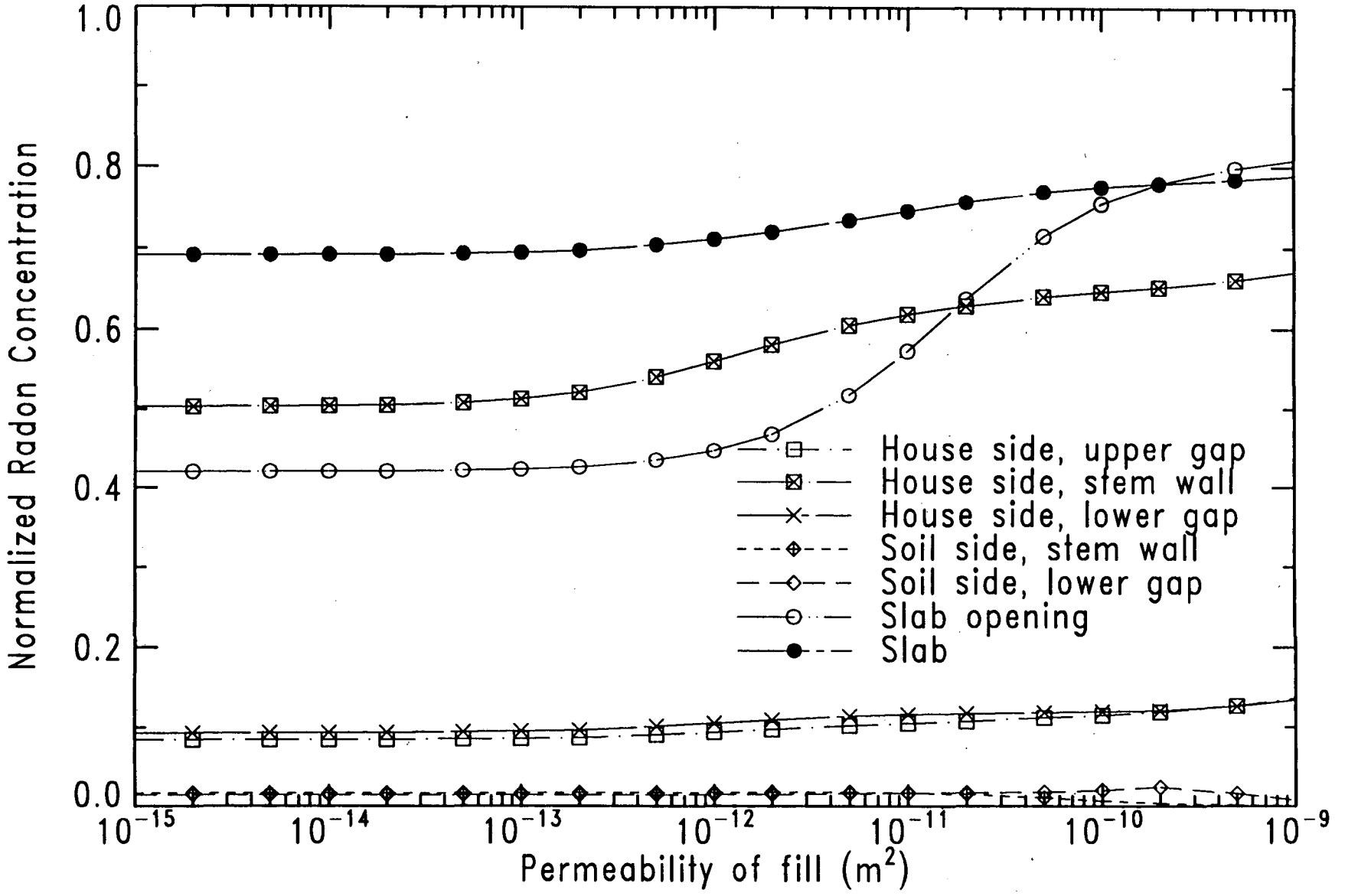

Figure A7C.
Normalized radon concentrations at the several entry points, with the backfill permeability as parameter.

10/03/91 10:47:17

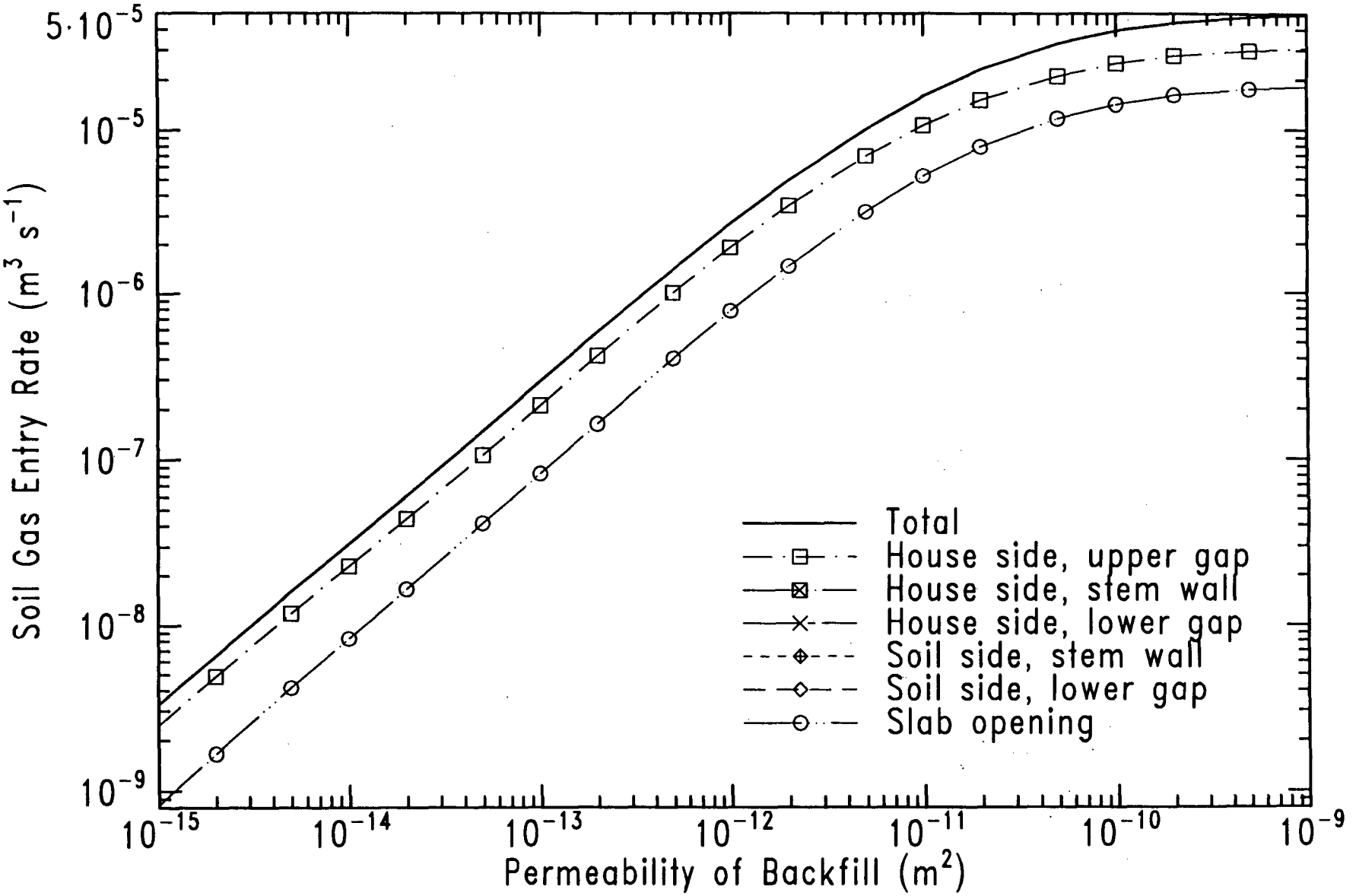

Figure A8S.
Soil-gas entry rates at the several entry points, with the backfill permeability as parameter (concrete-filled stem wall simulated).

10/03/91 10:38:48

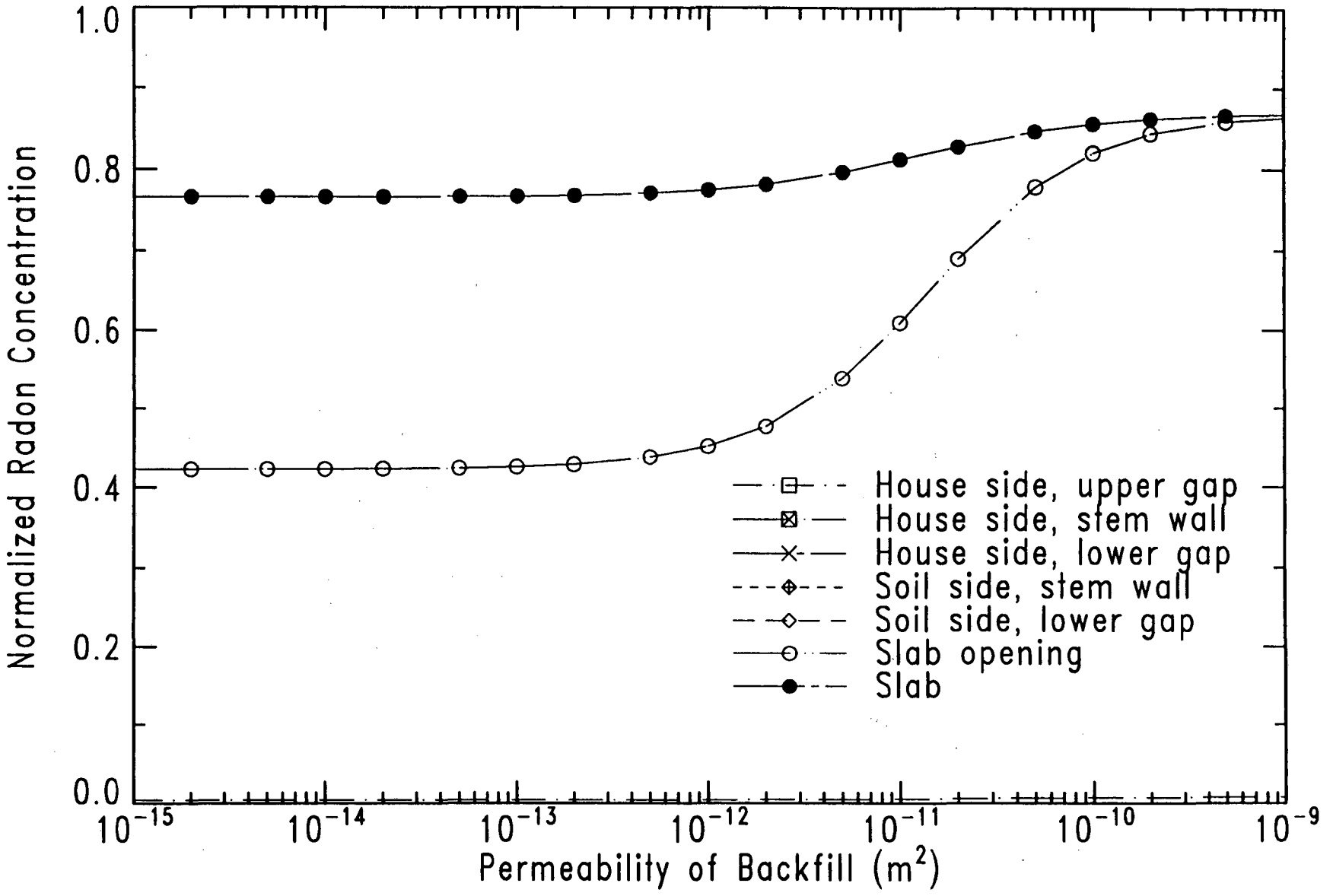

Figure A8C.
Normalized radon concentrations at the several entry points, with the backfill permeability as parameter (concrete-filled stem wall simulated).

10/03/91 10:47:22

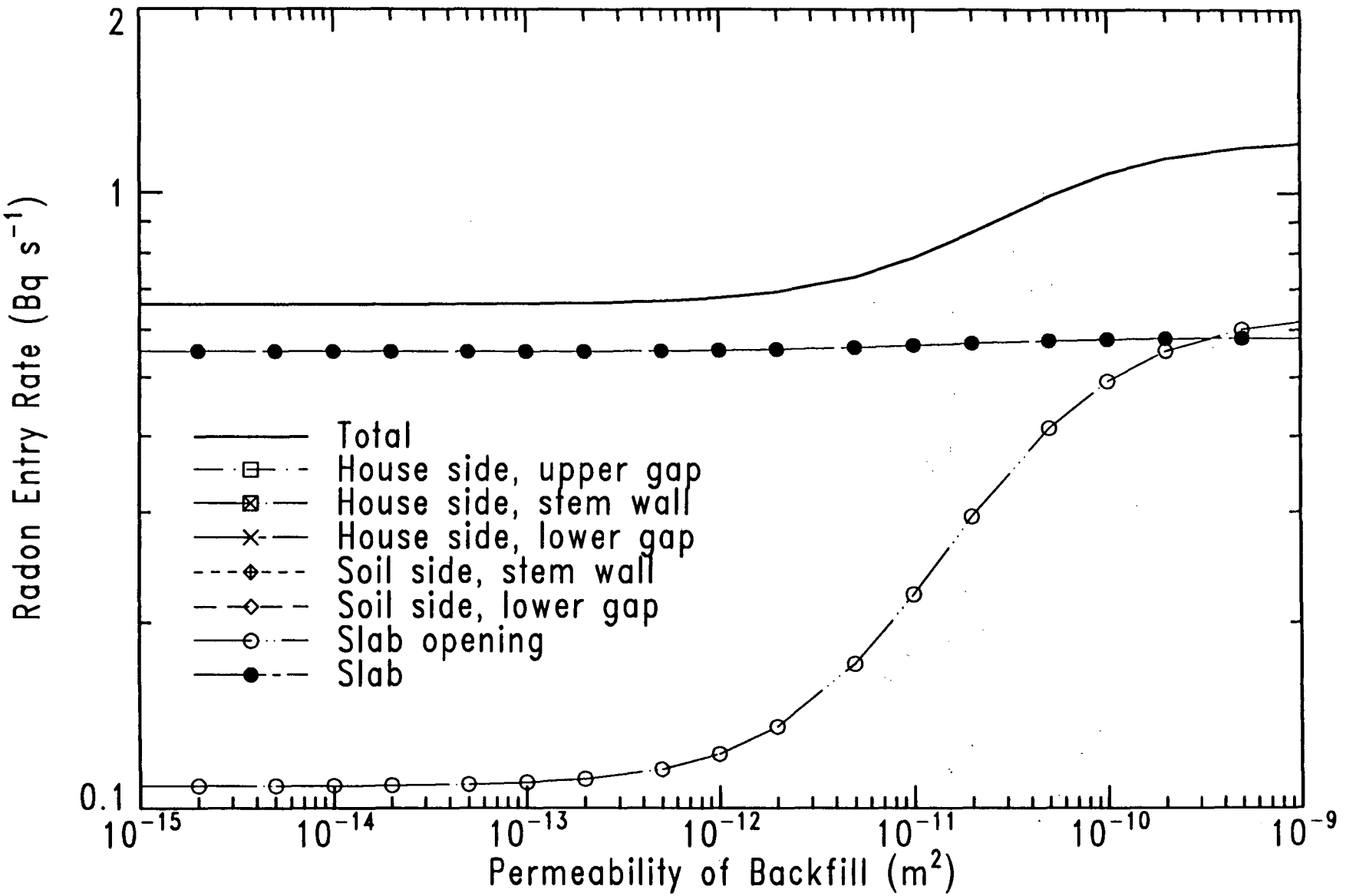

Figure A8R.
Radon entry rates at the several entry points, with the backfill permeability as parameter (concrete-filled stem wall simulated).

10/03/91 11:14:21

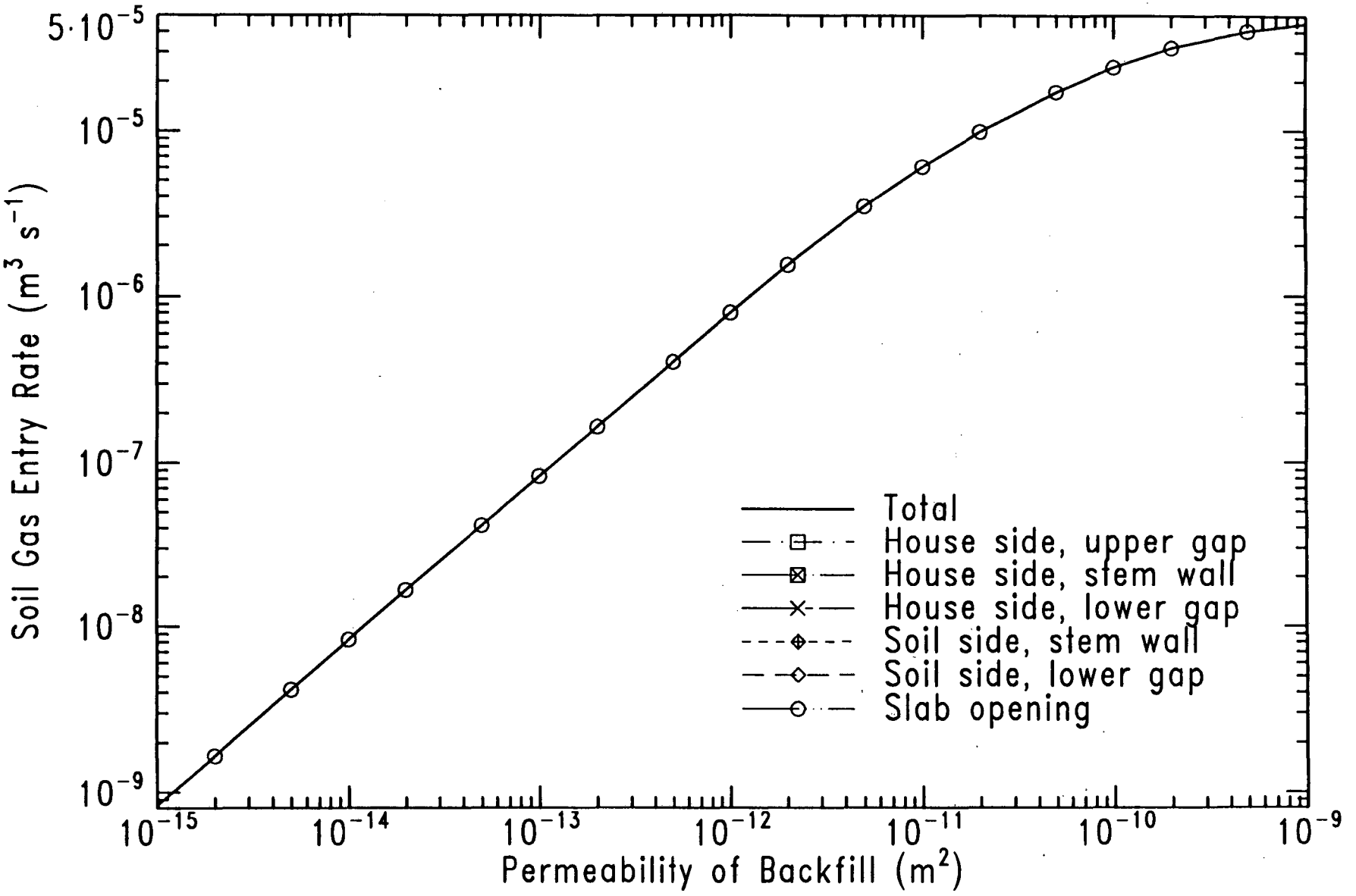

Figure A9S.
Soil-gas entry rates at the several entry points, with the backfill permeability as parameter (no entry except at the opening in the slab).

10/03/91 11:28:47

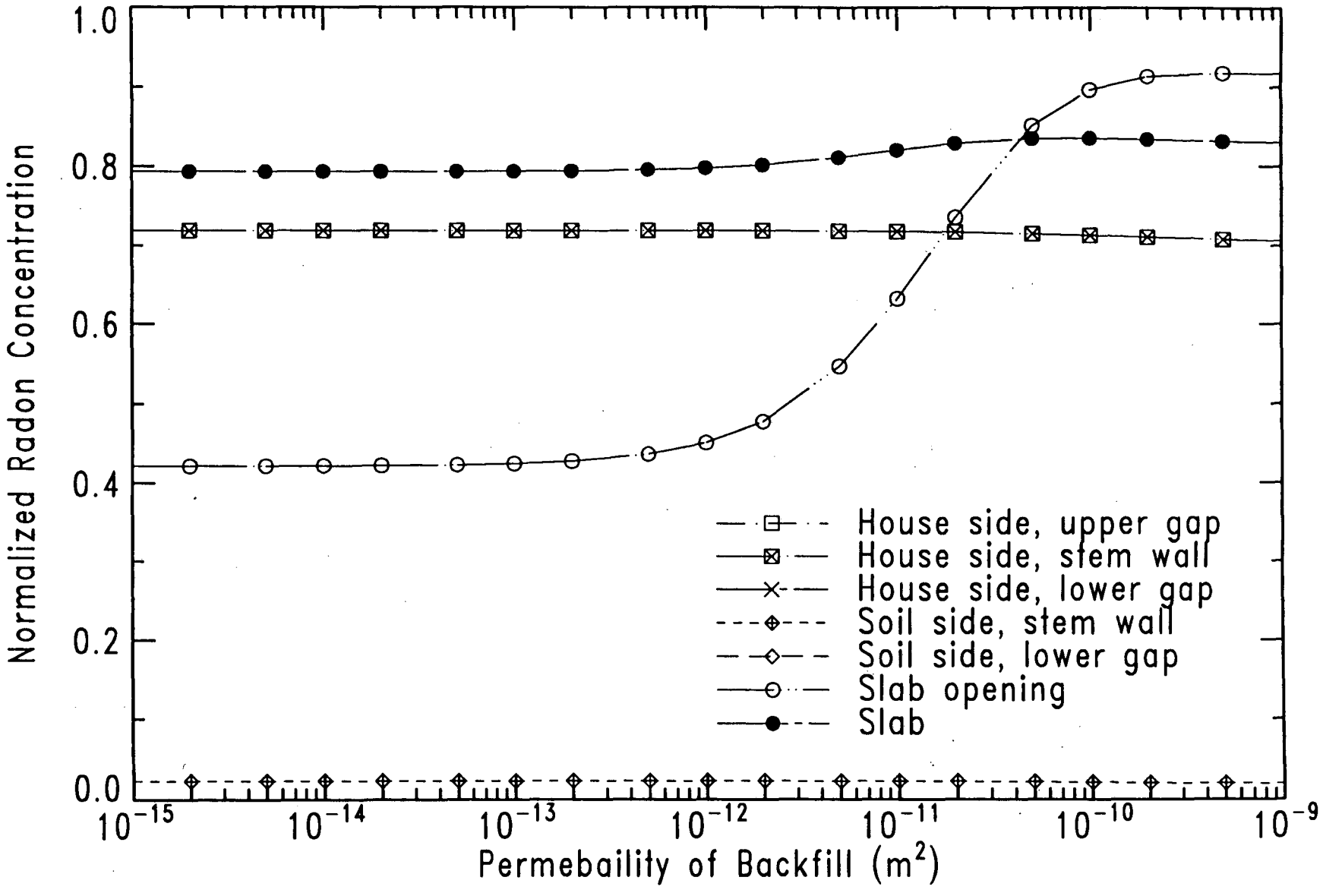

Figure A9C.
Normalized radon concentrations at the several entry points,
with the backfill permeability as parameter
(no soil-gas entry except at the opening in the slab).

10/03/91 13:15:18

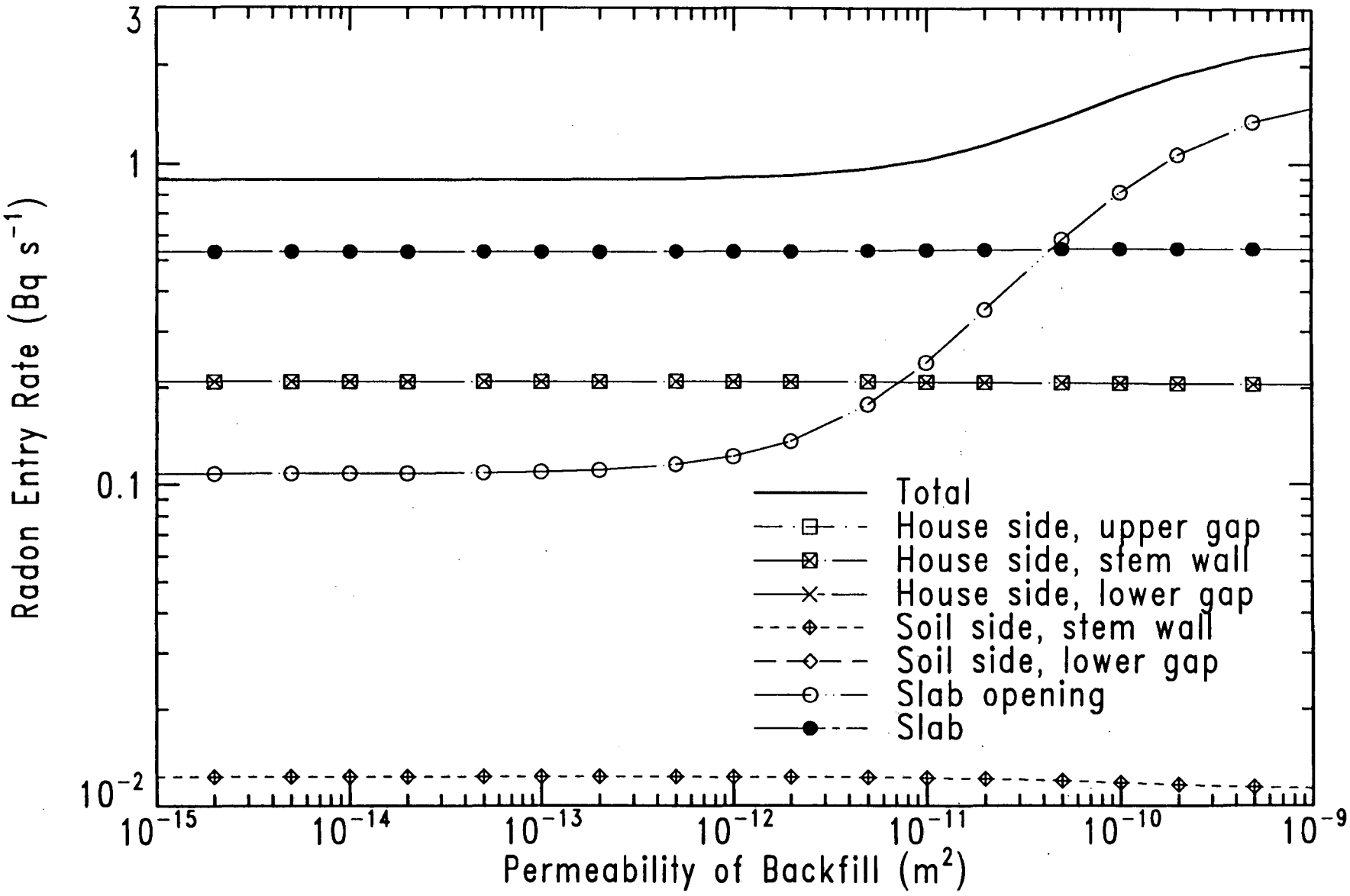

Figure A9R.
Radon entry rates at the several entry points,
with the backfill permeability as parameter
(no soil-gas entry except at the opening in the slab).

10/03/91 13:38:58

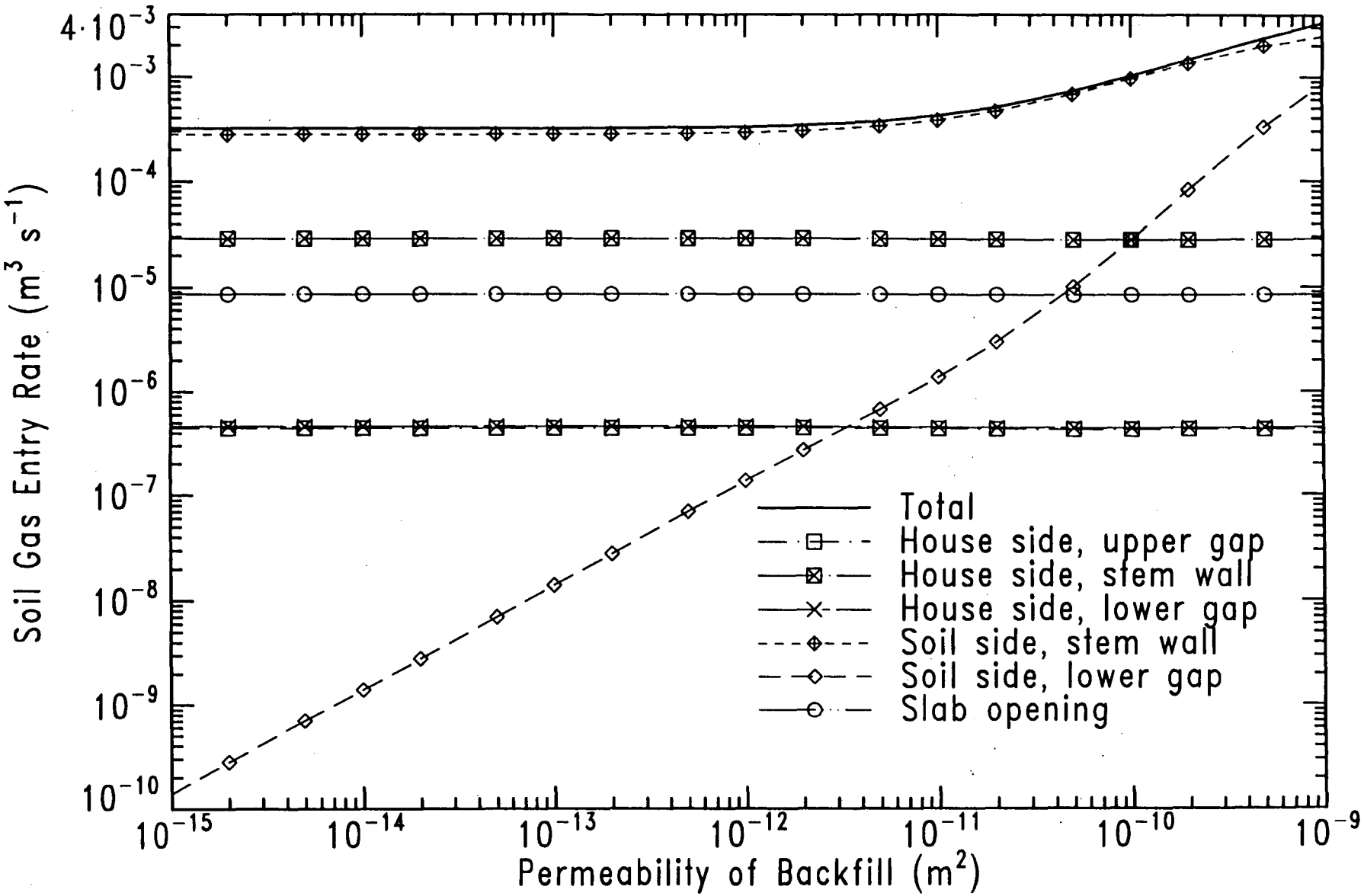

Figure A10S.
Soil-gas entry rates at the several entry points,
with the soil-side backfill permeability as parameter.

10/03/91 11:28:50

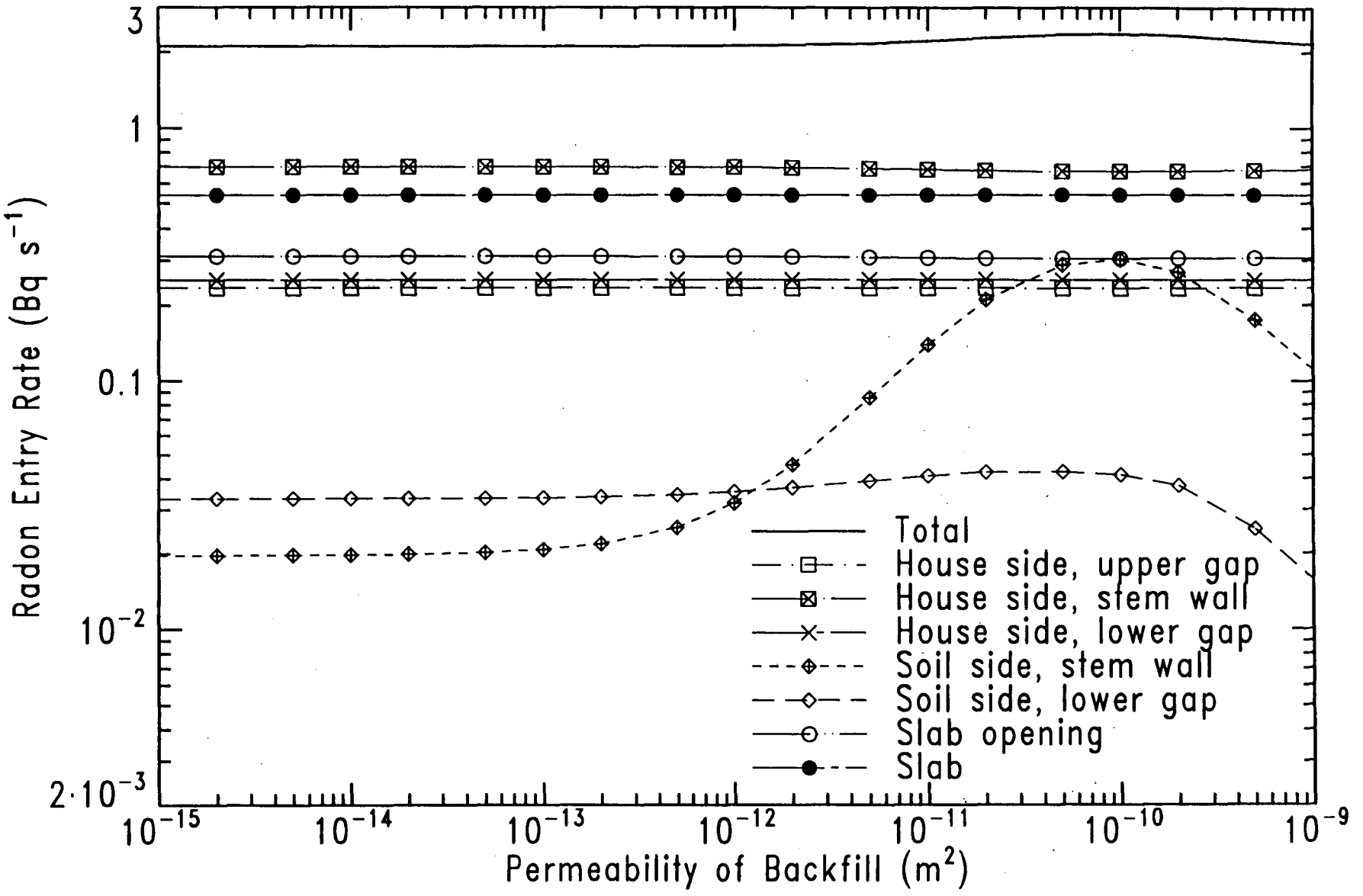

Figure A10R.
Radon entry rates at the several entry points,
with the soil-side backfill permeability as parameter.

10/03/91 13:46:31

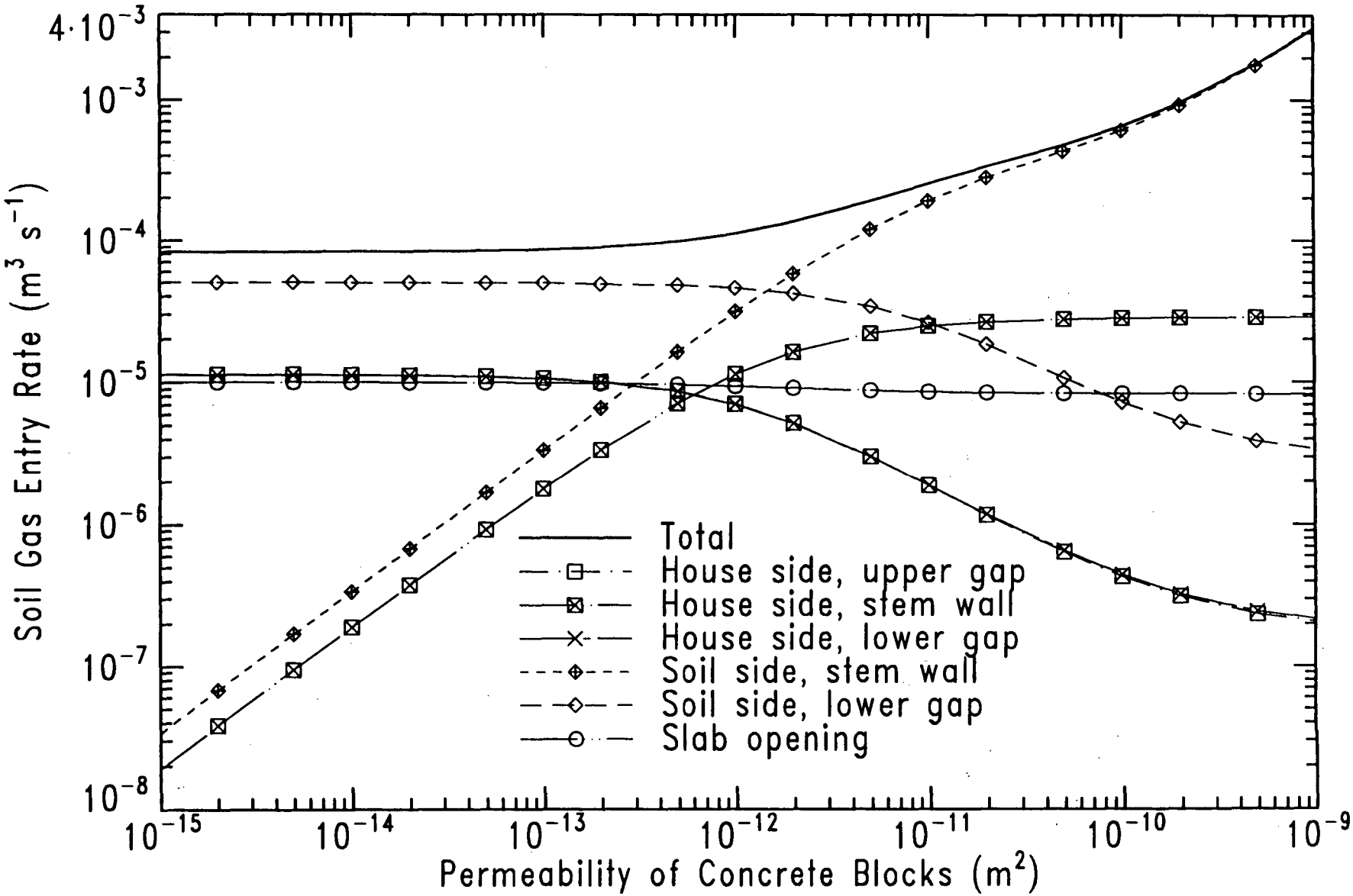

Figure A11S.
Soil-gas entry rates at the several entry points, with the stem wall permeability as parameter.

10/03/91 11:28:53

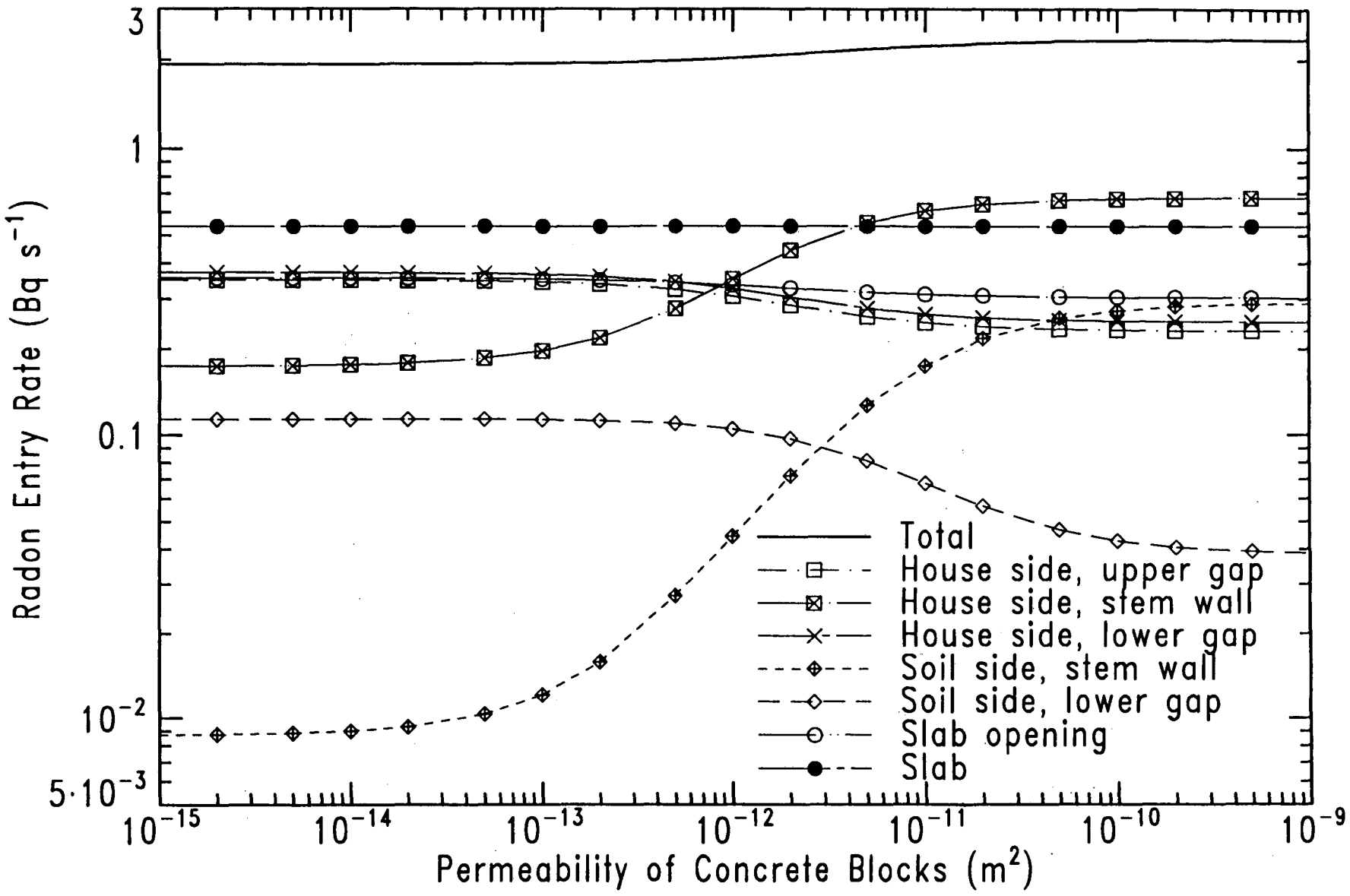

Figure A11R.
Radon entry rates at the several entry points,
with the stem wall permeability as parameter.

10/03/91 13:39:04

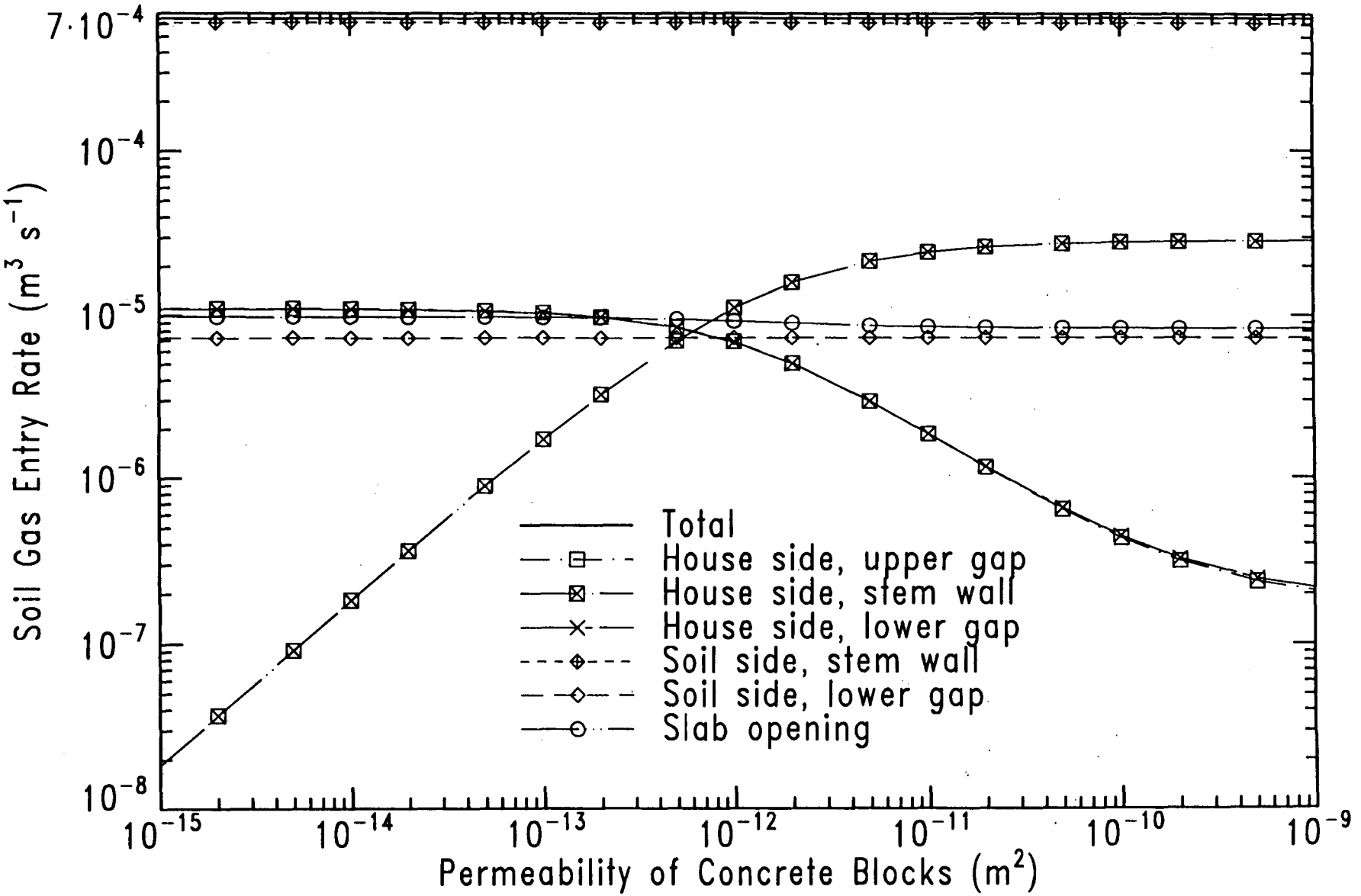

Figure A12S.
Soil-gas entry rates at the several entry points,
with the house-side stem wall permeability as parameter.

10/03/91 11:28:56

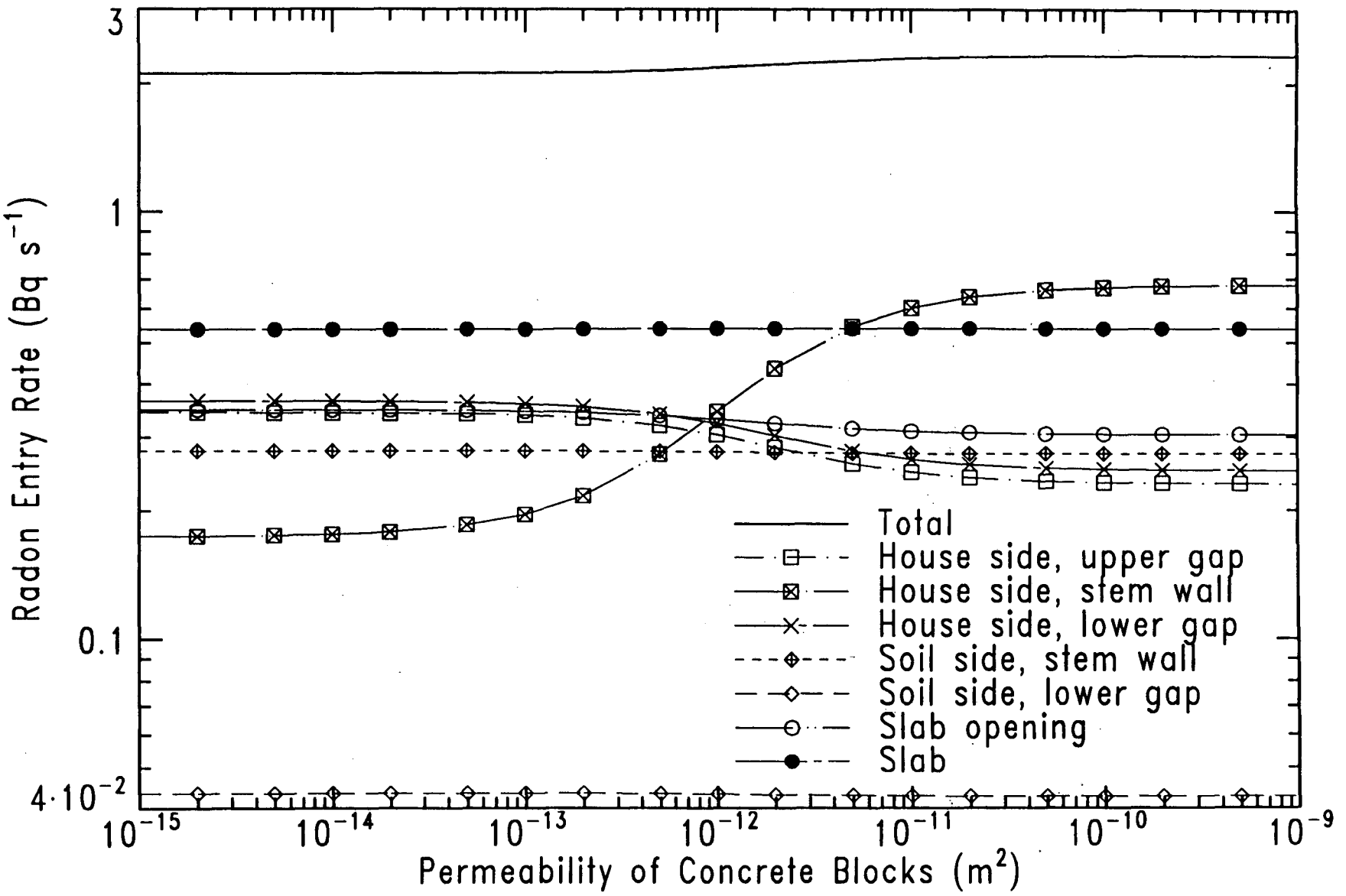

Figure A12R.
Radon entry rates at the several entry points,
with the house-side stem wall permeability as parameter.

10/03/91 13:39:07

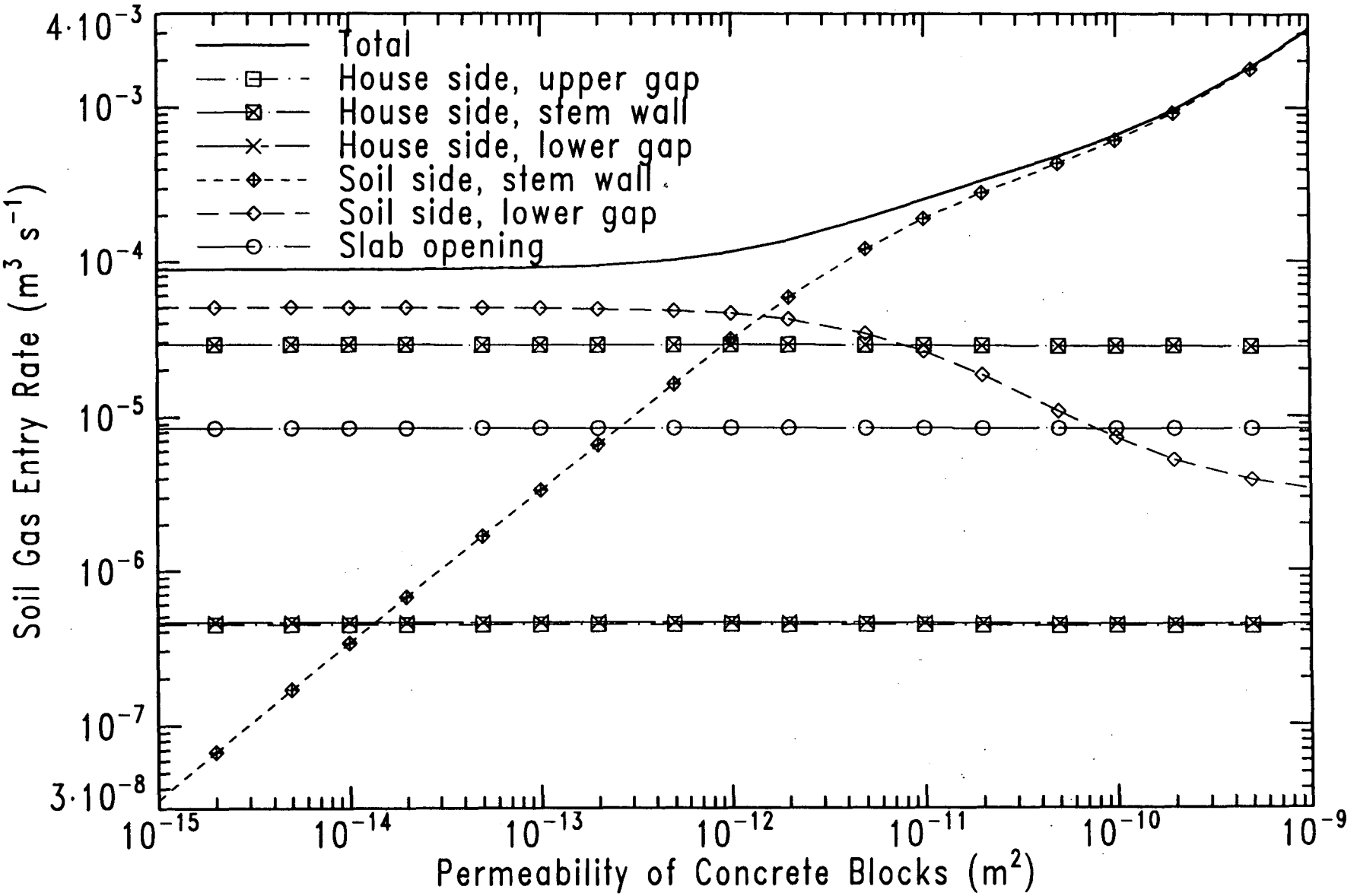

Figure A13S.
Soil-gas entry rates at the several entry points,
with the soil-side stem wall permeability as parameter.

10/03/91 11:28:59

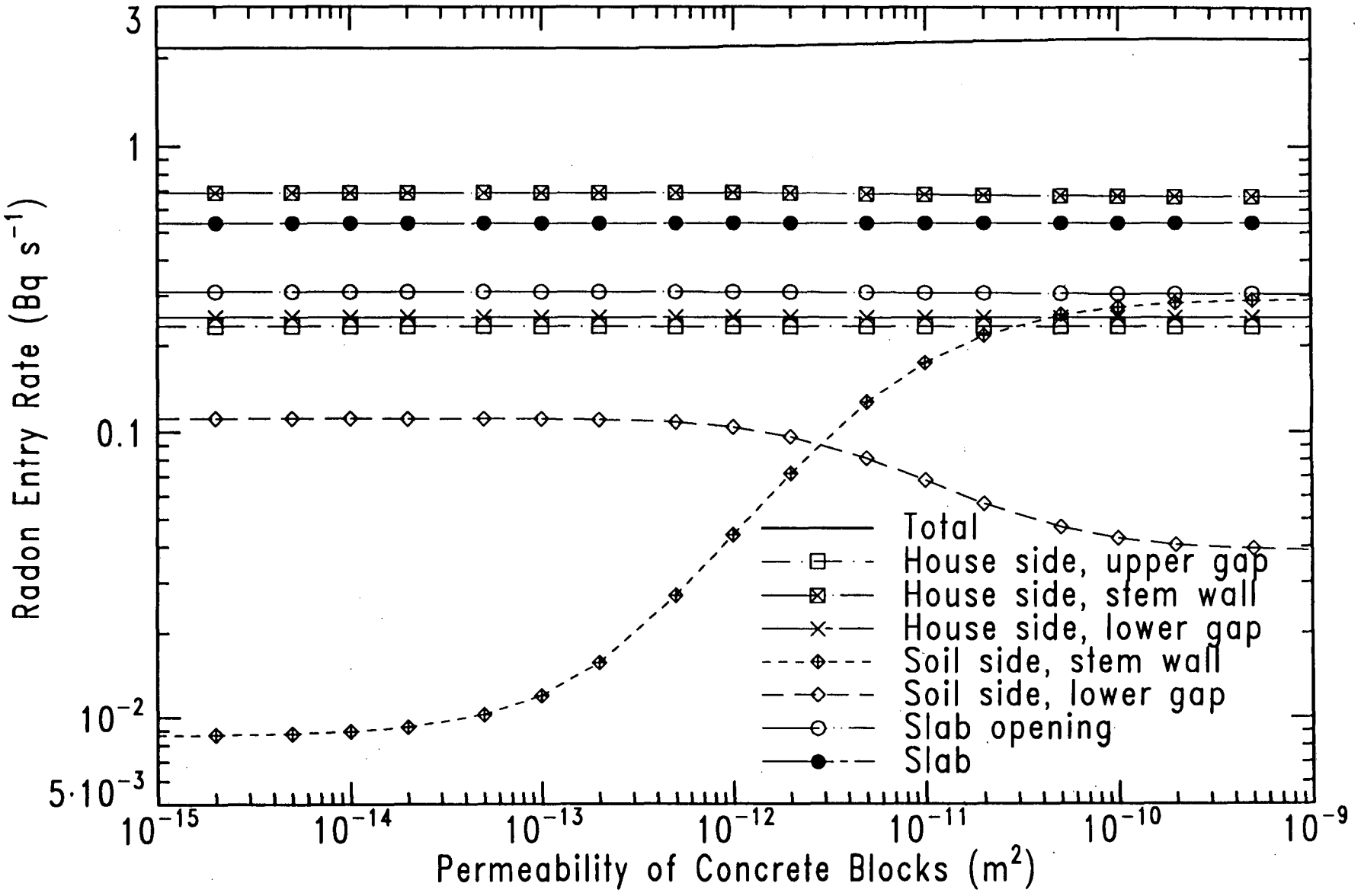

Figure A13R.
Radon entry rates at the several entry points,
with the soil-side stem wall permeability as parameter.

10/03/91 13:39:10

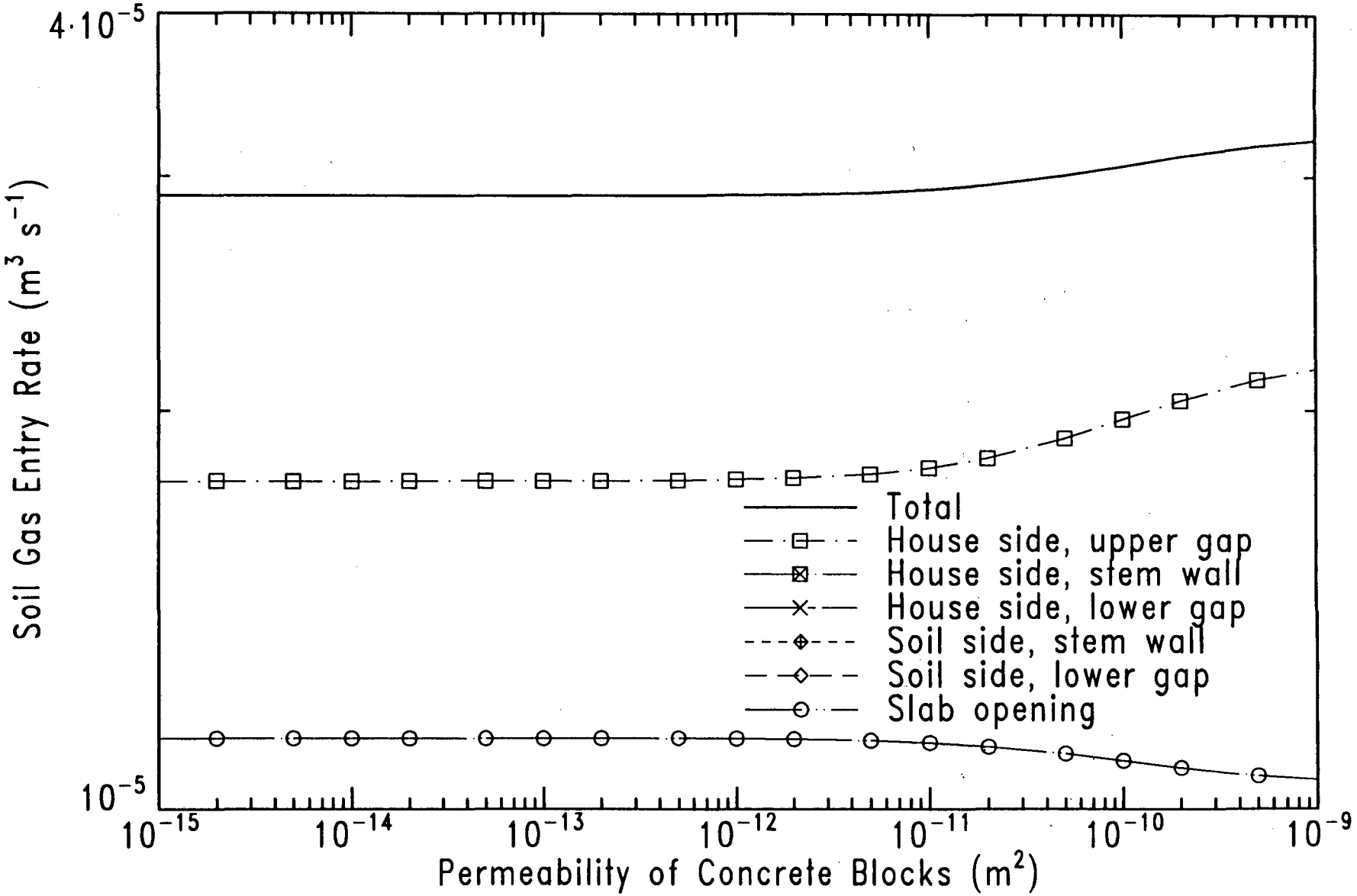

Figure A14S.
Soil-gas entry rates at the several entry points, with the stem wall permeability as parameter (concrete-filled stem wall simulated).

10/03/91 11:29:02

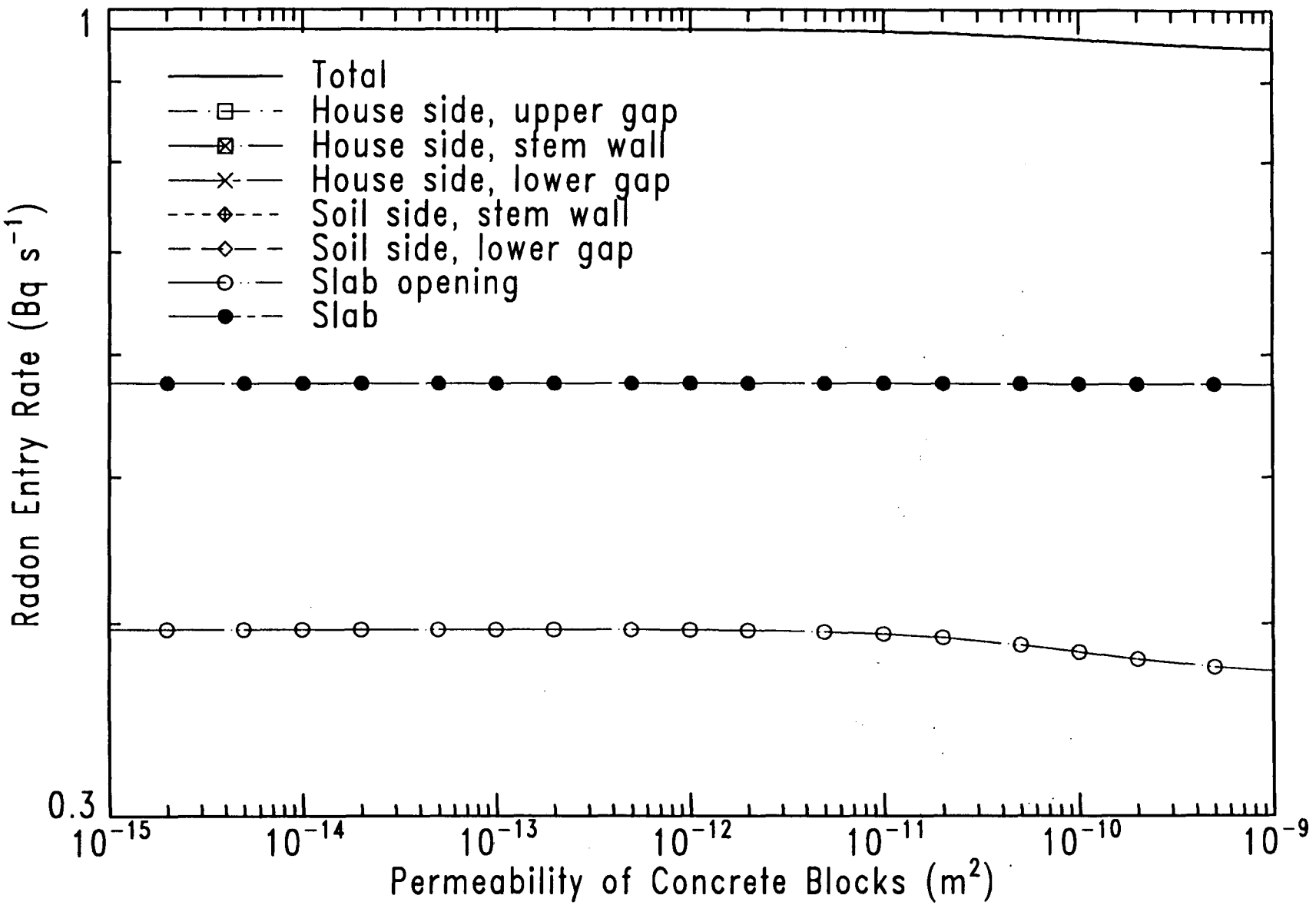

Figure A14R.
Radon entry rates at the several entry points, with the stem wall permeability as parameter (concrete-filled stem wall simulated).

10/03/91 13:39:17

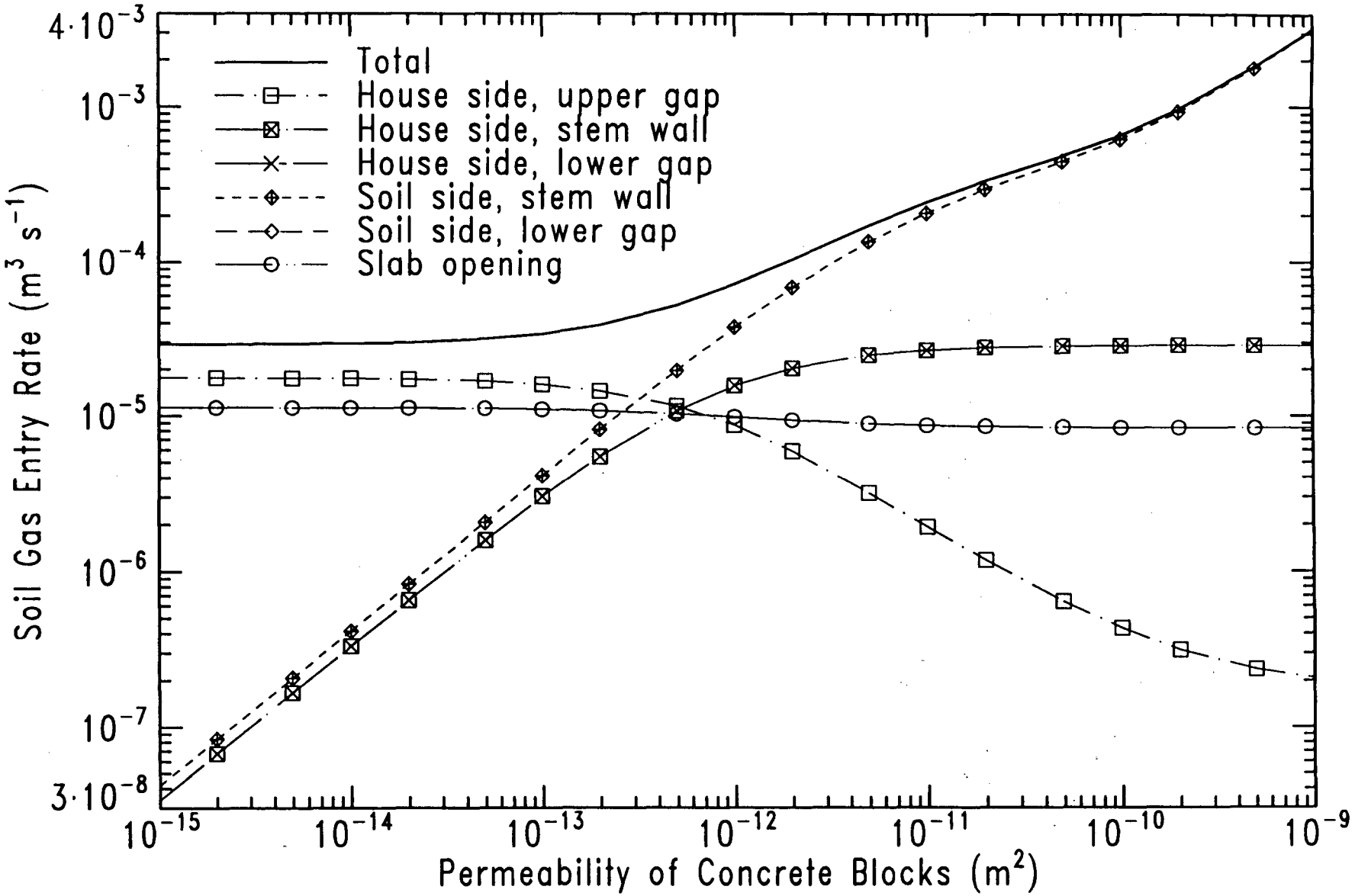

Figure A15S.
Soil-gas entry rates at the several entry points, with the stem wall permeability as parameter (wall-footer gaps closed)

10/03/91 11:29:05

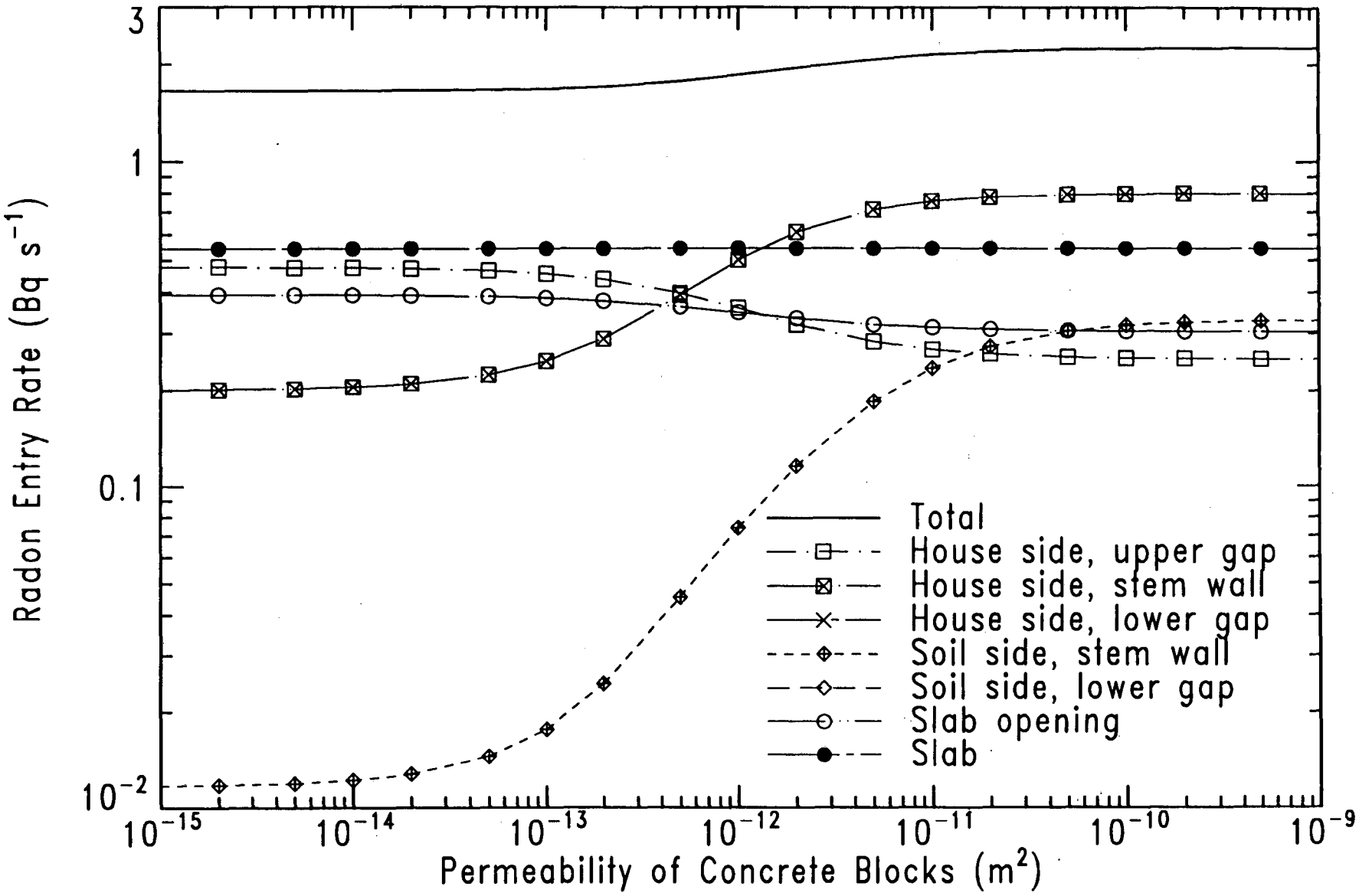

Figure A15R.
Radon entry rates at the several entry points,
with the stem wall permeability as parameter
(wall-footer gaps closed)

10/03/91 13:39:15

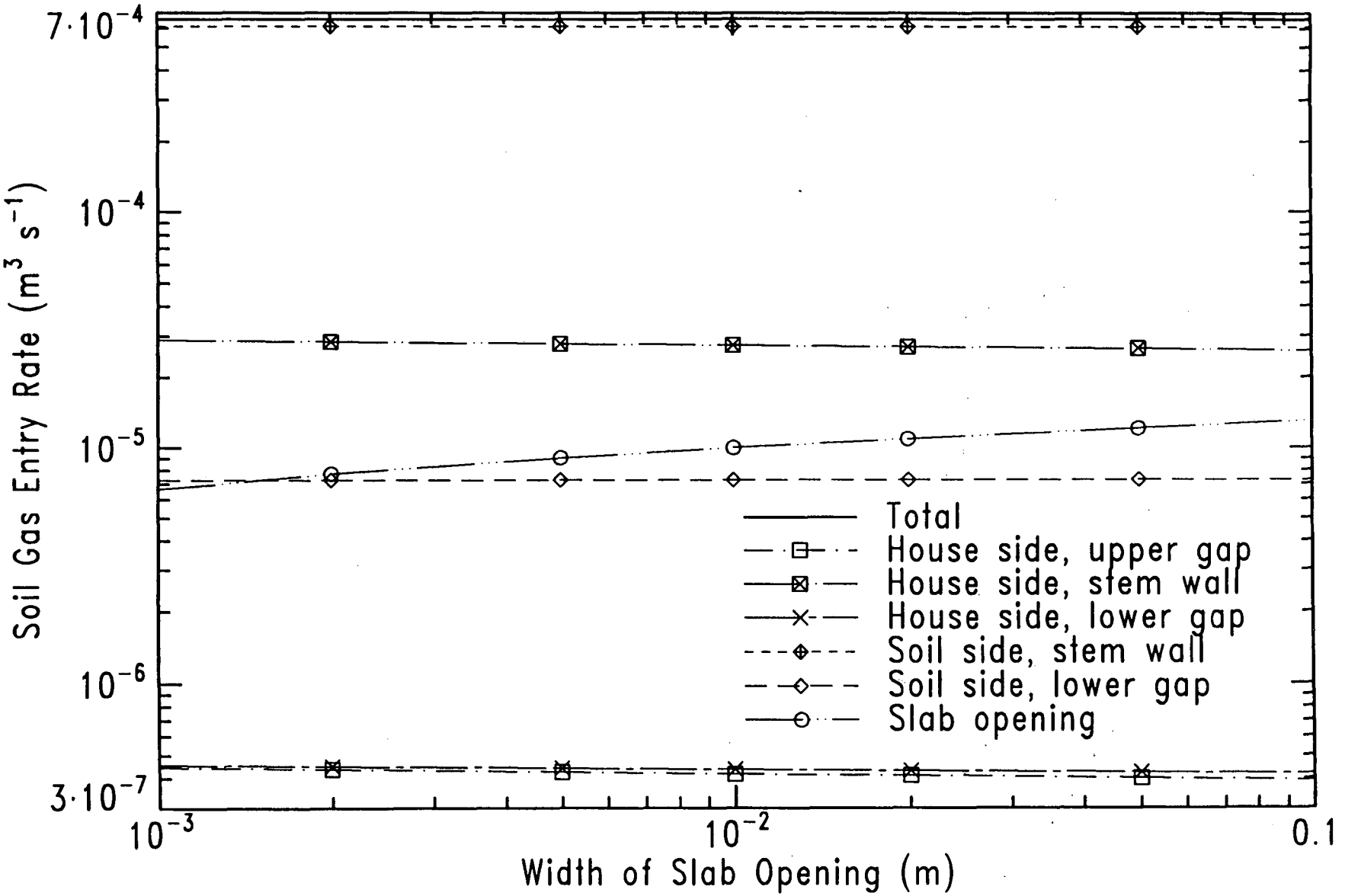

Figure A16S.
Soil-gas entry rates at the several entry points, with the width of the slab opening as parameter.

10/03/91 11:42:48

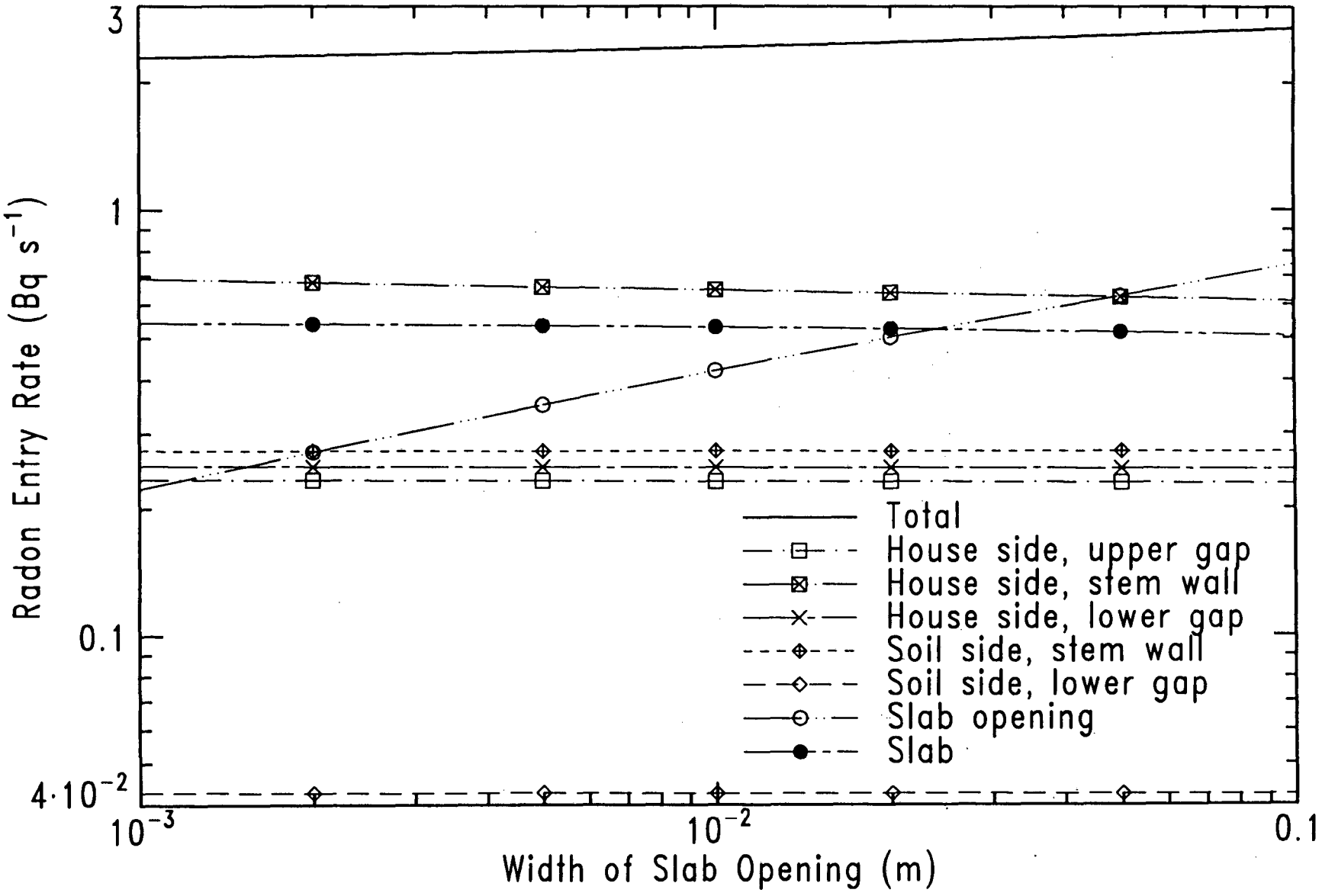

Figure A16R.
Radon entry rates at the several entry points,
with the width of the slab opening as parameter.

10/03/91 13:39:18

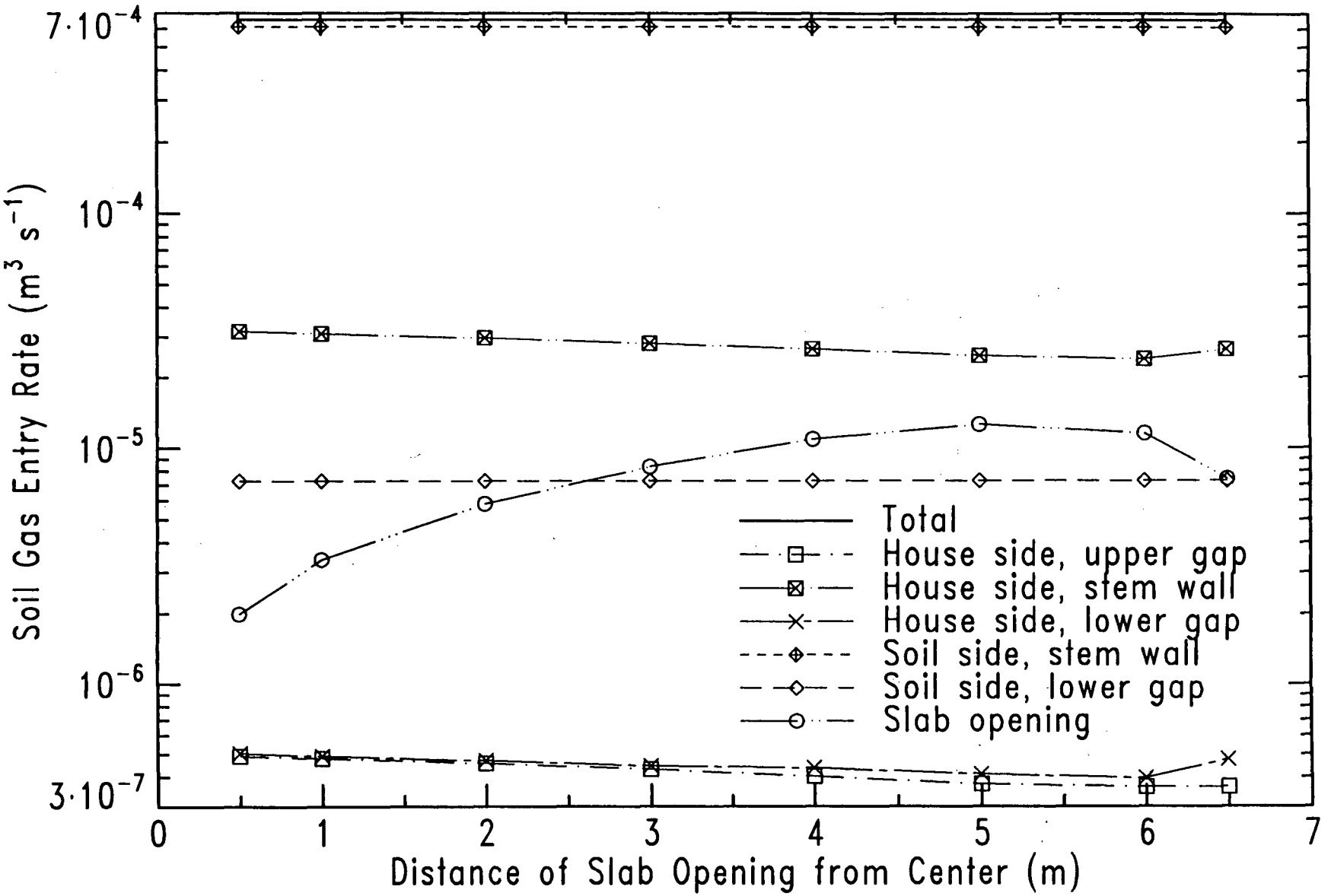

Figure A17S.
Soil-gas entry rates at the several entry points, with the distance of the slab opening from the center as parameter.

10/03/91 11:42:51

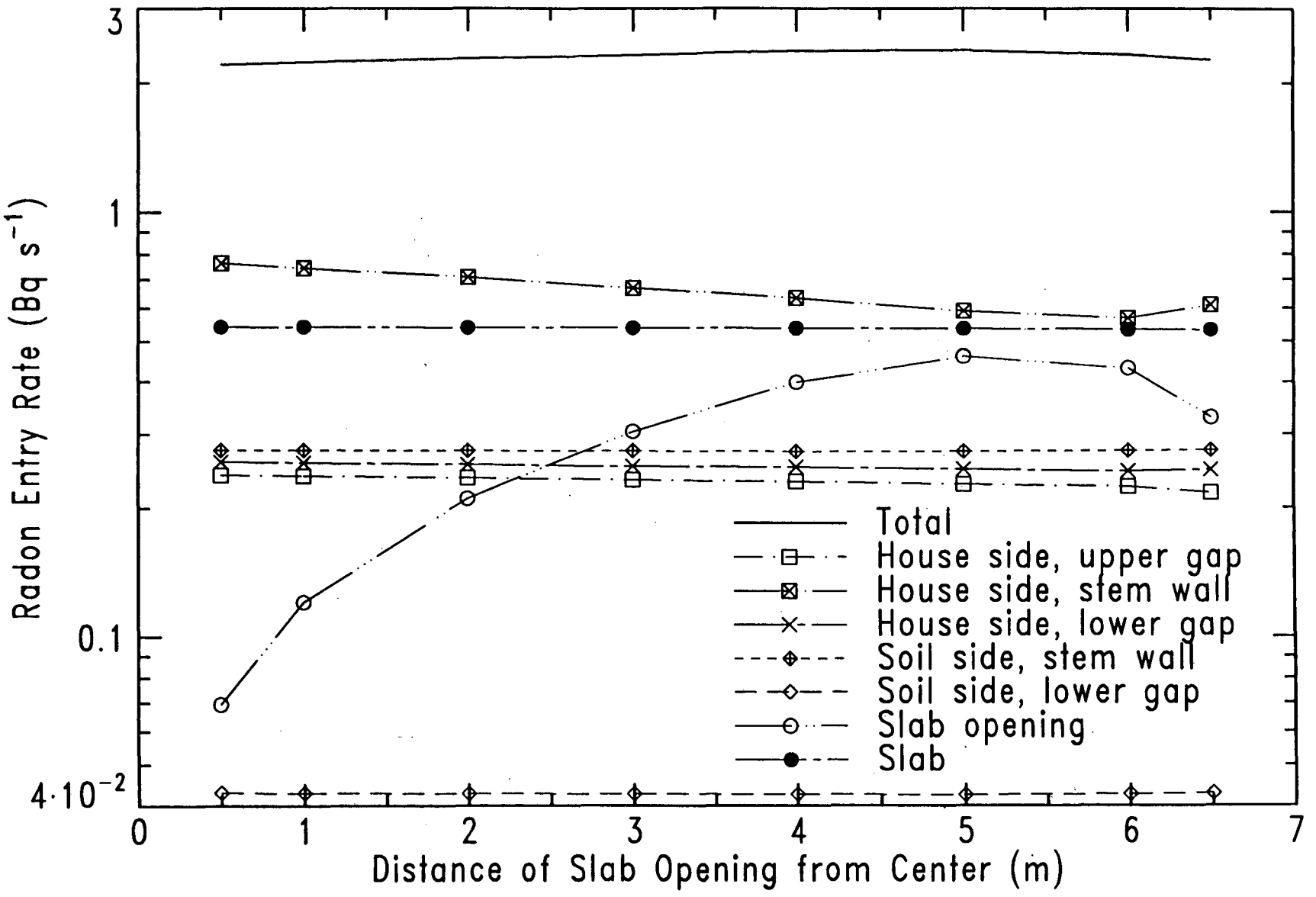

Figure A17R.
Radon entry rates at the several entry points, with the distance of the slab opening from the center as parameter.

10/03/91 13:56:02

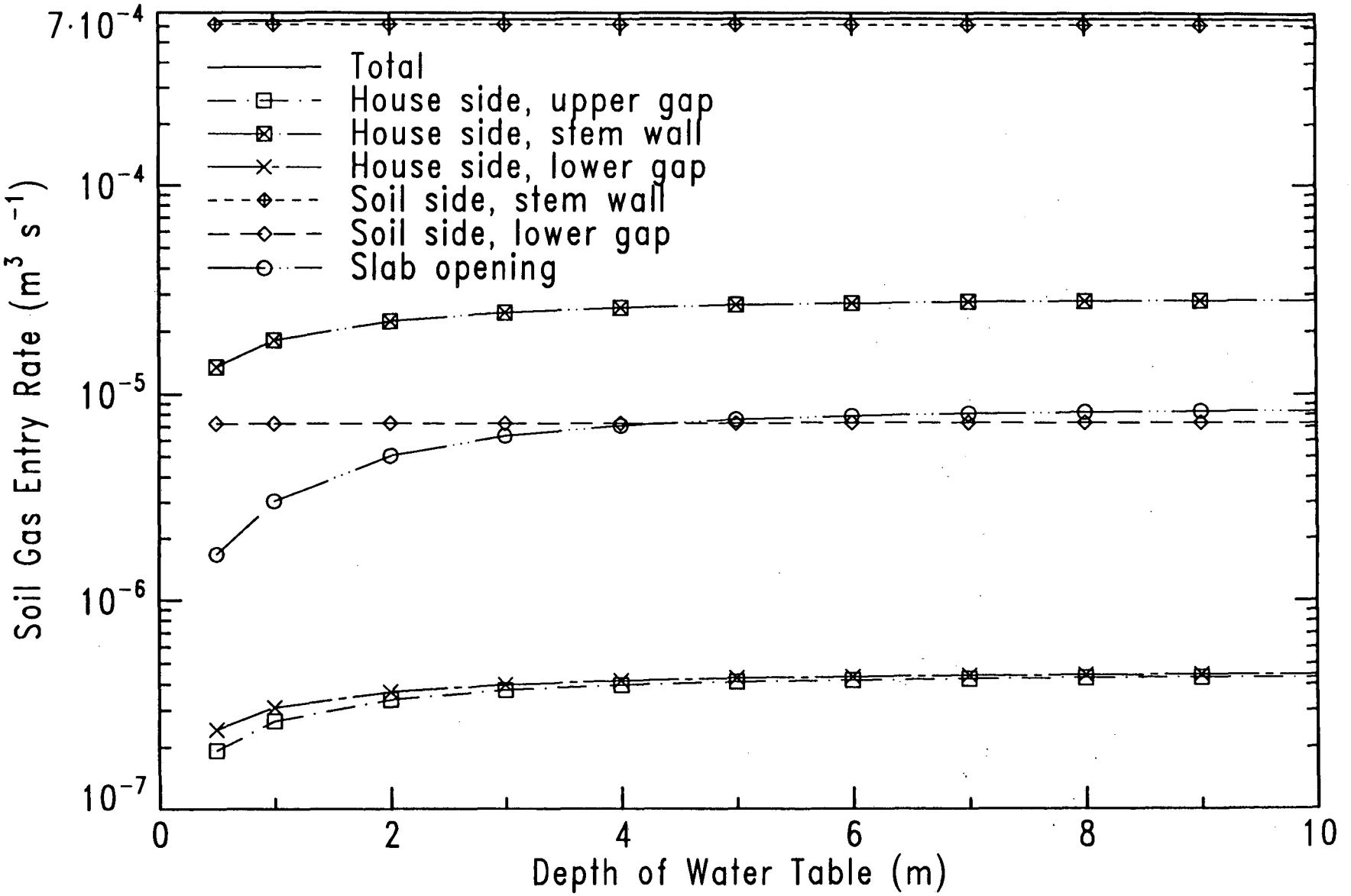

Figure A18S.
Soil-gas entry rates at the several entry points, with the water table depth as parameter.

10/03/91 11:42:53

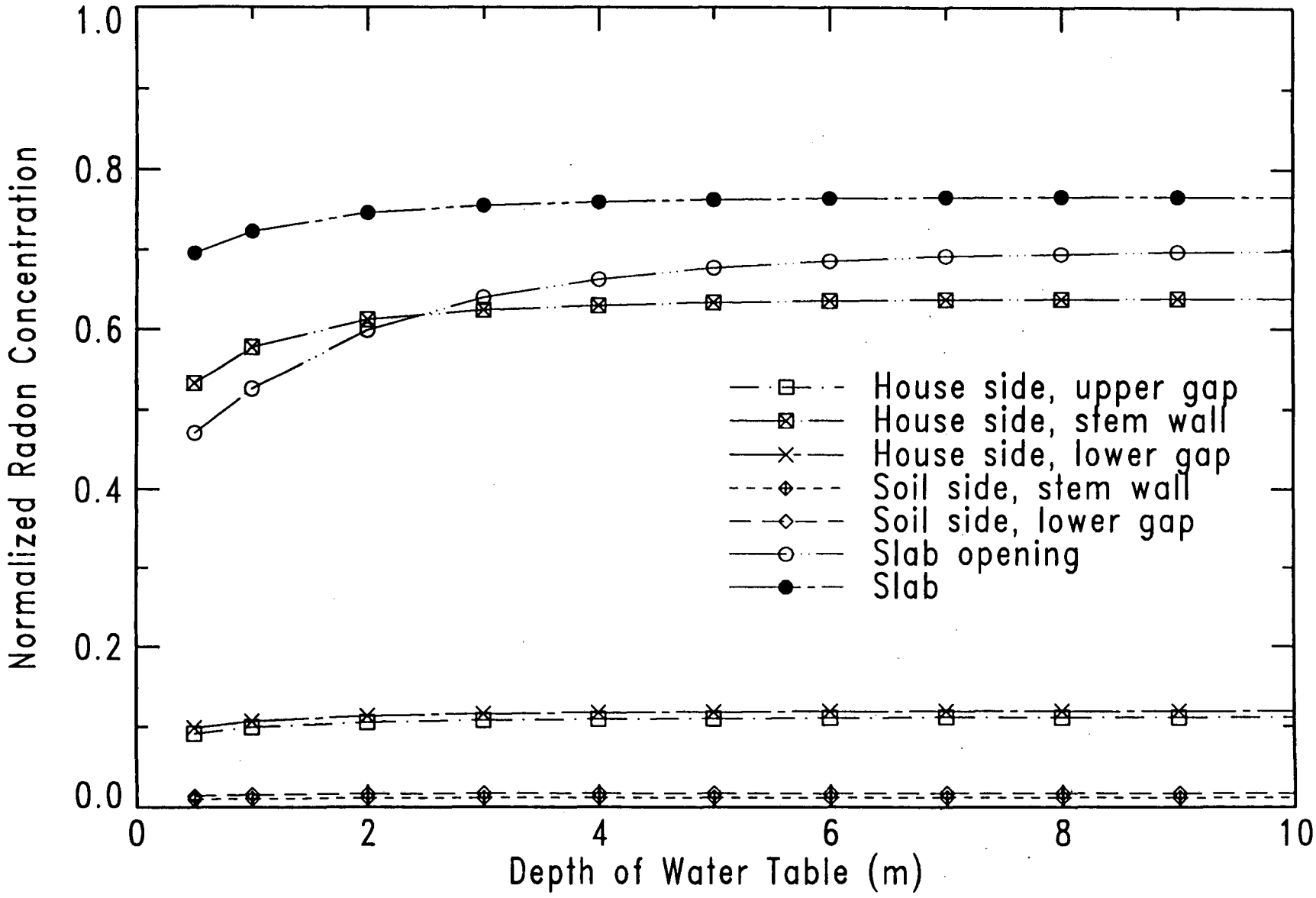

Figure A18C.
Normalized radon concentrations at the several entry points, with the water table depth as parameter.

10/03/91 13:15:23

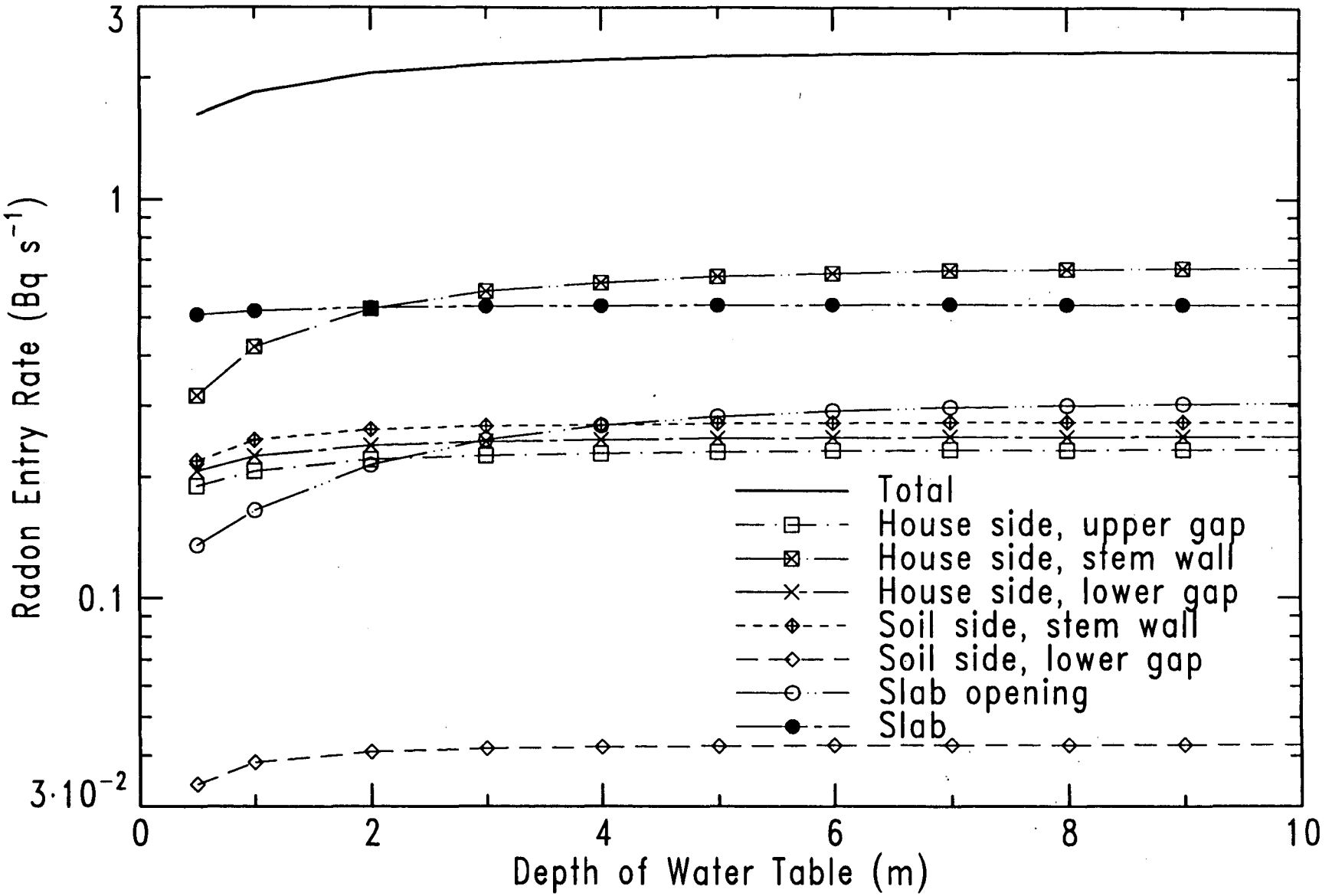

Figure A18R.
Radon entry rates at the several entry points,
with the water table depth as parameter.

10/03/91 13:56:05

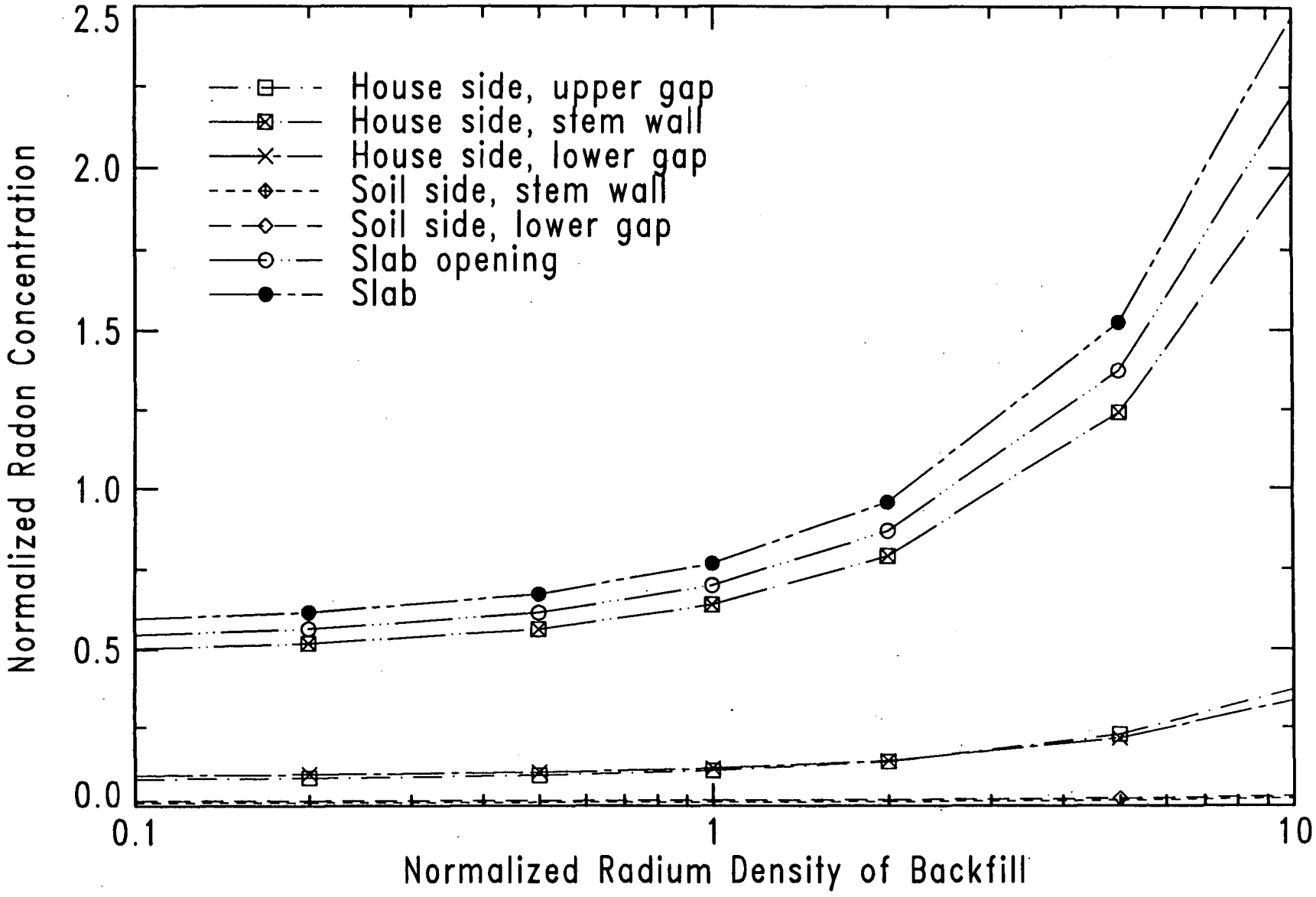

Figure A19C.
Normalized radon concentrations at the several entry points, with the radium content of the backfill as parameter.

10/03/91 13:15:26

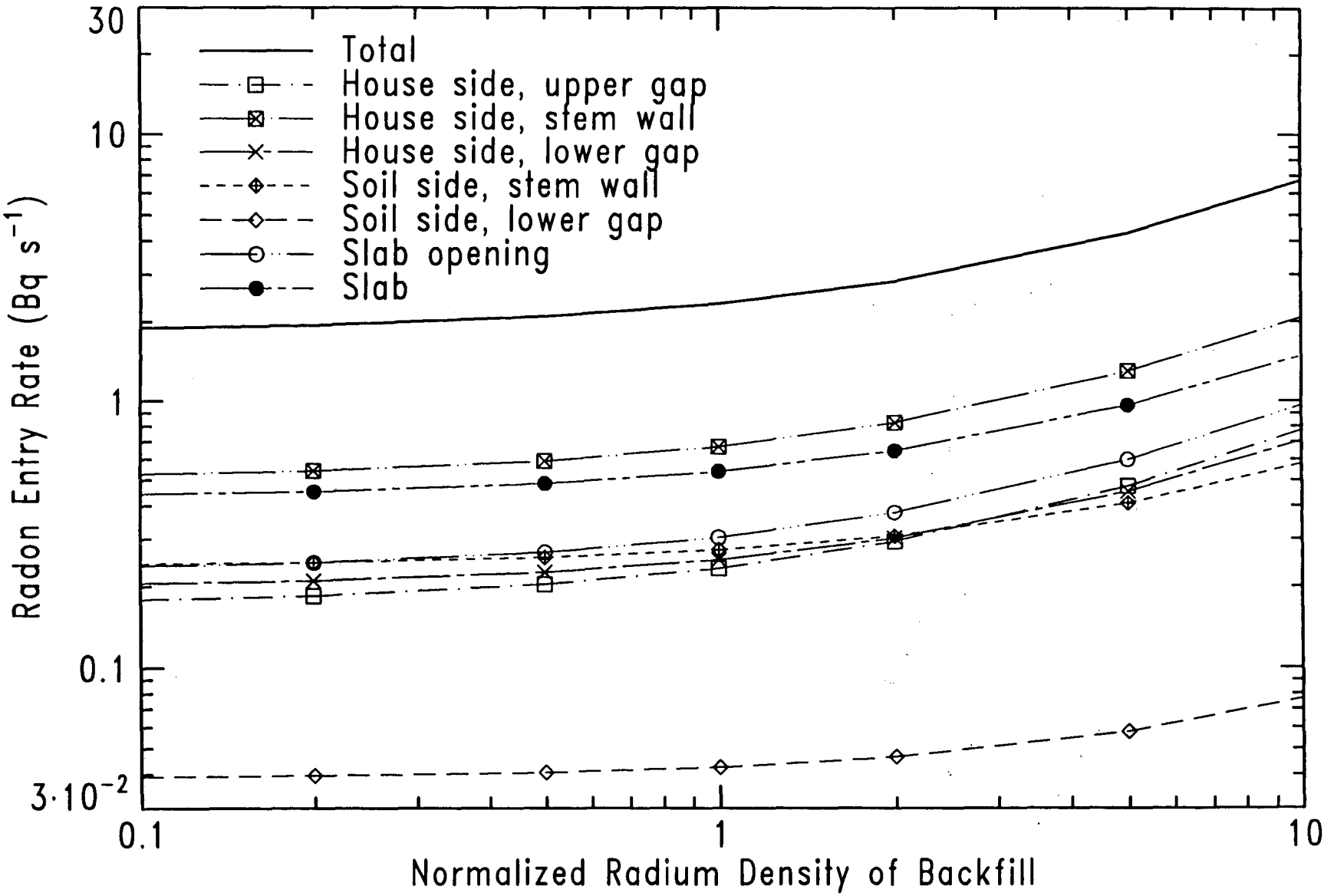

Figure A19R.
Radon entry rates at the several entry points,
with the radium content of the backfill as parameter.

10/03/91 14:21:44

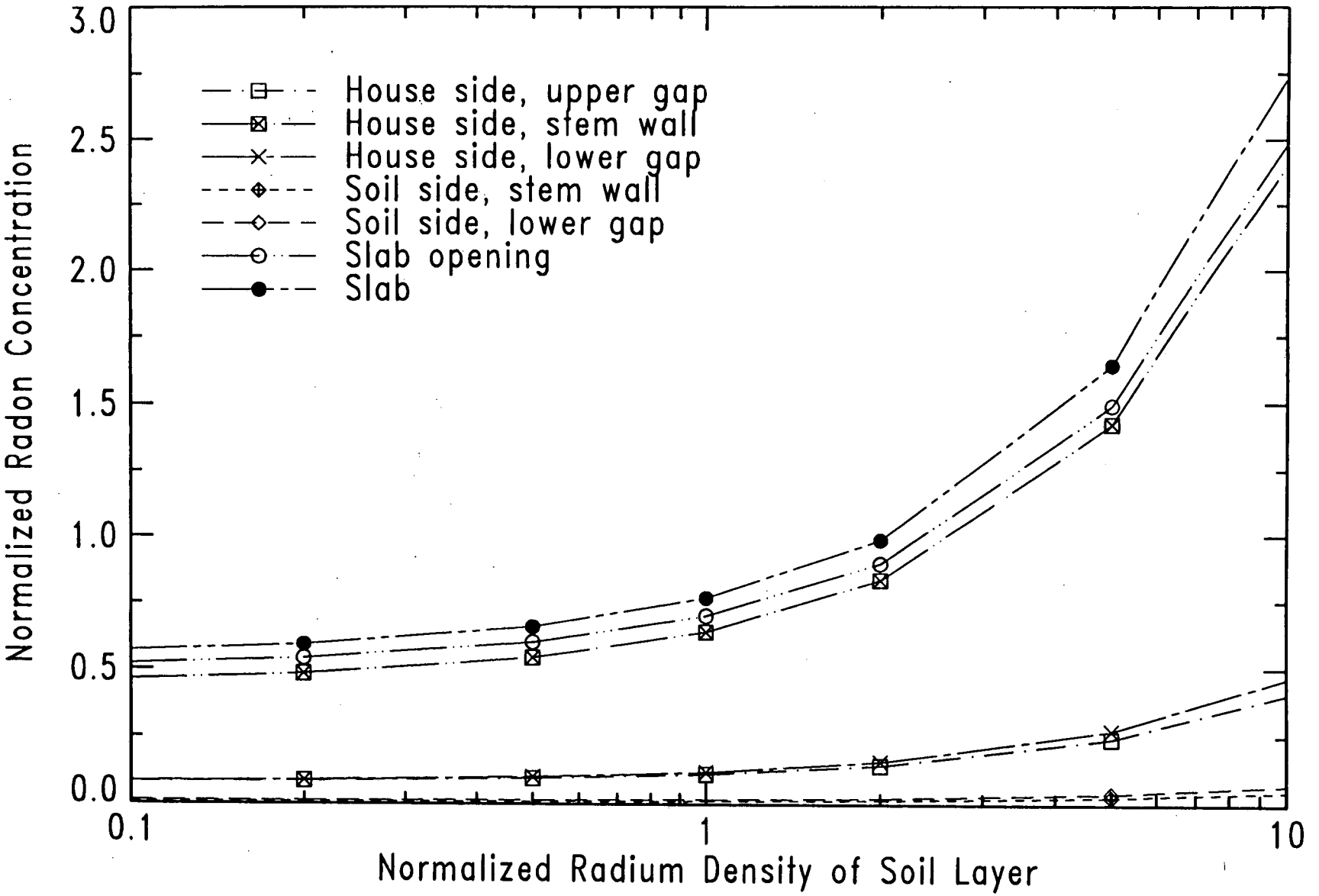

Figure A20C.
Normalized radon concentrations at the several entry points, with the radium content of the soil below 1 m depth as parameter.

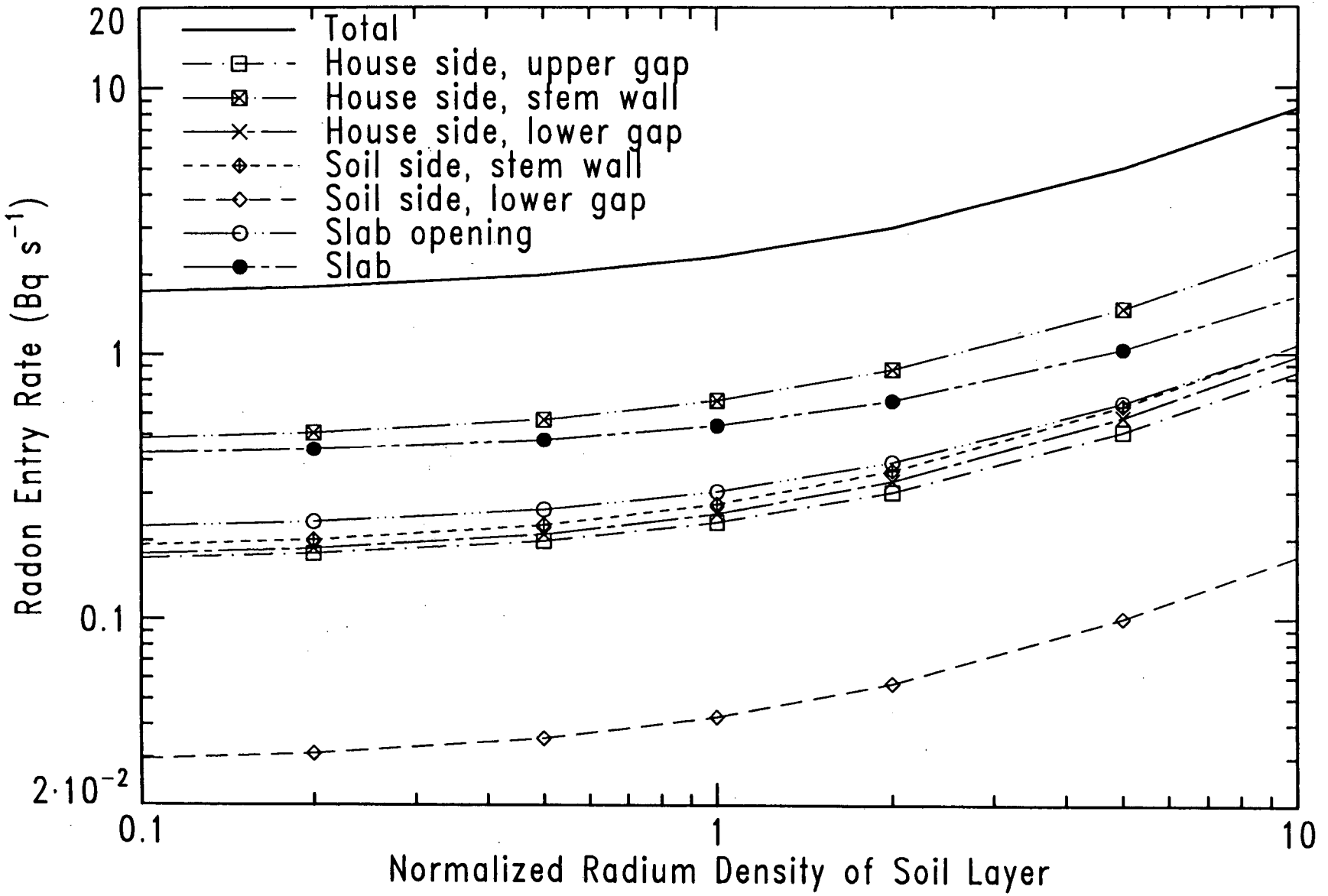

Figure A20R.
Radon entry rates at the several entry points, with the radium content of the soil below 1 m depth as parameter.

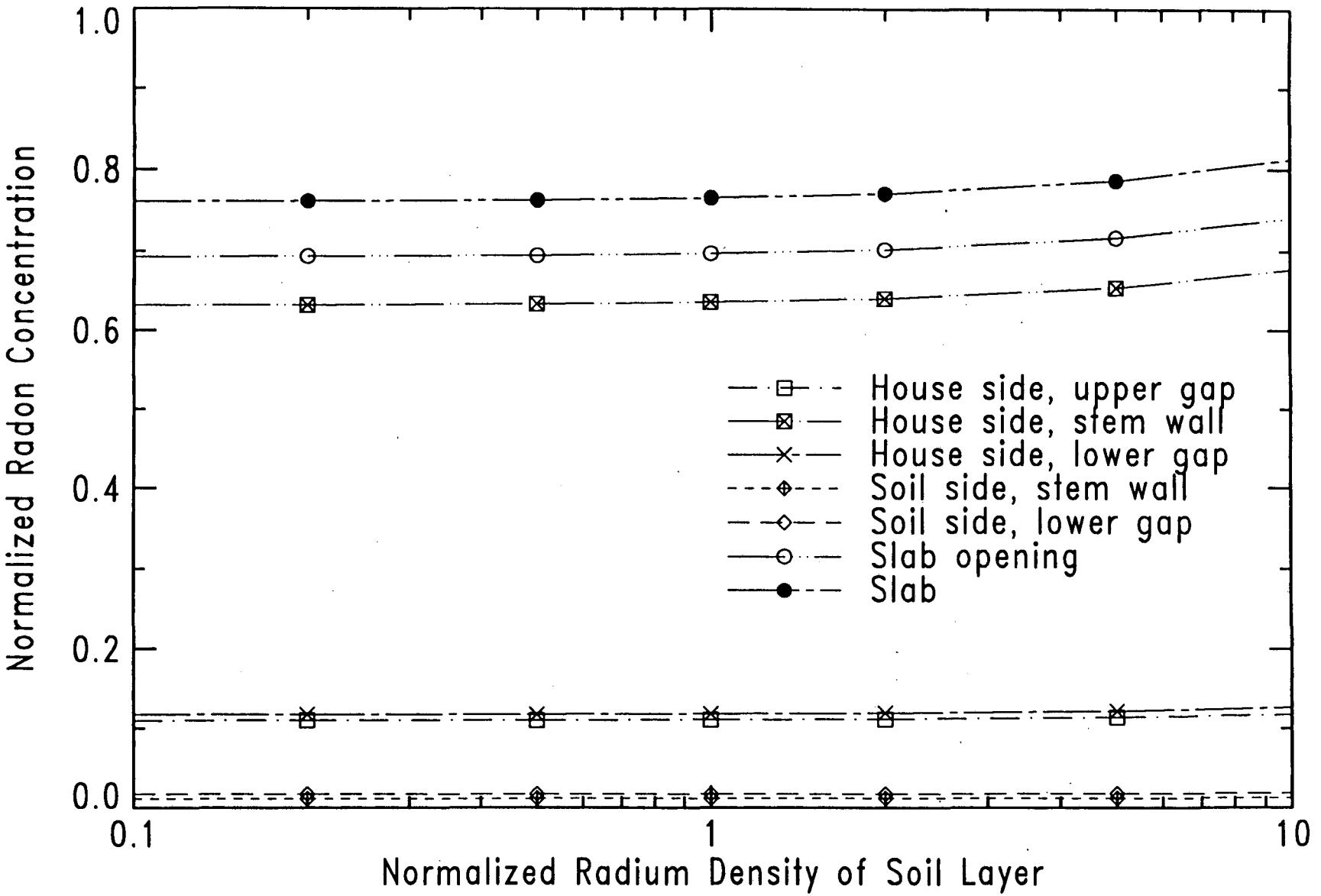

Figure A21C.
Normalized radon concentrations at the several entry points, with the radium content of the soil below 5 m depth as parameter.

10/03/91 13:15:31

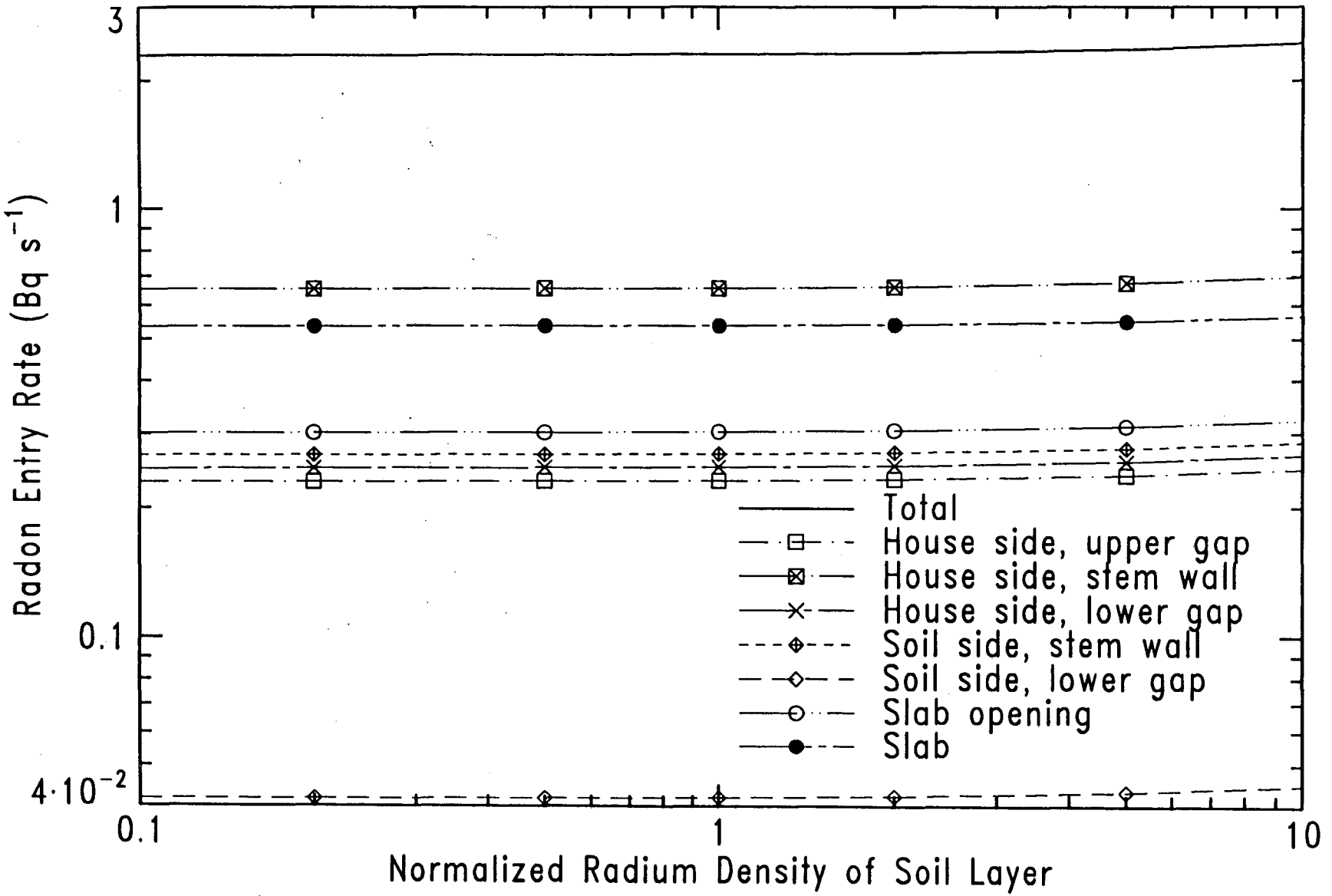

Figure A21R.
Radon entry rates at the several entry points, with the radium content of the soil below 5 m depth as parameter.

10/03/91 13:56:12

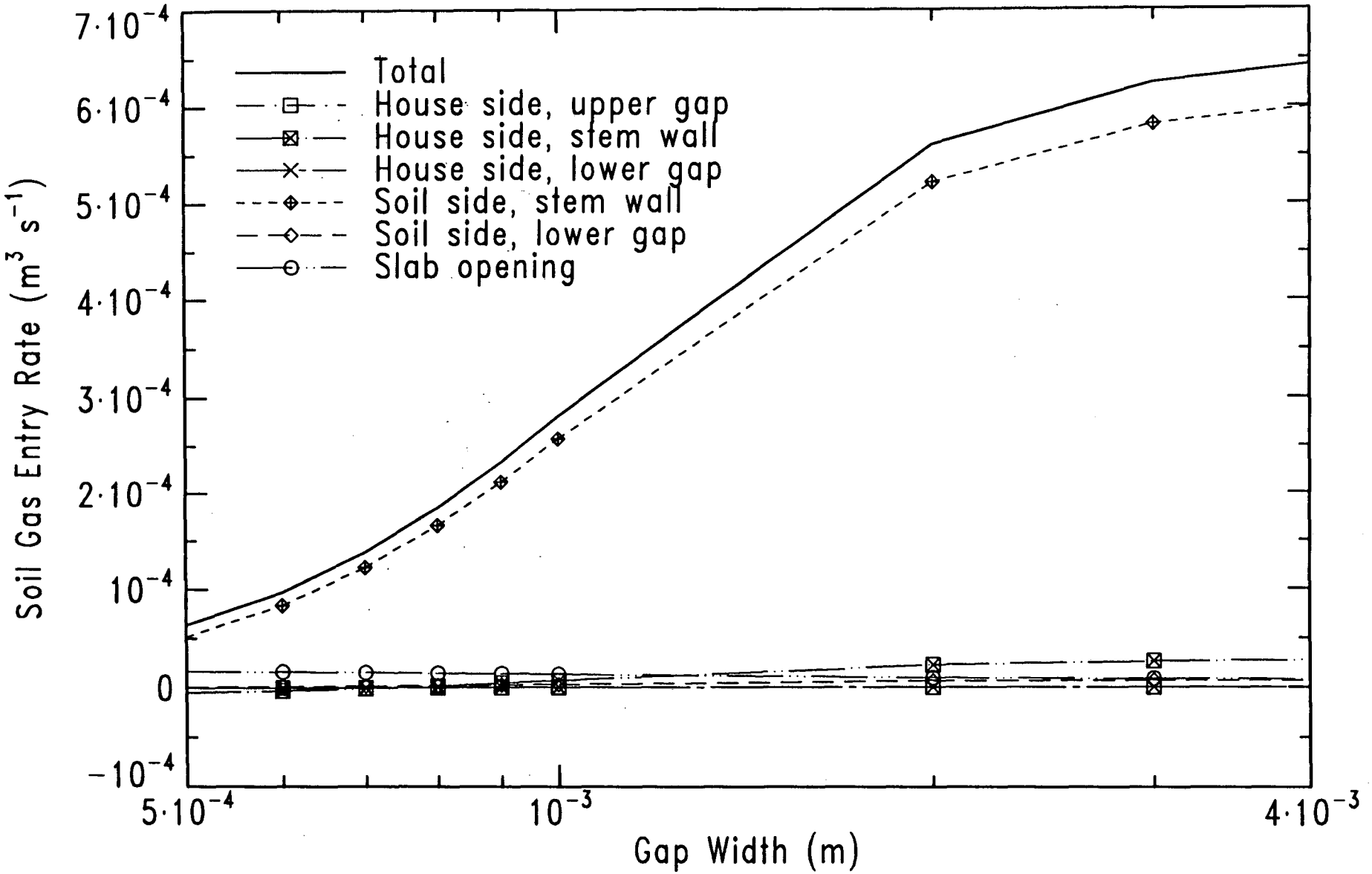

Figure A22S.
Soil-gas entry rates at the several entry points, with the width of the gap between slab and stem wall as parameter.

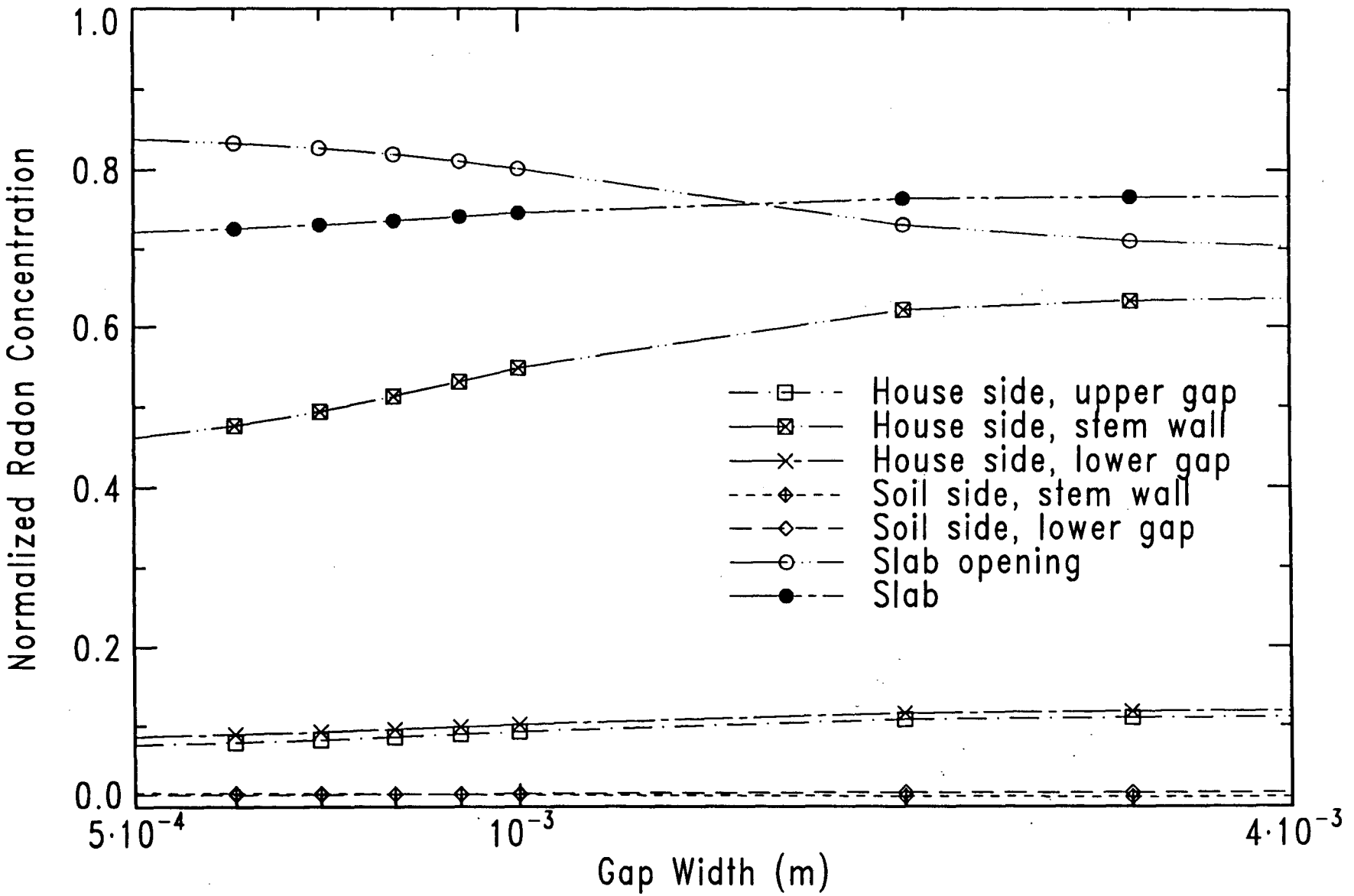

Figure A22C.
Normalized radon concentrations at the several entry points, with the width of the gap between slab and stem wall as parameter.

10/03/91 13:15:34

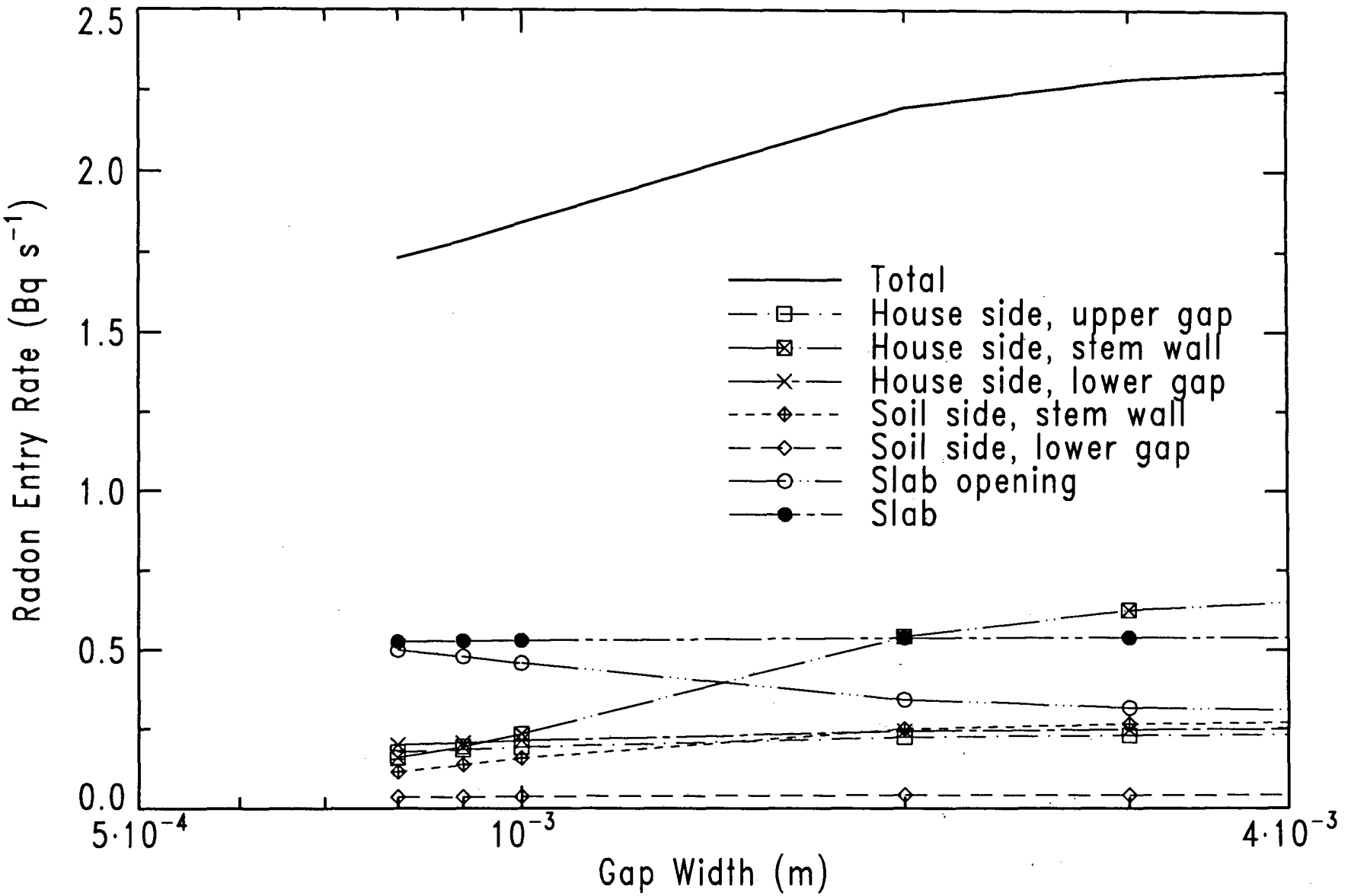

Figure A22R.
Radon entry rates at the several entry points, with the width of the gap between slab and stem wall as parameter. Values for gap widths less than 0.008 m are uncertain.

10/21/91 15:14:48

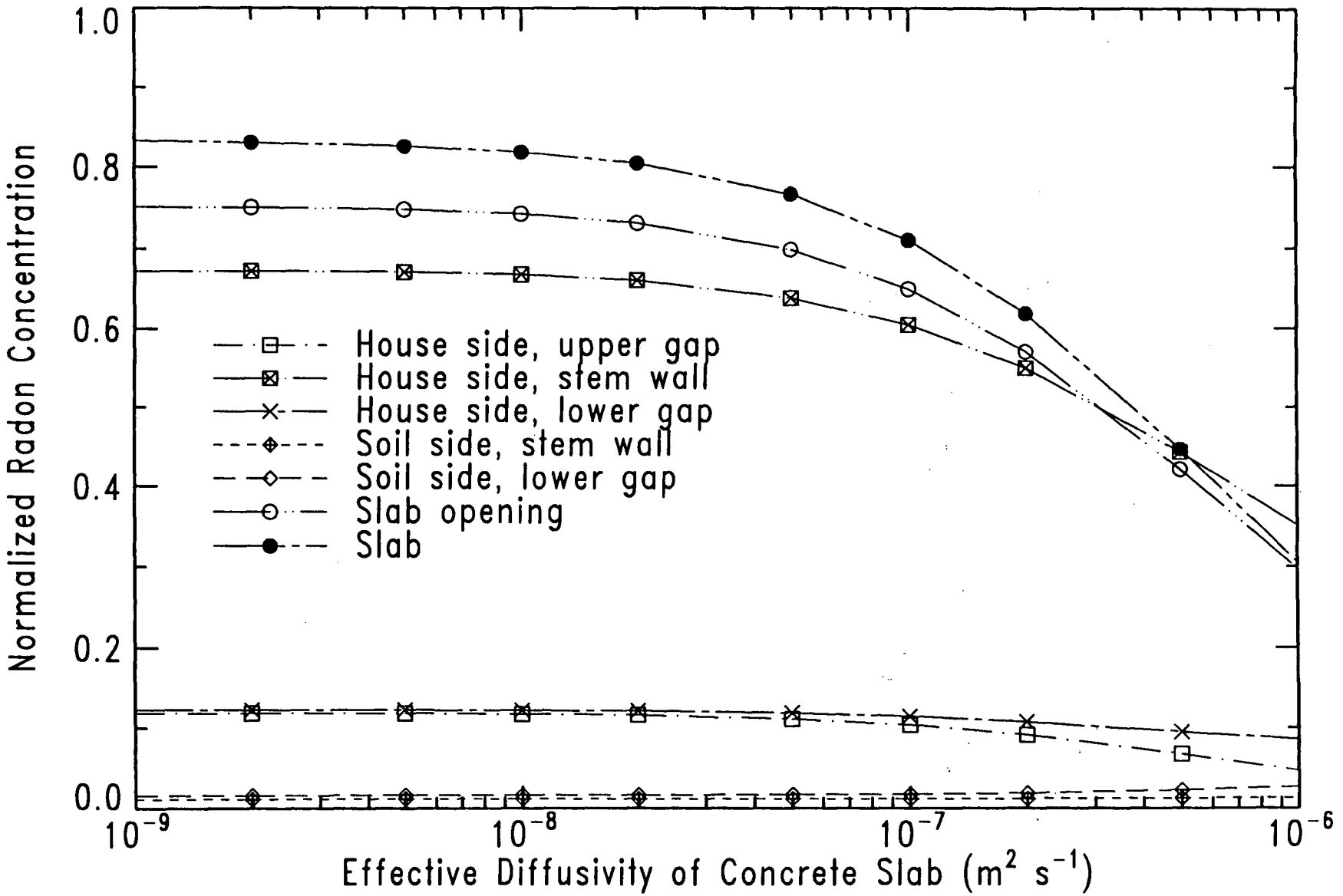

Figure A23C.
Normalized radon concentrations at the several entry points, with the effective diffusivity of the slab as parameter.

10/03/91 13:15:37

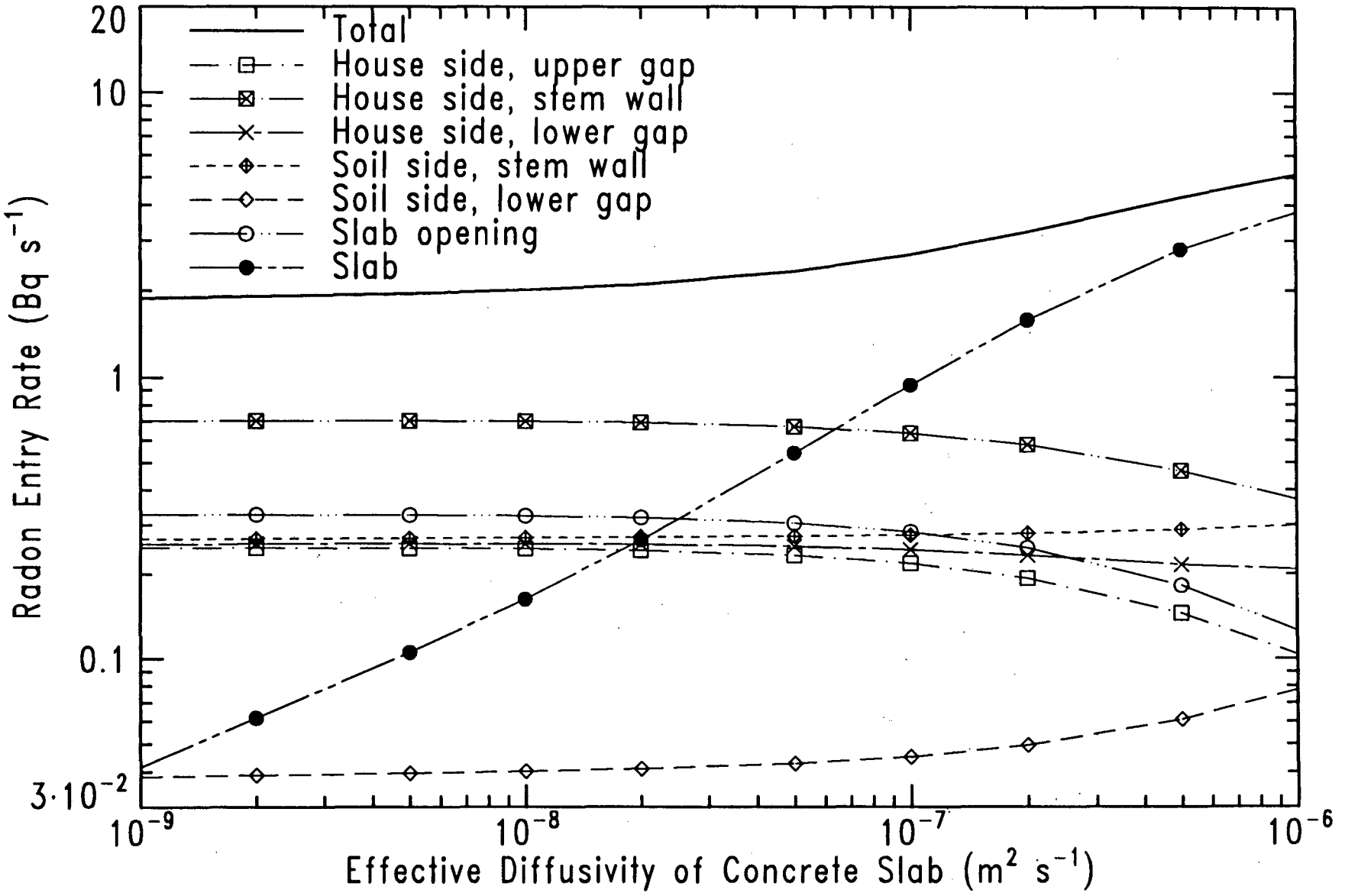

Figure A23R.
Radon entry rates at the several entry points,
with the effective diffusivity of the slab as parameter.

10/03/91 13:56:18

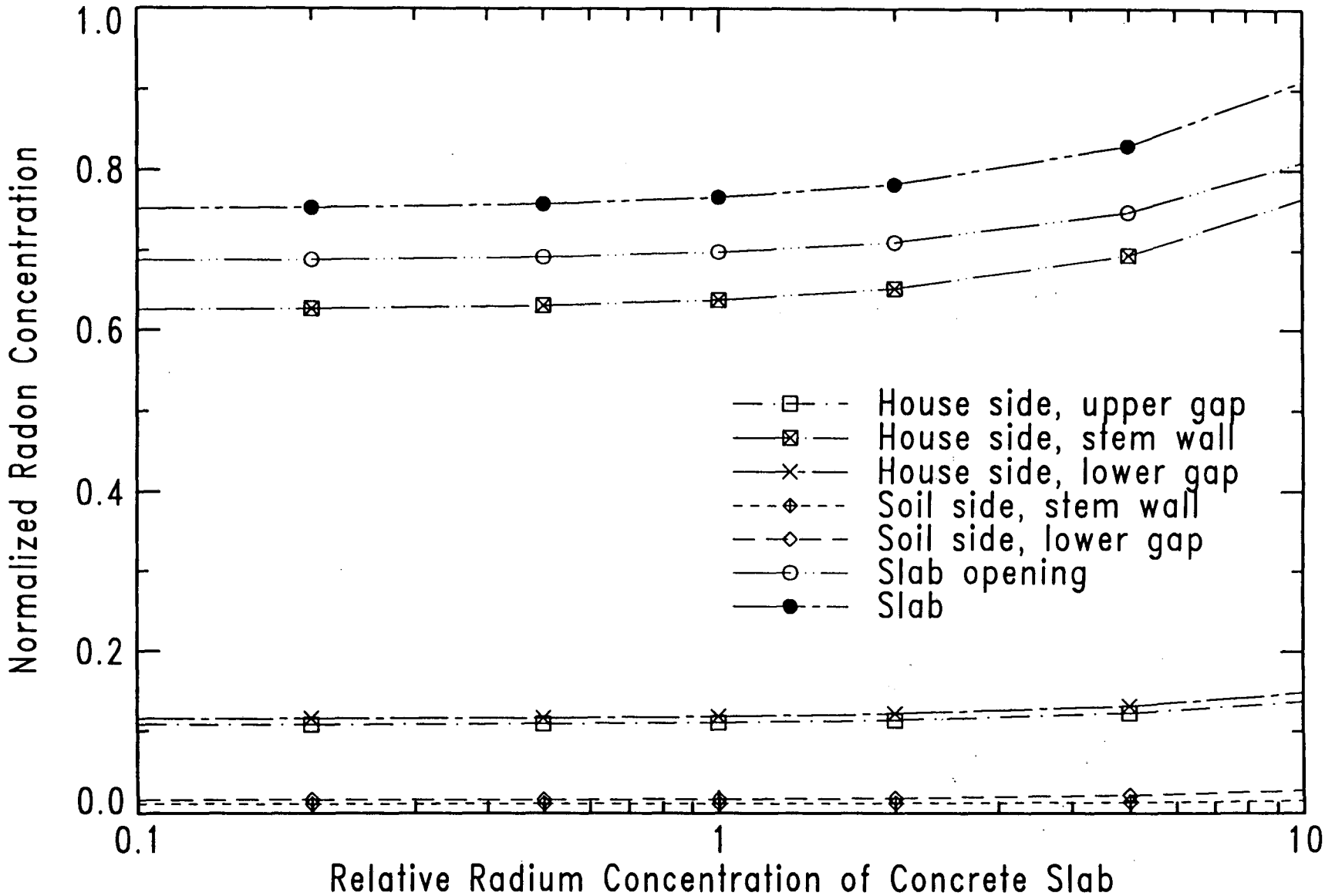

Figure A24C.
Normalized radon concentrations at the several entry points, with the radium content of the slab as parameter.

10/03/91 13:19:07

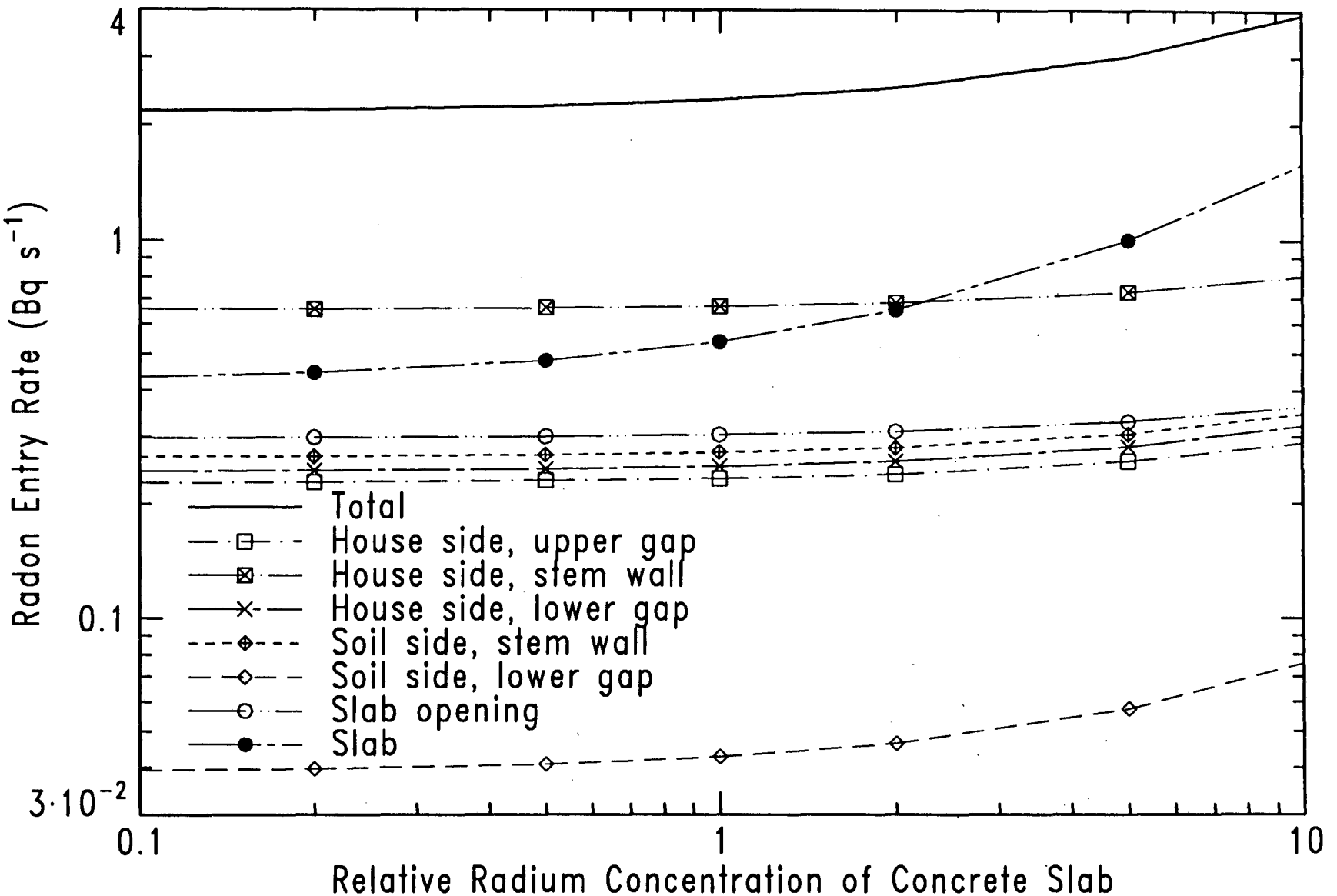

Figure A24R.
Radon entry rates at the several entry points,
with the radium content of the slab as parameter.

10/03/91 13:56:20

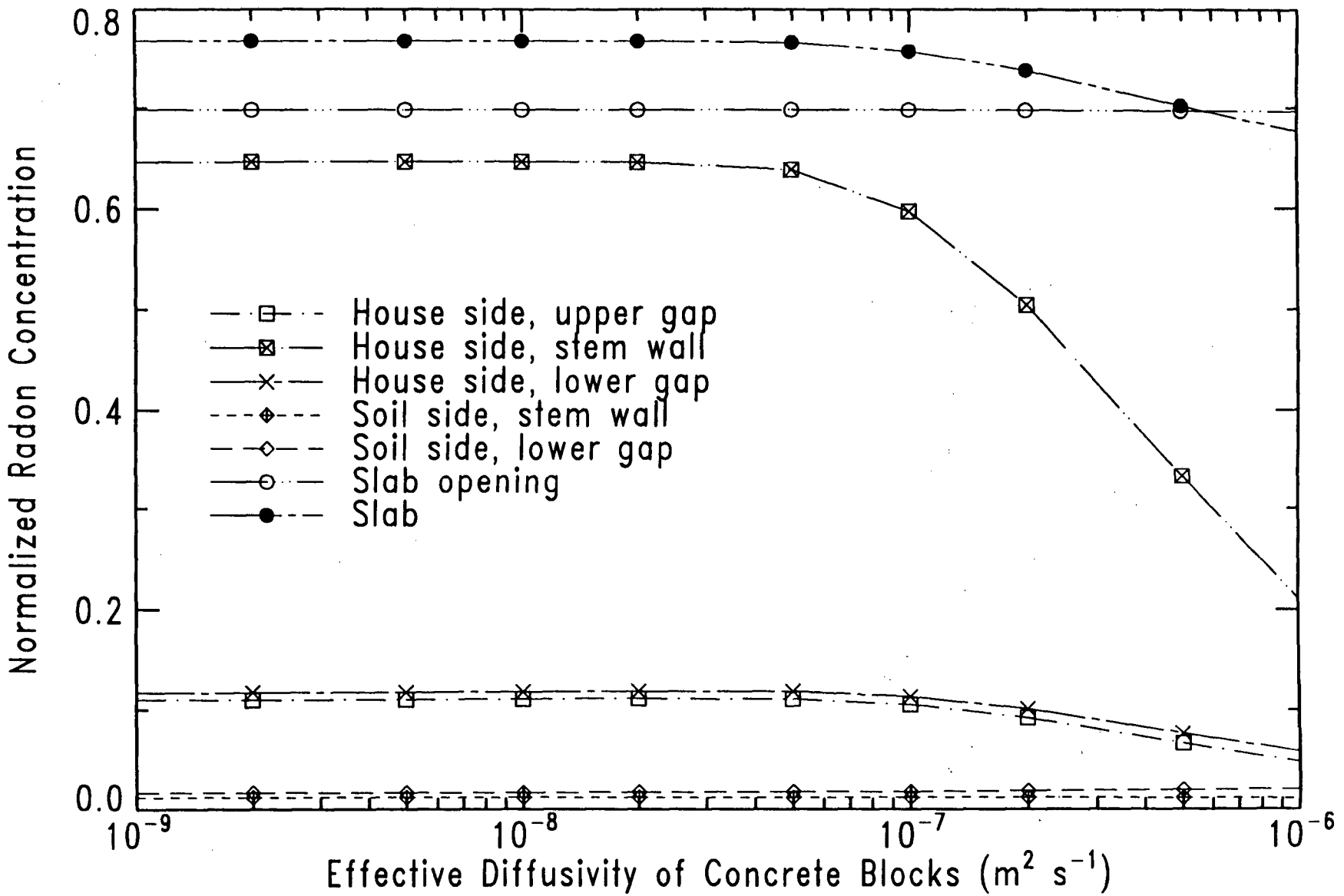

Figure A25C.
Normalized radon concentrations at the several entry points, with the effective diffusivity of the stem wall blocks as parameter.

10/03/91 13:19:10

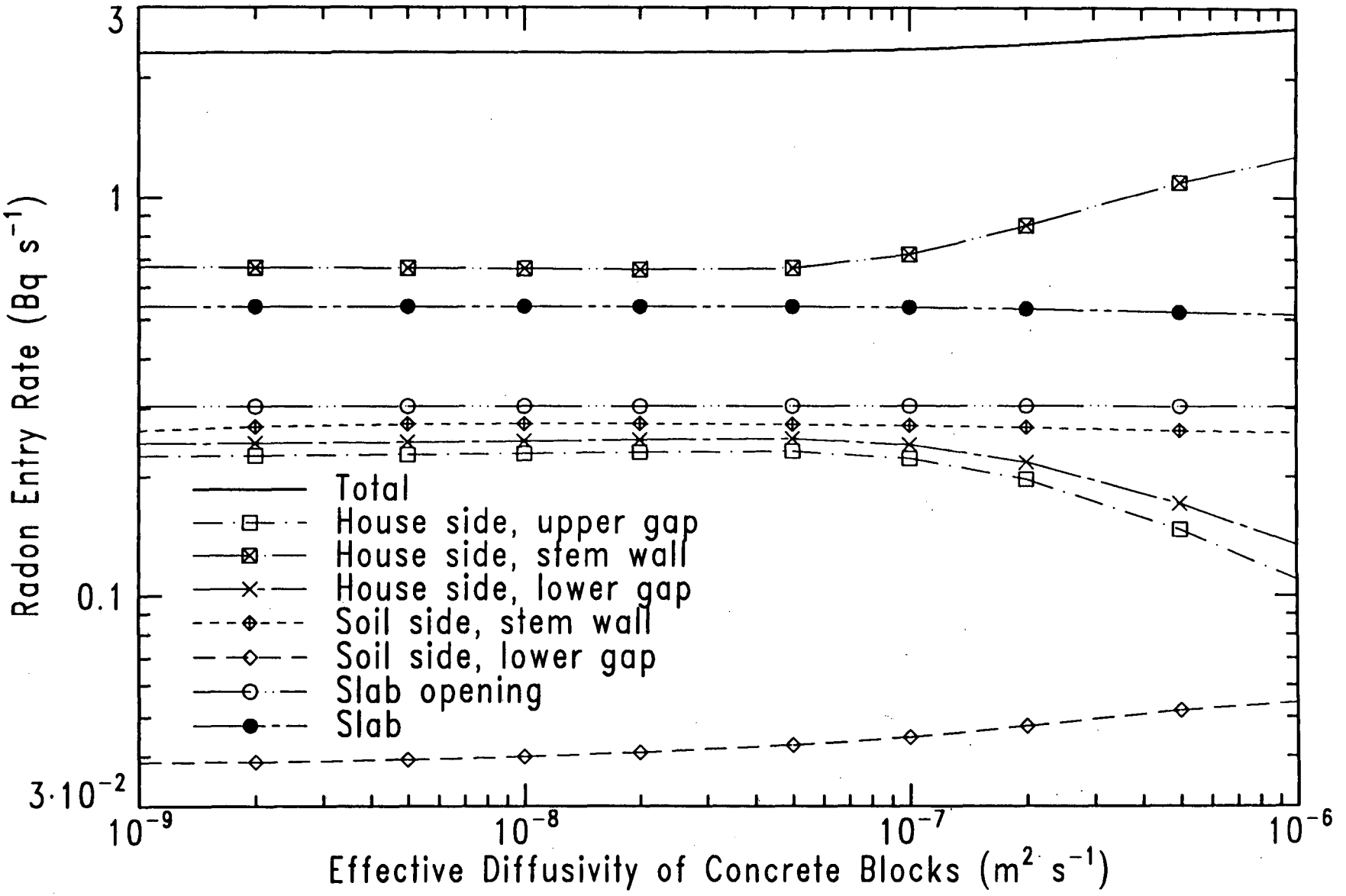

Figure A25R.
Radon entry rates at the several entry points, with the effective diffusivity of the stem wall blocks as parameter.

10/03/91 13:56:23

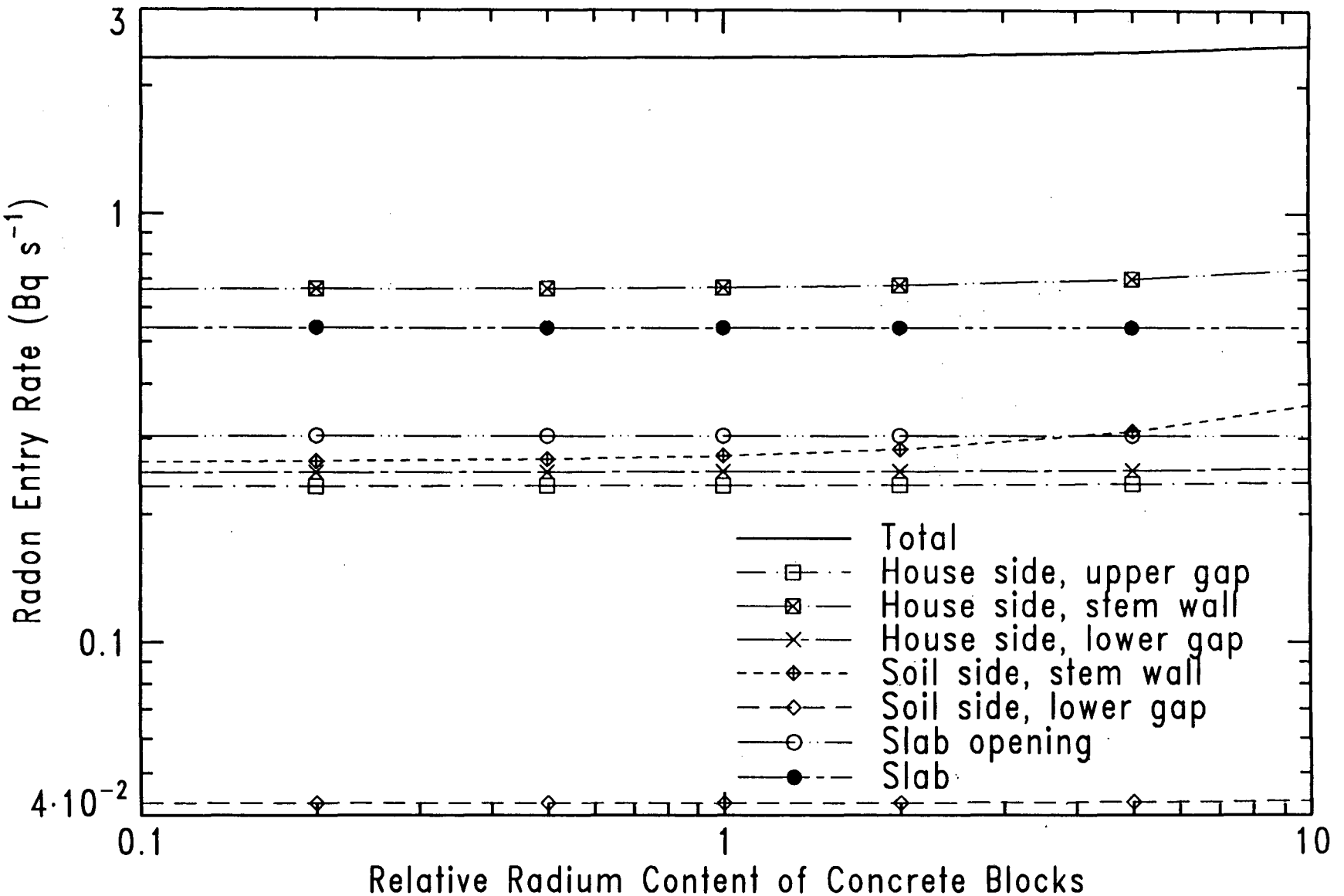

Figure A26R.
Radon entry rates at the several entry points,
with the radium content of the stem wall blocks as parameter.

10/03/91 13:56:26

LAWRENCE BERKELEY LABORATORY
UNIVERSITY OF CALIFORNIA
INFORMATION RESOURCES DEPARTMENT
BERKELEY, CALIFORNIA 94720